Minerals Processing Research Institute
Louisiana State University

Low-Cost Sorbent for Capturing Carbon Dioxide Emissions Generated by Existing Coal-Fired Power Plants

Final Report

submitted to

TDA Research, Inc.

for

Department of Energy Contract Number DE-NT0005497

Attn: Jeannine Elliott and Robert Copeland

by

Ralph W. Pike, Director and Horton Professor of Chemical Engineering
F. Carl Knopf, Associate Director and the Anding Distinguished Professor of Chemical Engineering
Debalina Sengupta, Graduate Research Assistant

May 10, 2010

MPRI-TDAR-2

Abstract

Simulation and economic analysis of the Conesville #5 Power Plant operations have been completed and expanded which includes the off-design case that produces steam for regeneration of the adsorbent. A significant cost is electricity for the sequestration process estimated at 85,516 kW. The levelized make-up power cost is 2.50 ¢/kW-hr which would result in an increased utility cost of 33.6 % based on current (no sequestration) Conesville No. 5 electricity cost of 6.4 ¢/kW-hr.

Table of Contents

Introduction

Coal-fired power plants generate more than 300 GW (gigawatts) which is about one-half of the electricity in the United States. The DOE/EIA estimates that coal-fired generating capacity will increase to more than 400 GW by 2030. More than 90% of the carbon dioxide emissions from 2007 to 2030 will come from today's existing plants because less than 4 GW of existing capacity will be retired during this period (Ciferno, 2009).

To minimize carbon dioxide emissions these plants must be operated optimally, unconstrained by regulations that currently cause inefficient plants to be operated without the best available technology. Even without carbon capture processes, significant reductions could be made in carbon dioxide emissions with plants operated optimally. Plants operating optimally with carbon capture processes could achieve the goal of a 90% reduction in emissions by the year 2020.

This project is in support of TDA Research, Inc.'s DOE contract for the design and fabrication of a pilot scale reactor for testing on coal stack gas that is based on adsorbent laboratory and life testing data with simulated coal stack gases. A flowsheet simulation is used to evaluate fixed, fluidized and moving bed reactor designs based on a minimum cost of carbon dioxide mitigated and other considerations. The simulation includes existing pulverized coal-fired power plants, such as AEP's Conesville Unit No. 5 (Ramezan, 2007a).

Possible configurations for contacting the flue gas with the solid particles include fixed, moving, and fluidized beds. Key technical challenges to sorbent based systems for capturing carbon dioxide from coal-fired power plants include: large flue gas volume, relatively low CO2 concentration, flue gas contaminants and high parasitic power demand for sorbent recovery. The TDA Research adsorbent pilot scale tests have considered these characteristics in the research to-date, and current research is demonstrating that these technical challenges can be met.

Solid sorbents are solid particles that can be used to capture CO_2 from flue gas through chemical adsorption, physical adsorption, or a combination of the two effects. TDA Research has developed a low cost, dry solid adsorbent that is regenerable and can undergo rapid cycling in a fixed bed. It adsorbs carbon dioxide over a wide temperature range with a 200^{o}C nominal operating temperature. It adsorbs sulfur dioxide and NO_x that is released with the carbon dioxide on regeneration. The sorbent can be reconditioned, restoring to initial activity even after being loaded with H_2SO_4 and HNO_3 (Copeland, 2008). In summary, the TDA Research solid sorbents have the capability for high CO_2 loading capacities while being able to maintain particle performance in the presence of flue gas contaminants.

For the design of a moving-bed adsorption unit, the sorbent is an extruded cylinder with a bulk density of 0.95 gm/cm^3 and pore volume of 0.19cm^3/gm with a dynamic loading of 0.75% and a theoretical maximum loading of 9.0%. The crush strength is 1.5 lb_f/mm in small batches and is 6.3 lb_f /mm in large batches. The sorbent is regenerated with saturated steam to 0% CO_2 at 1.0 atms. The cost of producing the adsorbent in this form is estimated to be $1.37/lb. Breakthrough curves have been determined, and this data is used in the design of a moving bed adsorber and regenerator for the power plant (Srinivas, et al, 2008 and 2009, Copeland, 2008).

The Aspen HYSYS flowsheet simulator was used to design the process for the adsorber, regenerator and downstream processing to produce pipeline quality carbon dioxide. With HYSYS, the process equipment, operating conditions and energy (power, cooing water, etc) requirements were determined. The economic analysis used Aspen Icarus In-Plant Cost Estimator to determine capital and operating costs, other manufacturing costs and economic returns. A description of these programs is given in Appendix B.

Power Plant Performance - Design and Off-Design Calculations

All carbon dioxide sequestration processes require sorbent regeneration, and this process utilizes steam extracted from the power plant for regeneration. This steam extraction will adversely affect power plant performance. Ultimate costing of the sequestration process requires accurate accounting for all sequestration costs (capital, labor, etc.) as well as accounting for the power furnished from the power plant.

Power plants are designed and optimized for full-load operation, which is termed the design case or base-case. All operations which are not full-load operation are termed off-design operation. Sequestration with steam extraction causes the power plant to operate in an off-design operation.

The first step in all power plant calculations is to determine design case plant performance including all pressures, temperatures, efficiencies, steam flows, turbine net heat rate, plant net heat rate, etc. All off-design performance calculations start from the design case.

In the next sections we discuss design and off-design power plant calculations. These calculations are particularized to the Conesville #5 Power Plant. The off-design calculations include steam extraction as needed for regeneration of the solid sorbent.

Power Plant Performance Design Case (Full-Load Operation)

Design case performance calculations for steam turbine systems are standard calculations. We can outline the calculation procedure as follows:

1.) Use the known turbine inlet conditions and exhaust conditions at each extraction point to determine enthalpy, entropy and steam quality in and out of each turbine section, as well as turbine section efficiency.

2.) Use the known pressure drops in the reheater and boiler, feedwater heater terminal temperature difference and the feedwater drain cooler approach temperature to determine steam properties at appropriate locations.

3.) Determine the steam extraction flowrates starting with feedwater heater (7) FWH-7, and continuing, FWH-6, FWH-5, …, until FWH-1 is reached (Figure 1).

4.) Calculate the power used by the auxiliary turbine and low-pressure feedwater pump.

5.) Calculate the turbine exhaust end loss using Spencer et al. (1963).

6.) Sum the output from all the turbines, account for all losses and determine turbine heat rate.

Normal full-load operational data for the Conesville #5 Power Plant were taken from the DOE report, DOE/NETL-401/110907, November 2007, page 19 (Ramezan, 2007a). This DOE report indicates the Conesville #5 plant has a steam turbine heat rate of 7773 Btu/kW-hr, a generator output of 463,478 kW and a net plant heat rate of 9,309 Btu/kW-hr. The initial design case simulation developed for the present study, with results shown in Figure 1, indicates a steam turbine heat rate of 7794 Btu/kW-hr, a generator output of 473,411 kW and a net plant heat rate of 9312 Btu/kW-hr. These later values are in agreement with the DOE report.

Power Plant Performance Off-Design Operation

The solution to the off-design problems involves:

1.) Supplying initial estimates for all pressures and efficiencies in the turbine system.

2.) Modifying pressures in the turbine system based on the off-design turbine inlet conditions.

3.) Modifying the efficiencies based on the off-design velocity into each turbine section.

In the design case, we solved the full load operation material and energy balances for the turbine system using thermodynamic functions and known P and T or P and $\hat{h}$ (for two-phase steam) at each turbine section inlet, outlet and extraction point. All standard commercial simulation packages – ASPEN, HYSYS, Pro/II, etc. – can determine power plant performance for the design case. However these packages cannot directly solve for off-design performance. Here user written subroutines must be added to account for off-design pressure and efficiency changes. Here we develop the needed subroutines to allow off-design calculation to be performed within the standard commercial packages. There are specialized commercial programs – GateCycle from General Electric – which can perform both design and off-design calculations for power systems.

We evaluated several methods for predicting off-design performance, for use with standard simulation packages, including the Spencer, Cotton, and Cannon Method (Spencer, et al, 1963) as well as methods involving modifications to the Willians line. The most consistent off-design results were obtained using the method developed by Erbes and Eustis (1986) with addition of the Spencer, Cotton, and Cannon Method to determine turbine exhaust end loss.

To start the off-design calculations, the pressure at each stage i is modified from the design pressure by multiplication with the flow ratio,

$$P_{i,Off-Design} = P_{i,Design} * Flow\_Ratio \tag{1}$$

where the $Flow\_Ratio$ = Off Design Flow Rate / Design Flow Rate.

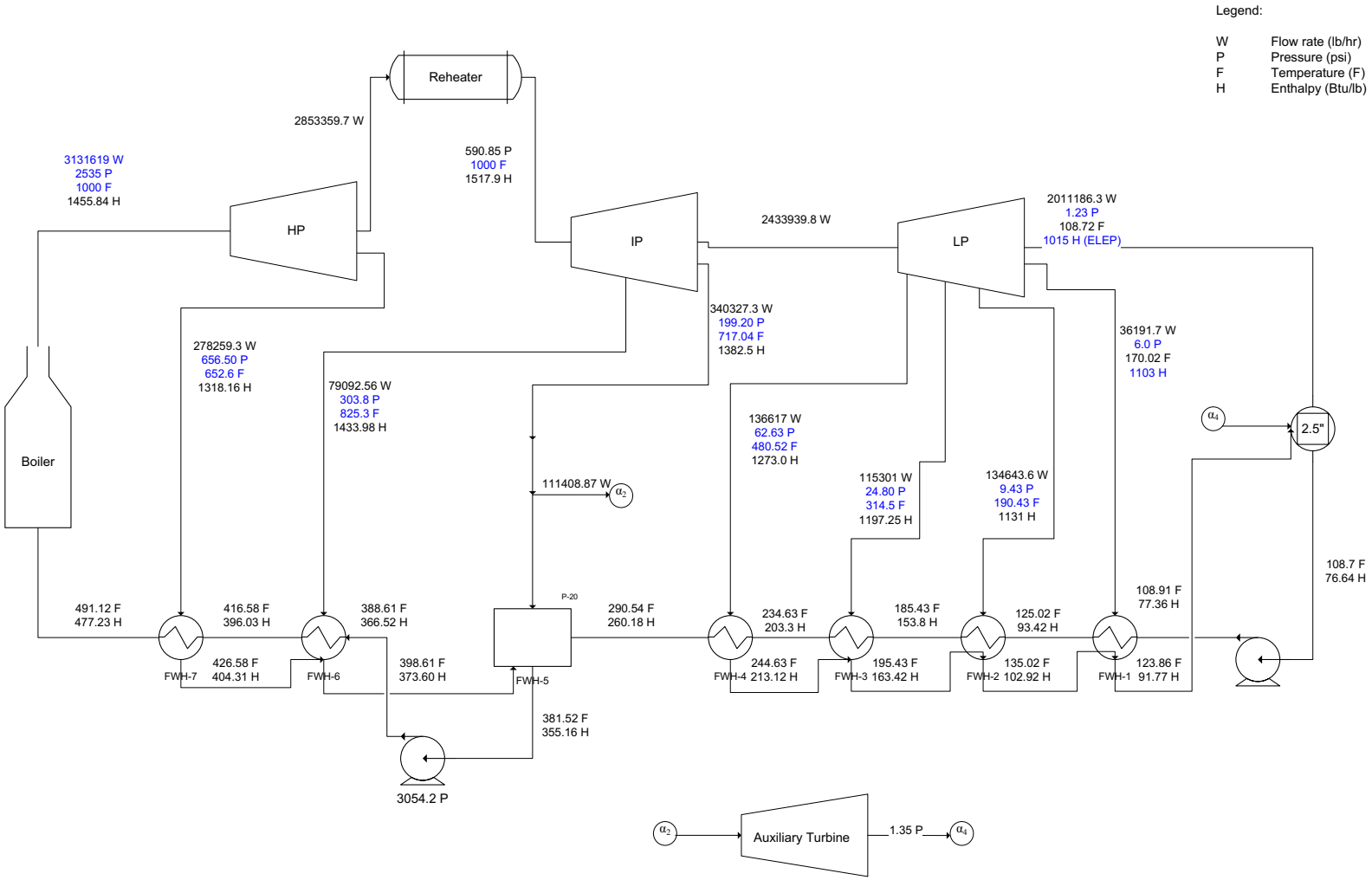

Figure 1 : Heat Balance diagram for design conditions (throttle steam flow ratio : 1.0).

Turbine Net Heat Rate: 7794 Btu/kW-hr **Turbine Net Output: 473411 kW**

In CO_2 sequestration applications, steam extraction will change the flow rates determined in the design case for the LP turbine section. The off-design system performance can now be solved for the given off-design steam flow rates and using the design-case efficiencies, estimated pressures and assuming that all other conditions, including pump efficiencies and feedwater heater approach temperatures remain at design conditions.

Update Pressures for Off-Design Case: The process begins with the Stodola's ellipse law (1954) which provides a relation between steam flow and pressure drop in a turbine section as,

$$F_{Turbine\,Section} = K\sqrt{1-\frac{P_{Out}}{P_{In}}} \tag{2}$$

where, $F_{Turbine\,Section}$ is the steam flow in the turbine section (lb/hr); K is a proportionality constant; and P_{Out} is pressure out of the section, and P_{In} is pressure in. But Equation (2) cannot be used for off-design calculations since it does not take into account the effect of varying inlet temperature. Erbes and Eustis (1986) utilize a modification of the ellipse law suggested by Sylvestri, which accounts for varying inlet conditions as,

$$F_{Turbine\,Section} = K\sqrt{\frac{P_{In}^2 - P_{Out}^2}{\nu_{In}\,P_{In}}} \tag{3}$$

where ν_{In} = the stage inlet specific volume (ft^3/lb) and the remaining terms are the same as Equation (2). In order to use Equation (3) the constant K is first determined for each turbine section, which is done using design conditions.

With each $K_{Design}^{Turbine\,Section}$ determined, we can use Equation (3) in a reverse-order iterative calculation, starting at the LP turbine outlet, to update the off-design pressure distribution in the turbine system. Equation (3) can be rearranged to solve for an updated value for P_{In} as,

$$P_{In}^{Stage\,i} = \frac{\nu_{In}^{Stage\,i}\left(\frac{F_{Turbine\,Section}^{Stage\,i}}{K_{Design}^{Stage\,i}}\right)^2 + \sqrt{\left(\nu_{In}^{Stage\,i}\left(\frac{F_{Turbine\,Section}^{Stage\,i}}{K_{Design}^{Stage\,i}}\right)^2\right)^2 + 4\left(P_{Out}^{Stage\,i}\right)^2}}{2} \tag{4}$$

All the terms on the RHS of Equation (4) are known from the initial estimate of the off-design conditions.

When updated values for all the P_{In}'s have been determined, these values can replace the initial estimated $P_{In}^{Stage\,i}$ values. These new P values can be used to generate new flow rates,

temperatures and steam specific volumes into each turbine section. The replacement (iteration process) continues until the pressure values remain unchanged.

With converged pressures for the IP and LP turbine sections, we next update the HP turbine stage. The HP section is not included in the iteration process as the pressure drop in the reheater, $\Delta P_{Reheater}^{Off-Design}$, fixes the outlet pressure of the HP turbine as,

$$P_{Out}^{HPT} = P_{In}^{IPT} + \Delta P_{Reheater}^{Off-Design} \tag{5}$$

The pressure drop in the reheater can be determined by assuming a homogeneous flow model.

Update Efficiencies for the Off Design Case: In the off-design calculations we have utilized the $\eta^{Isentropic}$ values found in the design case. We next want to update these efficiency values using internal turbine considerations. Steam turbines are generally classified as impulse or reactive. In actual operation, most turbine sections show both impulse and reactive characteristics. Erbes and Eustis (1987) assume 50% reaction balding for each turbine section. From Salisbury (1950), stage efficiency can be found as,

$$\eta_{Design}^{Isentropic} = 2y\left[(a-y)+\sqrt{(a-y)^2+1-a^2}\right] \tag{6}$$

where $a = \sqrt{1-x}$, x = fraction of stage energy released in the bucket system, $y = \dfrac{W_{Design}}{V_{Design}}$, W_{Design} = turbine rotational speed and, V_{Design} = inlet steam velocity to the turbine section. For a 50% reaction stage, x = 0.5 and a = 0.7071. Furthermore, for a 50% reaction stage, the maximum efficiency $y_{Optimal} = \left(\dfrac{W_{Design}}{V_{Design}}\right)_{Optimal} = 0.7071.$

In addition to the assumption of 50% reaction stages, Erbes and Eustis (1987) further suggest that the turbine rotational speed will remain constant in both the design and off design cases allowing us to write,

$$\frac{\left(\dfrac{W_{Off-Design}}{V_{Off-Design}}\right)}{\left(\dfrac{W_{Design}}{V_{Design}}\right)_{Optimal}} = \frac{\left(V_{Design}\right)_{Optimal}}{V_{Off-Design}} \tag{7}$$

It is then possible to use equation (6) to ratio the off-design and design efficiencies. For additional discussion of design and off-design power plant performance calculations see Knopf, 2010.

Impact of CO_2 Sequestration on Power Plant Performance

We want to evaluate the impact of adding CO_2 sequestration to the Conesville #5 Power Plant base case power plant. Here we utilize a solid adsorbent to adsorb CO_2. Regeneration of the sequestration system, when capturing 90% of the base-case generated CO_2, will require 345,076 lbs/hr of low pressure steam. This steam flow rate is ~ 11% of the total HP steam generated in the boiler.

We evaluated steam extraction from extraction point (4) which is point α_1 on Figure 2. Steam extraction will lower the pressure in the turbine system both at the extraction point and downstream of the extraction. There will also be some lowering of pressure up-steam of the extraction point, but this will be to a much lesser extent. Plant performance with extraction is shown in Figure 2. Key results for power plant performance for the base case (full-load operation) and the off-design steam extraction case are summarized in Table 1.

Table 1 Impact of CO_2 Sequestration on Power Plant Performance

	Base Case	Case 1
Percent CO2 capture	0%	90%
Extraction Point		(4)
Steam Turbine System (F, P, T, $\hat{h}$)		
Steam flow from Boiler (lb/hr)	3,131,619	3,131,619
Steam Pressure from Boiler (psia)	2,535	2,535
Steam Temperature from Boiler (F)	1,000	1,000
Steam Enthalpy from Boiler (Btu/lb)	1,455.835	1,455.835
Water Enthalpy into Boiler (Btu/lb)	477.23	476.80
Steam Pressure to IP Turbine Section (psia)	590.85	588.21
Steam Pressure to LP Turbine Section (psia)	199.20	193.38
Steam Extraction Rate for Regeneration (lb/hr)	NA	345,076
Steam Turbine System Heat Rate		
Turbine Net Output (kW)	473,411	448,855
Generator Efficiency (%)	98.5	98.5
Generator Net Output (kW)	466,310	442,123
Turbine Net Heat Rate (Btu/kW-hr)	7,794	8,225
Boiler Efficiency (%)	88.1	88.1
Steam Plant Auxiliary Power Consumption (%)	7.0	7.0
Plant Output (kW)	433,668	411,174
Plant Net Heat Rate (Btu/kW-hr)	9,513	10,039
Steam Turbine System CO_2 Emissions		
Coal Carbon wt %	63.2	63.2
Coal LHV (Btu/lb)	10,785	10,785
Coal Required, LHV (lb/hr)	382,526	382,717
CO_2 Produced (lb CO2 / lb Coal)	2.3159	2.3159
Total CO_2 produced (lb/hr)	885,903	886,346

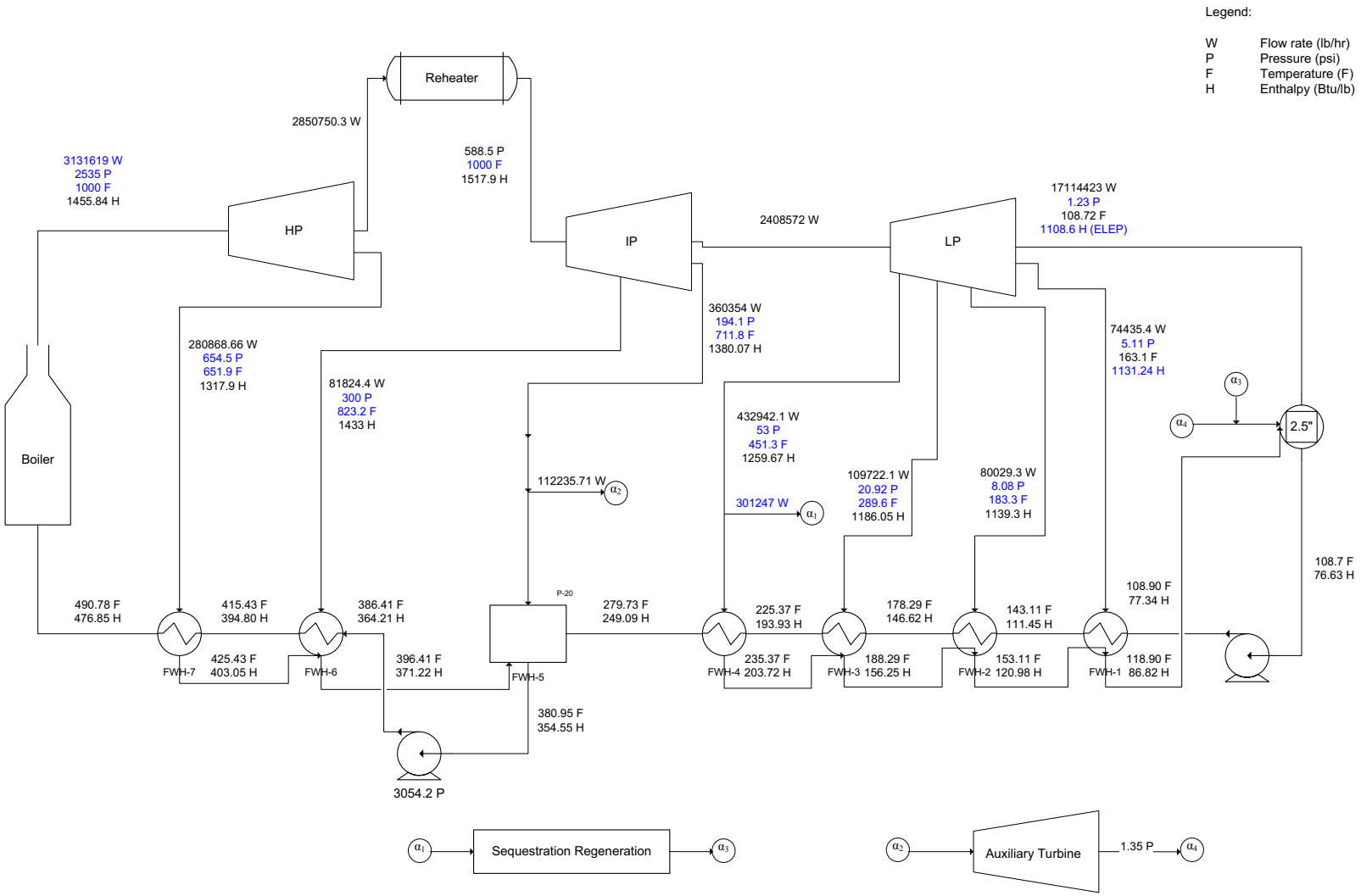

Figure 2 : Heat Balance diagram for the Off-design conditions (throttle steam flow ratio : 1.00)
Sequestration Steam Extraction: 4

Turbine Net Heat Rate: 8167 Btu/kW-hr **Turbine Net Output: 451999 kW**

Extraction steam flow is set at 345,076 lbs/hr. With extraction after the first stage of the LP turbine – the steam turbine heat rate is 8,225 Btu/kW-hr and generator output is 442,123 kW. The results from Table 1 show that the power plant will deliver 22,494 kW less electricity due to steam extraction for the sequestration regeneration process.

Impact of CO_2 Sequestration on Power Plant Economics

In order to properly determine the economics of the sequestration process we need to purchase make-up electricity (22,494 kW). In addition, the regeneration process itself has associated capital costs, operations and maintenance costs, and utility costs as summarized in Table 2. The equipment breakdown for the $72.2 MM capital investment is provided in Table 7. Capital costs were estimated using Aspen Icarus and correlations from Garrett, 1989. Operating costs in Table 5 were estimated using Aspen Icarus. These costs have been brought to a levelized energy cost basis to determine the impact of sequestration on utility pricing; a 20 year basis was assumed for all levelized cost calculations. Water / Steam lost in regeneration is estimated by TDA at 408,950 lb/hr. The dominate cost is electricity for the sequestration process estimated at 85,516 kW. The levelized make-up power cost is 2.50 ¢/kW-hr which would result in an increased utility cost of 33.6 %.

Before sequestration the power plant is delivering 433,668 kW. With sequestration, steam is extracted for the sequestration process which impacts the power plant. With steam extraction the power plant can only deliver 411,174 kW (this is a loss of 22,494 kW). Electricity at 85,515.6 kW is also required in the sequestration process itself.

Table 2 Economic Evaluation of CO_2 Sequestration

	Base Case	Case 1
Percent CO2 capture	0%	90%
Extraction Point		(4)
Steam Turbine System Heat Rate		
Turbine Net Output (kW)	473,411	448,855
Generator Efficiency (%)	98.5	98.5
Generator Net Output (kW)	466,310	442,123
Turbine Net Heat Rate (Btu/kW-hr)	7,794	8,225
Boiler Efficiency (%)	88.1	88.1
Steam Plant Auxiliary Power Consumption (%)	7.0	7.0
Plant Output (kW)	433,668	411,174
Plant Net Heat Rate (Btu/kW-hr)	9,513	10,039
Costs		
Total Capital Investment ($)		72,200,000
Capital Recovery Factor		0.175
Annualized Capital Cost ($/yr)		12,635,000
O&M (5.33 % TCI)		0.0533
Annual O&M Cost (5.33 % TCI)		3,848,260
O&M escalation 1.89%		0.0189
Equivalent discount		0.0796
O&M Levelization Factor		1.1567
Levelized O&M Cost ($/yr)		4,451,388
Steam Lost (gallons/hr)		49,094
Steam Cost ($/1000 gallons)		1.8
Lost Steam Cost ($/yr)		706,949
Sequestration Electricity (kW)		85,516
Make-Up Electricity (kW)		22,494
Electricity Cost ($/kW-hr)		0.064
Electricity Cost ($/yr)		55,301,040
Fuel escalation 1.89%		0.0198
Equivalent discount		0.0786
Fuel Levelization Factor		1.1650
Levelized NG + E Cost ($/yr)		65,247,989
Sequestration Cost Summary		
Total Levelized Annual Cost ($/yr)		82,334,327
Total Levelized Make-Up Power Cost (¢/kW-hr)		2.50
Increase In Electricity Costs (%)		33.57

Process Design for Adsorbent Capture of Carbon Dioxide from Coal-Fired Power Plants

The Aspen HYSYS process design for capturing carbon dioxide from a coal-fired power plant using the TDA adsorbent is shown in Figure 3 and the associated work book for physical properties and flow rates for material streams is given in Table 3 and in the Excel spreadsheet; *Moving Bed Adsorber and Regenerator Design with Downstream Processing rev 5-3-10.xls*. The Aspen UNIQUAC thermodynamic model was used to describe physical and transport properties. The process uses an adsorber to remove 90% of the carbon dioxide from the flue gas from a coal-fired power plant. The carbon dioxide is separated from the adsorbent by regenerating the adsorbent. This stream is sent to two serial steps of compression, heat exchange and two-phase separation to increase the pressure to 132 psia. Then, a silica gel packed bed removes the remaining water. Additional compression and cooling is used to remove the nitrogen. The purified carbon dioxide is sent to a pump to increase the pressure to 2,200 psia, which is required for sequestration.

Process Description: Referring to Figure 3, the desulfurized flue gas from the flue gas desulfurization (FGD) unit, 1-Flue Gas, was combined with the recycle flue gas stream 10-RCY-1 Out in MIX-105. Flow from this mixer was 2-Flue Gas. The 2-Flue Gas stream was split in sevenths and sent to parallel blowers (K-1 to K-7). The blowers increased the pressure from 14.7 to 15.7 psi. Then heater E-105 was used to increase the temperature of the flue gas from 132^{o}F to 356^{o}F to have it at the correct temperature to be introduced into the Adsorber/Regenerator system. The Adsorber/Regenerator system removed 90% of the carbon dioxide from the flue gas in the adsorber, and 3.65 moles-steam/mole-CO_2 were used to regenerate the adsorbent in the regenerator (Copeland, 2009a).

The carbon dioxide was removed in the regenerator in the 5 CO2+N2+H2O stream at 365^{o}F. The exit stream from the adsorber was sent to the stack as flue gas in stream 3-Flue Gas X CO2+Steam. The 5 CO2+N2+H2O stream was cooled in E-106 to 197^{o}F before introducing in the compressor system. The pressure of the 5-CO2+N2+H2O stream was increased from 15.5 psia to 44.09 psia (1 to 3 atm) using three compressors in parallel (K-100-1 – K-100-3). A single compressor was too large to process the volumetric flow rate of gas, so it was necessary to split the flow into three parallel streams, using compressor maximum inlet flow specification from Icarus.

The hot compressed gases from the compressors were combined in mixer, MIX-101 and were passed through interstage heat exchanger E-100 and cooled to 200^{o}F. The heat exchanger E-100 was designed as a counter current heat exchanger with three shells in series and six tube passes per shell. The maximum inlet temperature for the compressors required by Icarus is 200^{o}F; hence the exit stream MIX-101out from the three compressors was cooled to 200^{o}F in heat exchanger E-100. The heat transferred from MIX-101 out in E-100 was used to produce steam at 365^{o}F and 16 psi in stream E-100 steam to MIX-102, and this stream was sent to mixer MIX-102. The cooled stream, E-100 out, was a mixture of flue gas, steam and water. This mixture was flash separated in V-100. The bottom stream, V-100 water to MIX-103, contained 0.11% (wt) CO_2 in the aqueous phase at 200^{o}F and was sent to mixer MIX-103.

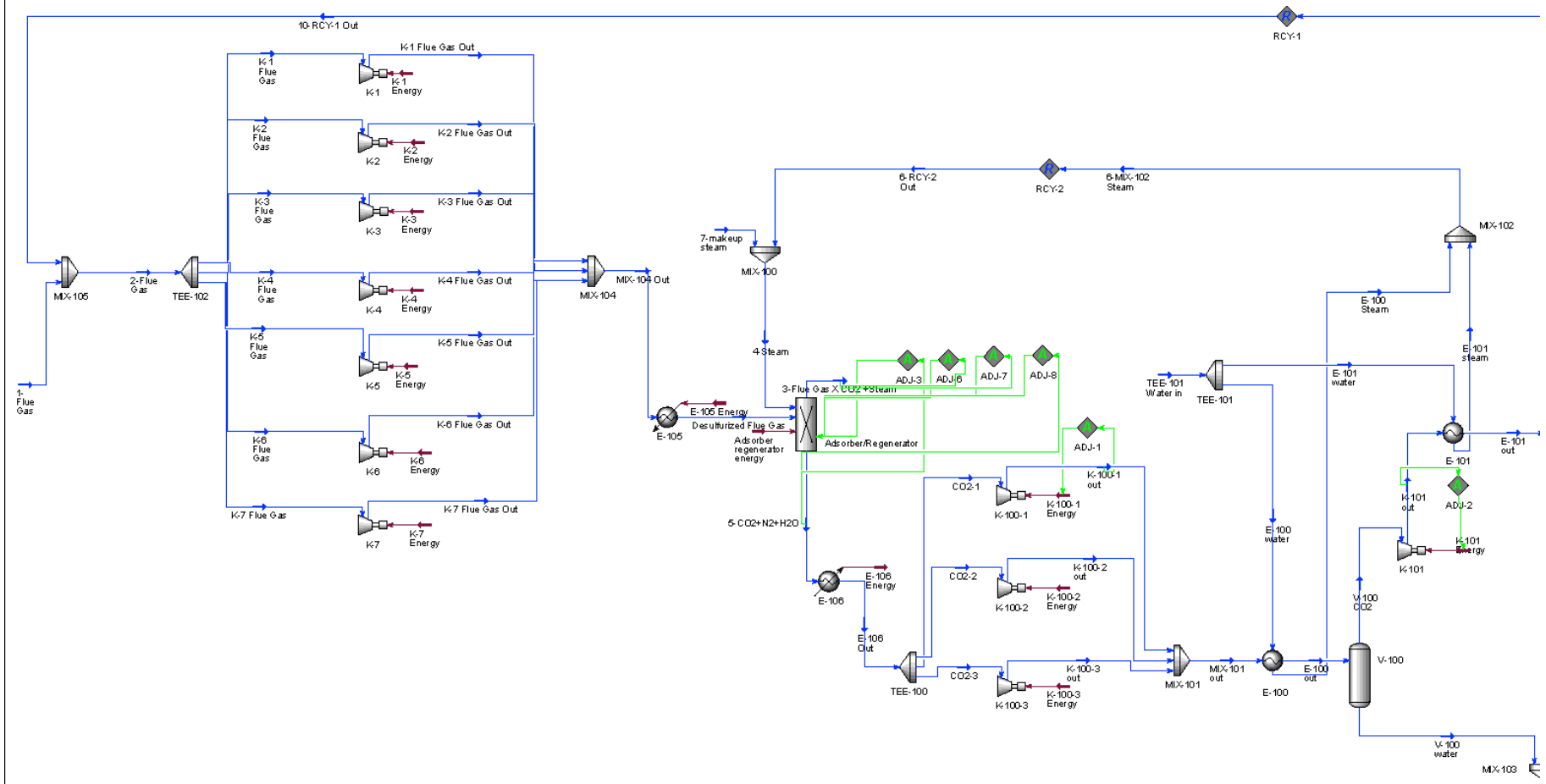

Figure 3 Aspen HYSYS Process Flow Diagram for Capturing Carbon Dioxide from a Coal-Fired Power Plant using the TDA A

Table 3 Aspen HYSYS Workbook for the Process Shown in Figure 3

aspentech

LOUISIANA STATE UNIVERSI
Calgary, Alberta
CANADA

Case Name: C:\Backup\TDA Proposal 2008\Final Report 2-7-10\TDA ADSORBER_DS
Unit Set: Field
Date/Time: Thu May 06 16:43:15 2010

Workbook: Case (Main)

Material Streams

Fluid Pkg: All

Name		1- Flue Gas	2-Flue Gas	3-Flue Gas X CO2 +St	4-Steam	5-CO2+N2+H2O
Vapour Fraction		1.0000	1.0000	1.0000	1.0000	1.0000
Temperature	(F)	116.6	115.0 *	347.0 *	365.0	365.0 *
Pressure	(psia)	14.50	14.50 *	15.20 *	16.00	15.50 *
Molar Flow	(lbmole/hr)	1.457e+005	1.471e+005 *	1.483e+005	6.708e+004 *	6.589e+004
Mass Flow	(lb/hr)	4.276e+006	4.320e+006	3.850e+006	1.208e+006	1.679e+006
Liquid Volume Flow	(barrel/day)	3.535e+005	3.572e+005	3.127e+005	8.291e+004	1.274e+005
Heat Flow	(Btu/hr)	-4.873e+009	-4.914e+009	-3.715e+009	-6.791e+009	-7.731e+009
Name		6-RCY-2 Out	7-makeup steam	8-V-101 CO2	9-P-100 CO2 liquid	10-RCY-1 Out
Vapour Fraction		1.0000	1.0000	1.0000	0.0000	1.0000
Temperature	(F)	365.0 *	365.0 *	115.0	-36.05	-46.00 *
Pressure	(psia)	16.00 *	16.00 *	132.3	2200 *	800.0 *
Molar Flow	(lbmole/hr)	4.791e+004 *	1.917e+004	1.993e+004	1.812e+004	1457 *
Mass Flow	(lb/hr)	8.630e+005	3.454e+005	8.498e+005	7.974e+005	4.478e+004
Liquid Volume Flow	(barrel/day)	5.921e+004	2.370e+004	7.047e+004	6.615e+004	3738
Heat Flow	(Btu/hr)	-4.850e+009	-1.941e+009	-3.123e+009	-3.203e+009	-4.080e+007
Name		E-102 out	E-102 cooling water in	E-102 cooling water ou		
Vapour Fraction		1.0000	0.0000	0.0000		
Temperature	(F)	125.0 *	86.00 *	106.0 *		
Pressure	(psia)	800.0	30.00 *	25.00		
Molar Flow	(lbmole/hr)	1.958e+004	2.420e+005	2.420e+005		
Mass Flow	(lb/hr)	8.422e+005	4.360e+006	4.360e+006		
Liquid Volume Flow	(barrel/day)	6.989e+004	2.991e+005	2.991e+005		
Heat Flow	(Btu/hr)	-3.098e+009	-2.960e+010	-2.951e+010		

Molar Flow Rate

Fluid Pkg: All

Name	1- Flue Gas	2-Flue Gas	3-Flue Gas X CO2 +St	4-Steam	5-CO2+N2+H2O
Master Comp Molar Flow (Oxygen) (lbmole/hr)	4571.1845	4627.0000 *	4571.1000	0.0000 *	55.9000
Master Comp Molar Flow (Nitrogen) (lbmole/hr)	106409.6837	107578.0000 *	106278.8000	0.0000 *	1299.2000
Master Comp Molar Flow (H2O) (lbmole/hr)	14524.9962	14525.0000 *	35454.0000	67077.0000 *	46148.0000
Master Comp Molar Flow (CO2) (lbmole/hr)	20150.6938	20384.0000 *	1993.0000	0.0000 *	18391.0000
Master Comp Molar Flow (SO2) (lbmole/hr)	0.3100	0.3100 *	0.3100	0.0000 *	0.0000
Master Comp Molar Flow (Argon) (lbmole/hr)	0.0000	0.0000 *	0.0000	0.0000 *	0.0000
Name	6-RCY-2 Out	7-makeup steam	8-V-101 CO2	9-P-100 CO2 liquid	10-RCY-1 Out
Master Comp Molar Flow (Oxygen) (lbmole/hr)	0.0000 *	0.0000	55.8155	0.0000	55.8155 *
Master Comp Molar Flow (Nitrogen) (lbmole/hr)	0.0000 *	0.0000	1298.1282	0.0000	1168.3163 *
Master Comp Molar Flow (H2O) (lbmole/hr)	47906.1049 *	19170.8951	221.9180	0.0036	0.0038 *
Master Comp Molar Flow (CO2) (lbmole/hr)	0.0000 *	0.0000	18351.3607	18118.0545	233.3062 *
Master Comp Molar Flow (SO2) (lbmole/hr)	0.0000 *	0.0000	0.0000	0.0000	0.0000 *
Master Comp Molar Flow (Argon) (lbmole/hr)	0.0000 *	0.0000	0.0000	0.0000	0.0000 *
Name	E-102 out	E-102 cooling water in	E-102 cooling water ou		
Master Comp Molar Flow (Oxygen) (lbmole/hr)	55.8155	0.0000 *	0.0000		
Master Comp Molar Flow (Nitrogen) (lbmole/hr)	1168.3163	0.0000 *	0.0000		
Master Comp Molar Flow (H2O) (lbmole/hr)	0.0074	242000.0336 *	242000.0336		
Master Comp Molar Flow (CO2) (lbmole/hr)	18351.3607	0.0000 *	0.0000		
Master Comp Molar Flow (SO2) (lbmole/hr)	0.0000	0.0000 *	0.0000		
Master Comp Molar Flow (Argon) (lbmole/hr)	0.0000	0.0000 *	0.0000		

* Specified by user.

Table 3 continued Aspen HYSYS Workbook for the Process Shown in Figure 3

aspentech

LOUISIANA STATE UNIVERSI
Calgary, Alberta
CANADA

Case Name:	C:\Backup\TDA Proposal 2008\Final Report 2-7-10\TDA ADSORBER_DS
Unit Set:	Field
Date/Time:	Thu May 06 16:43:15 2010

Workbook: Case (Main) (continued)

Mass Flow Rate

Fluid Pkg: All

Name	1- Flue Gas	2-Flue Gas	3-Flue Gas X CO2 +St	4-Steam	5-CO2+N2+H2O
Master Comp Mass Flow (Oxygen) (lb/hr)	146277.9048	148064.0000 *	146275.2000	0.0000 *	1788.8000
Master Comp Mass Flow (Nitrogen) (lb/hr)	2.980854522e+06	3.013582567e+06 *	2.977188076e+06	0.0000 *	36394.4902
Master Comp Mass Flow (H2O) (lb/hr)	261669.2656	261669.3345 *	638707.3724	1.208398895e+06 *	831360.8569
Master Comp Mass Flow (CO2) (lb/hr)	886826.0045	897093.7406 *	87711.3336	0.0000 *	809382.4070
Master Comp Mass Flow (SO2) (lb/hr)	19.8595	19.8595 *	19.8595	0.0000 *	0.0000
Master Comp Mass Flow (Refrig-290) (lb/hr)	0.0000	0.0000 *	0.0000	0.0000 *	0.0000

Name	6-RCY-2 Out	7-makeup steam	8-V-101 CO2	9-P-100 CO2 liquid	10-RCY-1 Out
Master Comp Mass Flow (Oxygen) (lb/hr)	0.0000 *	0.0000	1786.0952	0.0000	1786.0952 *
Master Comp Mass Flow (Nitrogen) (lb/hr)	0.0000 *	0.0000	36364.4937	0.0001	32728.0443 *
Master Comp Mass Flow (H2O) (lb/hr)	863033.2935 *	345365.6014	3997.8755	0.0645	0.0688 *
Master Comp Mass Flow (CO2) (lb/hr)	0.0000 *	0.0000	807637.8934	797370.1574	10267.7361 *
Master Comp Mass Flow (SO2) (lb/hr)	0.0000 *	0.0000	0.0000	0.0000	0.0000 *
Master Comp Mass Flow (Refrig-290) (lb/hr)	0.0000 *	0.0000	0.0000	0.0000	0.0000 *

Name	E-102 out	E-102 cooling water in	E-102 cooling water ou		
Master Comp Mass Flow (Oxygen) (lb/hr)	1786.0952	0.0000 *	0.0000		
Master Comp Mass Flow (Nitrogen) (lb/hr)	32728.0444	0.0000 *	0.0000		
Master Comp Mass Flow (H2O) (lb/hr)	0.1333	4.359654921e+06 *	4.359654921e+06		
Master Comp Mass Flow (CO2) (lb/hr)	807637.8934	0.0000 *	0.0000		
Master Comp Mass Flow (SO2) (lb/hr)	0.0000	0.0000 *	0.0000		
Master Comp Mass Flow (Refrig-290) (lb/hr)	0.0000	0.0000 *	0.0000		

Compositions

Fluid Pkg: All

Name	1- Flue Gas	2-Flue Gas	3-Flue Gas X CO2 +St	4-Steam	5-CO2+N2+H2O
Comp Mole Frac (Oxygen)	0.0314	0.0315 *	0.0308	0.0000 *	0.0008
Comp Mole Frac (Nitrogen)	0.7306	0.7313 *	0.7167	0.0000 *	0.0197
Comp Mole Frac (H2O)	0.0997	0.0987 *	0.2391	1.0000 *	0.7003
Comp Mole Frac (CO2)	0.1383	0.1386 *	0.0134	0.0000 *	0.2791
Comp Mole Frac (SO2)	0.0000	0.0000 *	0.0000	0.0000 *	0.0000
Comp Mole Frac (Refrig-290)	0.0000	0.0000 *	0.0000	0.0000 *	0.0000

Name	6-RCY-2 Out	7-makeup steam	8-V-101 CO2	9-P-100 CO2 liquid	10-RCY-1 Out
Comp Mole Frac (Oxygen)	0.0000 *	0.0000	0.0028	0.0000	0.0383 *
Comp Mole Frac (Nitrogen)	0.0000 *	0.0000	0.0651	0.0000	0.8016 *
Comp Mole Frac (H2O)	1.0000 *	1.0000	0.0111	0.0000	0.0000 *
Comp Mole Frac (CO2)	0.0000 *	0.0000	0.9209	1.0000	0.1601 *
Comp Mole Frac (SO2)	0.0000 *	0.0000	0.0000	0.0000	0.0000 *
Comp Mole Frac (Refrig-290)	0.0000 *	0.0000	0.0000	0.0000	0.0000 *

Name	E-102 out	E-102 cooling water in	E-102 cooling water ou		
Comp Mole Frac (Oxygen)	0.0029	0.0000 *	0.0000		
Comp Mole Frac (Nitrogen)	0.0597	0.0000 *	0.0000		
Comp Mole Frac (H2O)	0.0000	1.0000 *	1.0000		
Comp Mole Frac (CO2)	0.9375	0.0000 *	0.0000		
Comp Mole Frac (SO2)	0.0000	0.0000 *	0.0000		
Comp Mole Frac (Refrig-290)	0.0000	0.0000 *	0.0000		

Energy Streams

Fluid Pkg: All

Name	P-100 heat	K-100-1 Energy	K-101 Energy	X-101 energy	K-103 Energy
Heat Flow (Btu/hr)	3.867e+006	4.468e+007 *	5.778e+007 *	1.009e+007	7.425e+007 *
Power (hp)	1520	1.756e+004 *	2.271e+004 *	3964	2.918e+004 *

Name	K-100-2 Energy	K-100-3 Energy	E-105 Energy	K-1 Energy	K-2 Energy
Heat Flow (Btu/hr)	4.468e+007	4.603e+007	2.497e+008	2.581e+006	2.581e+006
Power (hp)	1.756e+004	1.809e+004	9.813e+004	1015	1015

* Specified by user.

Table 3 continued Aspen HYSYS Workbook for the Process Shown in Figure 3

aspentech

LOUISIANA STATE UNIVERSI
Calgary, Alberta
CANADA

Case Name:	C:\Backup\TDA Proposal 2008\Final Report 2-7-10\TDA ADSORBER_DS
Unit Set:	Field
Date/Time:	Thu May 06 16:43:15 2010

Workbook: Case (Main) (continued)

Energy Streams (continued)

Fluid Pkg: All

Name		K-3 Energy	K-4 Energy	K-5 Energy	K-6 Energy	E-106 Energy
Heat Flow	(Btu/hr)	2.581e+006	2.581e+006	2.581e+006	2.581e+006	9.835e+007
Power	(hp)	1015	1015	1015	1015	3.865e+004
Name		K-7 Energy	Adsorber regenerator	E-104 energy		
Heat Flow	(Btu/hr)	2.563e+006	-8.717e+006	1.496e+008		
Power	(hp)	1007	-3426	5.879e+004		

Unit Ops

Operation Name	Operation Type	Feeds	Products	Ignored	Calc Level
X-100	Component Splitter		Flue Gas X Steam	Yes	500.0 *
			Steam Excess		
Adsorber/Regenerator	Component Splitter	Desulfurized Flue Gas	3-Flue Gas X CO2 +Steam	No	500.0 *
		4-Steam	5-CO2+N2+H2O		
		Adsorber regenerator energy			
X-101 - silica gel dehydration	Component Splitter	8-V-101 CO2	X-101 overhead	No	500.0 *
		X-101 energy	X-101 bottom		
K-100-1	Compressor	CO2-1	K-100-1 out	No	500.0 *
		K-100-1 Energy			
K-101	Compressor	V-100 CO2	K-101 out	No	500.0 *
		K-101 Energy			
K-103	Compressor	X-101 overhead	K-103 Out	No	500.0 *
		K-103 Energy			
K-100-2	Compressor	CO2-2	K-100-2 out	No	500.0 *
		K-100-2 Energy			
K-100-3	Compressor	CO2-3	K-100-3 out	No	500.0 *
		K-100-3 Energy			
K-1	Compressor	K-1 Flue Gas	K-1 Flue Gas Out	No	500.0 *
		K-1 Energy			
K-2	Compressor	K-2 Flue Gas	K-2 Flue Gas Out	No	500.0 *
		K-2 Energy			
K-3	Compressor	K-3 Flue Gas	K-3 Flue Gas Out	No	500.0 *
		K-3 Energy			
K-4	Compressor	K-4 Flue Gas	K-4 Flue Gas Out	No	500.0 *
		K-4 Energy			
K-5	Compressor	K-5 Flue Gas	K-5 Flue Gas Out	No	500.0 *
		K-5 Energy			
K-6	Compressor	K-6 Flue Gas	K-6 Flue Gas Out	No	500.0 *
		K-6 Energy			
K-7	Compressor	K-7 Flue Gas	K-7 Flue Gas Out	No	500.0 *
		K-7 Energy			
P-100	Pump	V-103 CO2 liquid	9-P-100 CO2 liquid	No	500.0 *
		P-100 heat			
ADJ-3	Adjust			No	3500 *
ADJ-5	Adjust			No	3500 *
ADJ-4	Adjust			No	3500 *
ADJ-6	Adjust			No	3500 *
ADJ-1	Adjust			No	3500 *
ADJ-2	Adjust			No	3500 *
ADJ-7	Adjust			No	3500 *
ADJ-8	Adjust			No	3500 *
E-100	Heat Exchanger	MIX-101 out	E-100 out	No	500.0 *
		E-100 water	E-100 Steam		

* Specified by user.

Table 3 continued Aspen HYSYS Workbook for the Process Shown in Figure 3

aspentech

LOUISIANA STATE UNIVERSI
Calgary, Alberta
CANADA

Case Name:	C:\Backup\TDA Proposal 2008\Final Report 2-7-10\TDA ADSORBER_DS
Unit Set:	Field
Date/Time:	Thu May 06 16:43:15 2010

Workbook: Case (Main) (continued)

Unit Ops (continued)

Operation Name	Operation Type	Feeds	Products	Ignored	Calc Level
E-101	Heat Exchanger	K-101 out	E-101 out	No	500.0 *
		E-101 water	E-101 steam		
E-103	Heat Exchanger	E-102 out	E-103 out	No	500.0 *
		E-103 refrigerant in	E-103 refrigerant out		
E-102	Heat Exchanger	K-103 Out	E-102 out	No	500.0 *
		E-102 cooling water in	E-102 cooling water out		
V-100	Separator	E-100 out	V-100 water	No	500.0 *
			V-100 CO2		
V-101	Separator	E-101 out	V-101 water	No	500.0 *
			8-V-101 CO2		
V-103	Separator	E-103 out	V-103 CO2 liquid	No	500.0 *
			V-103 N2		
MIX-102	Mixer	E-101 steam	6-MIX-102 Steam	No	500.0 *
		E-100 Steam			
MIX-103	Mixer	V-100 water	MIX-103 Water	No	500.0 *
		V-101 water			
MIX-101	Mixer	K-100-1 out	MIX-101 out	No	500.0 *
		K-100-2 out			
		K-100-3 out			
MIX-100	Mixer	6-RCY-2 Out	4-Steam	No	500.0 *
		7-makeup steam			
MIX-104	Mixer	K-1 Flue Gas Out	MIX-104 Out	No	500.0 *
		K-2 Flue Gas Out			
		K-3 Flue Gas Out			
		K-4 Flue Gas Out			
		K-5 Flue Gas Out			
		K-6 Flue Gas Out			
		K-7 Flue Gas Out			
MIX-105	Mixer	1- Flue Gas	2-Flue Gas	No	500.0 *
		10-RCY-1 Out			
TEE-100	Tee	E-106 Out	CO2-1	No	500.0 *
			CO2-2		
			CO2-3		
TEE-101	Tee	TEE-101 Water in	E-100 water	No	500.0 *
			E-101 water		
TEE-102	Tee	2-Flue Gas	K-1 Flue Gas	No	500.0 *
			K-2 Flue Gas		
			K-3 Flue Gas		
			K-4 Flue Gas		
			K-5 Flue Gas		
			K-6 Flue Gas		
			K-7 Flue Gas		
E-106	Cooler	5-CO2+N2+H2O	E-106 Out	No	500.0 *
			E-106 Energy		
E-104	Cooler	E-103 refrigerant out	E-103 refrigerant in	No	500.0 *
			E-104 energy		
E-105	Heater	MIX-104 Out	Desulfurized Flue Gas	No	500.0 *
		E-105 Energy			
RCY-1	Recycle	V-103 N2	10-RCY-1 Out	No	3500 *
RCY-2	Recycle	6-MIX-102 Steam	6-RCY-2 Out	No	3500 *

* Specified by user.

The top stream, V-100 CO2 from separator V-100, contained 83.1% (wt) CO_2 and was sent to second stage compressor K-101. A pressure increase from 44.09 psi to 132.3 psi (3 to 9 atm) was obtained in the second stage compressor. The exit stream, K-101 out, was cooled to 115^{o}F in heat exchanger E-101. Heat exchanger E-101 consisted of one shell and one tube pass per shell. The heat gained was used to produce steam in stream, E-101 steam to MIX-102, and this stream was sent to mixer M-102, being combined with stream, E-100 steam. The cooled stream E-101out was flash separated in V-101. The bottom stream, V-101 water, contained 0.76% (wt) CO_2 in aqueous phase and was sent to mixer MIX-103 being combined with stream V-100 water.

The top stream, 8-V-101 CO_2 from separator V-101, contained 95.0% (wt) CO_2 and 0.47% (wt) water, and it was sent to the silica gel dehydration unit. Water was removed from 8-V-101CO2 to pipeline quality specifications of less than 0.0002 % (mol) (Ramezan, 2007a) using a silica gel dehydration unit, X-101 silica gel dehydration. The design was based on the CO_2 Dryer described by Ramezan, M., et al., 2007a which used vacuum regeneration. The composition of the dried gas stream, X-101overhead, was 95.90% (wt) CO_2, 3.89% (wt) nitrogen and 0.21% (wt) oxygen. Stream X-101bottom, the water removed by the silica gel dehydration unit, X-101, had a composition of 52.4% (wt) water, 47.6% (wt) nitrogen**.**

Stream X-101 overhead from the silica gel dehydration unit was compressed in K-103 from 132.3 psi to 800 psi pressure. Stream K-103 out from the compressor was 574.3^{o}F, and it was sent to a heat exchanger, E-102, to cool the gas to 125^{o}F. In heat exchanger E-103 the gas was cooled and partially liquefied (liquid fraction 0.926) to -46^{o}F in stream E-103 out. The propane refrigerant E-103 refrigerant out was sent to heat exchanger E-104 to cool the propane from -43.46^{0}F to -50^{0}F, following the design described by Ramezan, 2007a.

Stream E-103 out was sent to flash drum V-103 where CO_2 and N_2 were separated. Stream V-103N2 was 73.08% (wt) N_2, 3.99% (wt) O_2 and 22.93% (wt) CO_2. It was recycled to the adsorber/regenerator system as 10-RCY-1 Out and was mixed with 1-Flue Gas stream in MIX-105. Stream V-103CO2 liquid was pipeline quality CO_2 at -46^{o}F and 800psia.

Pump P-100 was used to increase the pressure of Stream V-103 CO2 liquid to 2,200 psia. Stream 9-P-100 CO2 liquid was pipeline quality CO_2 .

Steam obtained from heat exchangers E-100 and E-101 were combined in mixer MIX-102, and the total mass flow rate was 863,033 lb/hr. The total amount of steam required by the process was 1,208,398 lb/hr and make-up steam required was 345,365 lb/hr.

Water obtained from separators V-100 and V-101 were combined in MIX-103, and the total was 829,140 lb/hr at a temperature of 187.3^{o}F and 44.09 psia. The concentrations were 99.79% (wt) water 0.21% (wt) CO_2. This water was not used as cooling water for heat exchangers E-100 and E-101 since it contained dissolved carbon dioxide, and the outlet temperature from these heat exchangers was 200^{0}F.

The following table summarizes the net removal of CO_2 from the flue gas. It accounts for the CO_2 lost in the water from the separators. The mandated removal is 90%.

CO_2 in Flue Gas entering Adsorber	896,896 lb/hr
CO_2 removed by the Adsorber	809,204
CO_2 lost in water from separators	833
Net CO_2 removed	809,204 – 833 = 808,371
Percent CO_2 removal	808,371/896,896*100 = 90.1%

Make-up steam at the rate of 345,076 lb/hr is required for the process in stream 7-Makeup Steam. There is 829,140 lb/hr of water containing 0.21% (wt) CO_2 and from the separators. An outside energy source could be used to make steam from this stream to replace the make-up steam from the power plant.

Adsorber/Regenerator Design: The Moving Bed Adsorber/Regenerator configuration was provided by TDA Research and is shown in Figure 5 (Srinivas, et al, 2009). Reactor 1 is the Adsorber with dimensions of 21 ft. tall by 37 ft in diameter, with a pressure drop of 0.5 psi. Reactor 2 is the Regenerator with dimensions of 20 ft. tall by 35 ft in diameter, with a pressure drop of 0.3 psi (Copeland, 2009). The flue gas to the Adsorber was the same as the mass flow rate and composition specified to match the conditions for the AEP Conesville Unit #5 with the modified Flue Gas Desulfurization Unit, Table 3-18, p.33 (Ramezan, 2007a, Elliott, 2009) and is given below in Table 4. Carbon dioxide capture was to be 10% and 9.1% was used in this design. The steam required to regenerate the adsorbent was specified by TDA Research to be 1,207,386 lb/hr or a 3.65 mole ratio of steam to CO_2 (Elliott, 2009).

The adsorber, regenerator, and the packing for the two vessels were separately designed in ICARUS. The dimensions of the adsorber and regenerator specified by TDA Research were used to size the vessels in Icarus. The packing in the vessels was selected as silica gel, a placeholder for the actual adsorbent. The mass balance for inlet and outlet streams in the adsorber/regenerator system is shown in Figure 4.

Details of the computations and HYSYS results are given in Aspen HYSYS Workbook, Table 3 and the related Excel spreadsheet; *Moving Bed Adsorber and Regenerator Design with Downstream Processing rev 5-10-10.xls*.

Table 4 Flue Gas from AEP Conesville Unit #5 with the Modified Flue Gas Desulfurization from Table 3-18, p.33, (Ramezan, 2007a and Elliott, 2009)

Component	Molar Flow Rate lb-mol/hr	Mass Flow Rate lb/hr
O_2	4,627	148,064
N_2	107,578	3,012,184
H_2O	14,525	261,450
CO_2	20,384	896,896
SO_2	0.31	20
Total	147,114	4,318,614

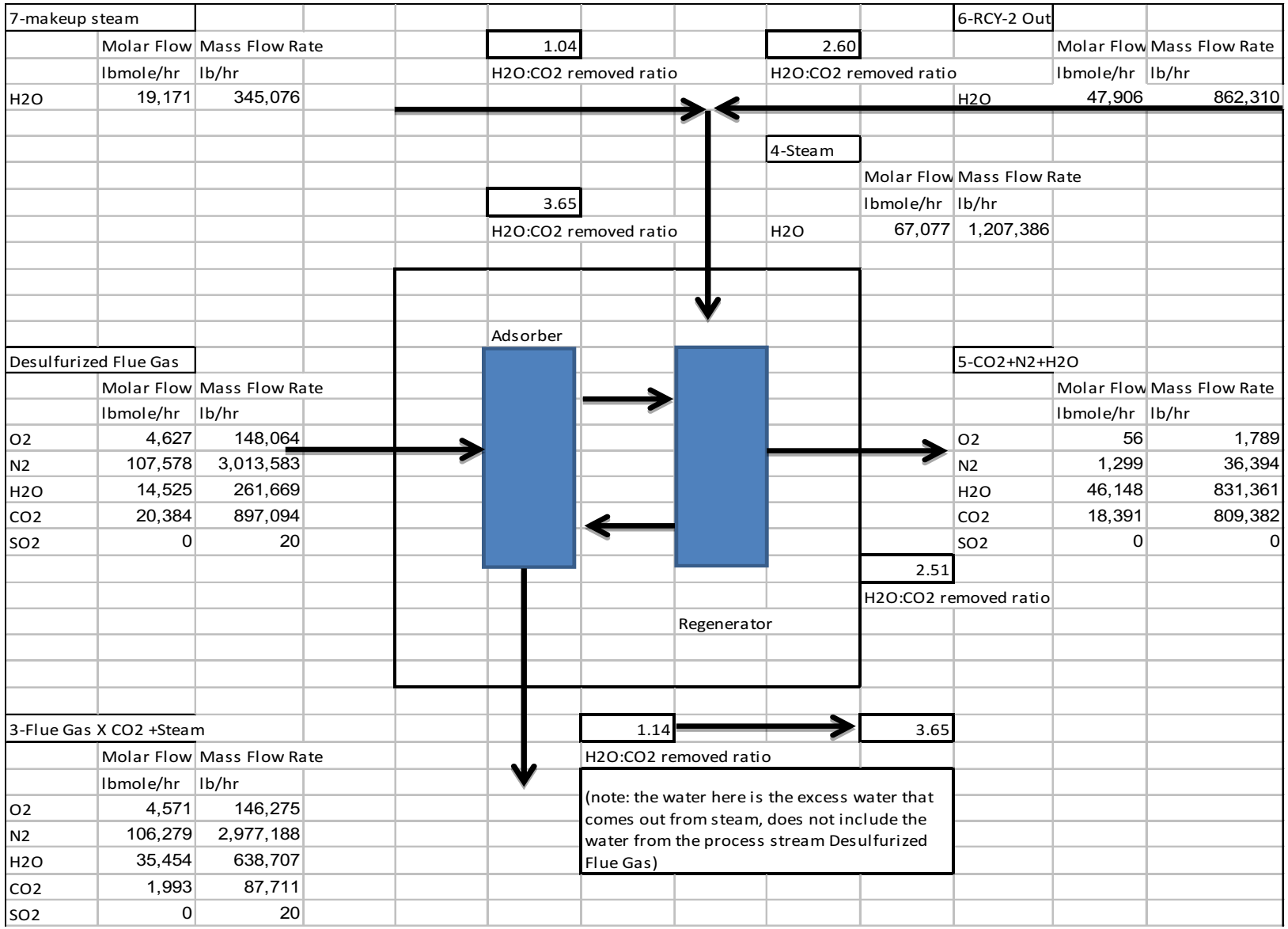

Figure 4. Mass Balance for Inlet and Outlet Streams in the Adsorber/Regenerator System

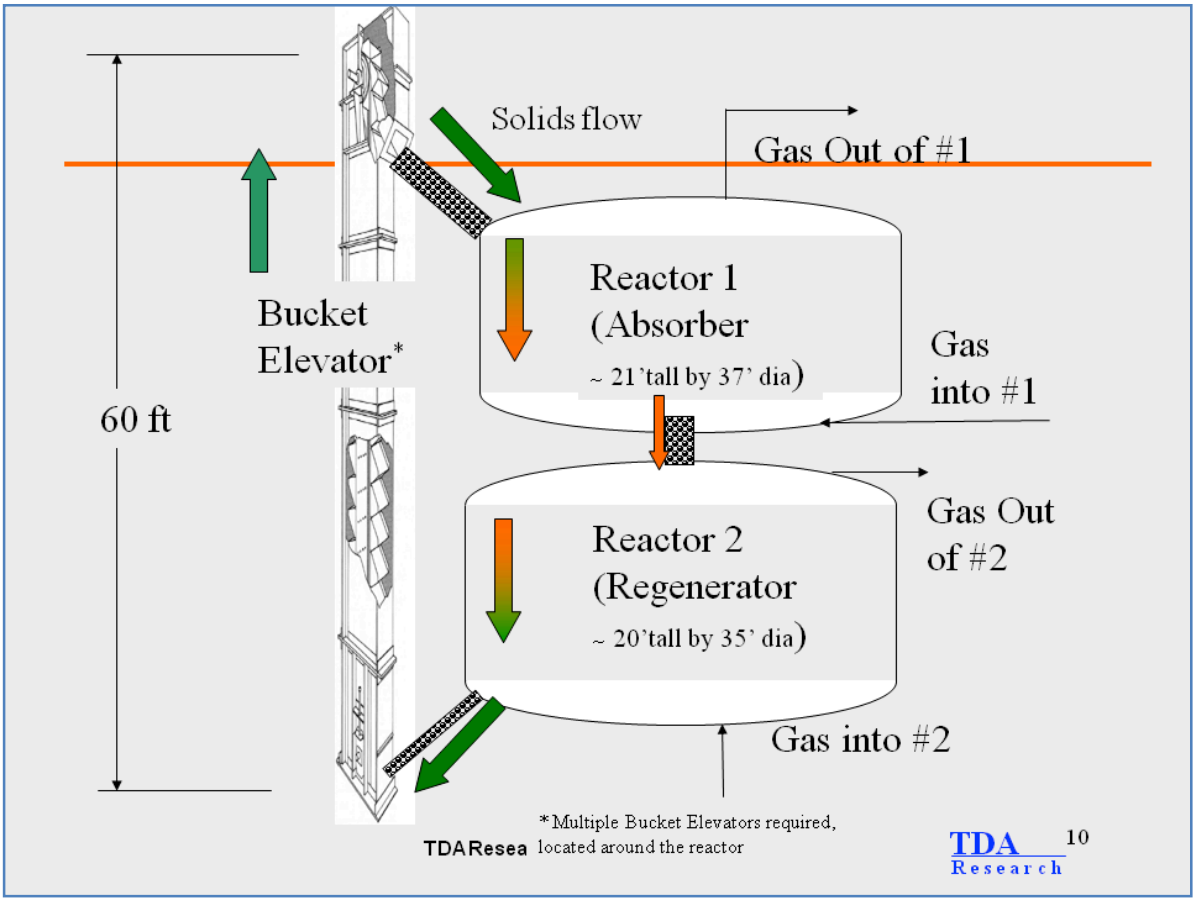

Figure 5. TDA Research Adsorber/Regenerator Configuration (Srinivas, et al, 2009)

The power required to pump the gas streams through the adsorber and regenerator is the product of the mass flow rate and the shaft work, W_s, from the Mechanical Energy Balance. Mechanical Energy Balance (MEB) is given below.

$$\frac{v_2^2 - v_1^2}{2g_c} + \frac{g}{g_c}(z_2 - z_1) + \frac{P_2 - P_1}{\rho} + W_s + \sum_{\substack{pipe \\ sections}} 4f\frac{L}{D}\frac{v^2}{2g_c} + \sum_{\substack{valves\& \\ fittings}} K\frac{v^2}{2g_c} + \sum_{\substack{entrance \\ \&exit\ loss}} K\frac{v^2}{2g_c} = 0 \qquad (8)$$

Simplifying the MEB, the following equation was obtained to compute the power required to pump the gas streams through the adsorber and the regenerator.

$$Power = massflowrate * \frac{(P_2 - P_1)}{\rho} \qquad (9)$$

For the adsorber the mass flow rate was 4,318,614 lb/hr, the density of the flue gas was 0.056 lb_m/ft^3 and the pressure drop ($P_2 - P_1$) was 0.5 psi. For the regenerator the mass flow rate was 1,678,034 lb/hr, the density of the flue gas was 0.0515 lb_m/ft^3 and the pressure drop ($P_2 - P_1$) was 0.3 psi.

The results are:

Adsorber	2,804 hp
Regenerator	711 hp

Computation details are in the Excel spreadsheet; *Moving Bed Adsorber and Regenerator Design with Downstream Processing rev 1-28-10.xls*.

Capital and Operating Costs for Adsorbent Capture of Carbon Dioxide from Coal-Fired Power Plants

The Aspen Icarus Economic Evaluation program was used to estimate the capital and operating costs. The following table was taken from the Executive Summary of the Icarus program.

Table 5 Icarus Summary for Adsorption Carbon Capture Process (Time period = 8000 hours)

Total Project Capital Cost (USD)	7.22E+07
Total Operating Cost (USD/period)	4.21E+07
Total Raw Materials Cost (USD/period)	0
Total Utilities Cost (USD/period)	3.51E+07

The following tables provide more details for these costs.

In Table 6, the power requirements for the process are listed. For the compressors and fans, the power was computed by Aspen Icarus. The power requirement for heat exchangers, pump and the silica gel dehydration unit was computed by Aspen HYSYS. The power requirements for the adsorber/regenerator unit were computed as described above. The power required for the adsorber/regenerator is comparable in magnitude to the fans and an order of magnitude less than the compressors.

In Table 7, Equipment costs, total direct (installed) costs and the total project capital cost are given for the process. The compressors and heat exchangers dominate the costs for the process. The cost for the adsorber/regenerator was for the vessel and the adsorbent with a conservative estimate for adsorbent cost given by ICARUS, a placeholder for the actual cost when it is available.

The cost for the silica gel dehydration unit, X-101, was estimated in ICARUS. The liquid entrainment method in ICARUS was used to compute the vessel size for X-101. Silica gel was used as packing material in the vessel X-101. The cost for silica gel was computed in ICARUS. The total cost for the dehydration equipment was comparable to costs reported by Aden, et al., 2002. No costs were assigned to mixers and tees as is the procedure for this level of design. Equipment costs for a capital approval design would include the costs of piping, valves, control systems, etc.

In Table 8, utility costs are given for the process. The compressors dominate the electrical requirements for the process. No potable water, natural gas or instrument air were specified for this design.

Table 6 Aspen HYSYS Summary of the Energy Requirements for Adsorption Carbon Capture Process

Component Name	Component Type	Energy Stream	Power (hp)
Compressors			
K-100-1	DGC CENTRIF	K-100-1 Energy	1.76E+04
K-100-2	DGC CENTRIF	K-100-2 Energy	1.76E+04
K-100-3	DGC CENTRIF	K-100-3 Energy	1.81E+04
K-101	DGC CENTRIF	K-101 Energy	2.27E+04
K-103	DGC CENTRIF	K-103 Energy	2.92E+04
Fans			
K-1	EFN CENTRIF	K-1 Energy	1.02E+03
K-2	EFN CENTRIF	K-2 Energy	1.02E+03
K-3	EFN CENTRIF	K-3 Energy	1.02E+03
K-4	EFN CENTRIF	K-4 Energy	1.02E+03
K-5	EFN CENTRIF	K-5 Energy	1.02E+03
K-6	EFN CENTRIF	K-6 Energy	1.02E+03
K-7	EFN CENTRIF	K-7 Energy	1.01E+03
High Pressure Pump			
P-100	DCP CENTRIF	P-100 heat	1.52E+03
Heat Exchangers			
E-104	DHE FLOAT HEAD	E-104 Energy	5.88E+04
E-105	DHE FLOAT HEAD	E-105 Energy	9.81E+04
E-106	DHE FLOAT HEAD	E-106 Energy	3.87E+04
X-101 - silica gel dehydration		X-101 energy	3.96E+03
Adsorber			2.804E+03
Regenerator			7.11E+02

Table 7 Total Direct (Installed) and Equipment Cost Estimation for Adsorption Carbon Capture Process based on Icarus Evaluation and Others

Component Name	**Component Type**	**Total Direct Cost**	**Equipment Cost**
		(USD)	**(USD)**
E-100	DHE FLOAT HEAD	2.47E+06	1.36E+06
E-101	DHE FLOAT HEAD	5.42E+05	3.24E+05
E-102	DHE FLOAT HEAD	3.59E+05	1.87E+05
E-103	DHE FLOAT HEAD	1.39E+06	9.31E+05
E-104	DHE FLOAT HEAD	6.79E+05	2.26E+05
E-105	DHE FLOAT HEAD	4.63E+06	2.65E+06
E-106	DHE FLOAT HEAD	1.50E+05	5.12E+04
K-100-1	DGC CENTRIF	8.21E+06	7.37E+06
K-100-2	DGC CENTRIF	8.21E+06	7.37E+06
K-100-3	DGC CENTRIF	8.24E+06	7.41E+06
K-101	DGC CENTRIF	7.24E+06	6.55E+06
K-103	DGC CENTRIF	5.11E+06	4.59E+06
MIX-100	C	0	0
MIX-101	C	0	0
MIX-102	C	0	0
MIX-103	C	0	0
MIX-104	C	0	0
MIX-105	C	0	0
P-100	DCP CENTRIF	4.35E+05	2.62E+05
TEE-100	C	0	0
TEE-101	C	0	0
TEE-102	C	0	0
V-100	DHT HORIZ DRUM	1.61E+05	3.55E+04
V-101	DHT HORIZ DRUM	7.84E+04	2.02E+04
V-103	DHT HORIZ DRUM	2.68E+05	1.25E+05
K-1	EFN CENTRIF	2.43E+05	1.34E+05
K-2	EFN CENTRIF	2.43E+05	1.34E+05
K-3	EFN CENTRIF	2.43E+05	1.34E+05
K-4	EFN CENTRIF	2.43E+05	1.34E+05
K-5	EFN CENTRIF	2.43E+05	1.34E+05
K-6	EFN CENTRIF	2.43E+05	1.34E+05
K-7	EFN CENTRIF	2.42E+05	1.34E+05
Adsorber Vessel	DVT CYLINDER	8.94E+05	3.95E+05
Regenerator Vessel	DVT CYLINDER	8.28E+05	3.52E+05
Adsorber Packing	EPAKPACKING	2.74E+06	2.63E+06
Regenerator Packing	EPAKPACKING	2.34E+06	2.24E+06

Component Name	**Component Type**	**Total Direct Cost**	**Equipment Cost**
		(USD)	**(USD)**
X-101 - silica gel dehydration	DVT CYLINDER	2.17E+05	7.75E+04
X-101-Silica Gel Packing	EPAKPACKING	1.95E+05	1.85E+05
Total Equipment Cost		5.71E+07	4.63E+07
Total Project Capital Cost		7.22E+07	

Table 8 Icarus Summary of Utility Cost Estimation for Adsorption Carbon Capture Process

UTILITIES COSTS		
		Units
Electricity		
Rate	85515.6	KW
Unit Cost	0.0354	Cost/KWH
Total Electricity Cost	2.42E+07	Cost/period
Potable Water		
Rate		
Unit Cost	0	Cost/MMGAL
Total Potable Water Cost	0	Cost/period
Fuel		
Rate		
Unit Cost	2.56	Cost/MMBTU
Total Fuel Cost	0	Cost/period
Instrument Air		
Rate		
Unit Cost	0	Cost/KCF
Total Instrument Air Cost	0	Cost/period
Subtotal Cost	**2.42E+07**	**Cost/period**
Process Utilities		
Steam @165PSI		
Rate	290.828	KLB/H
Unit Cost	4.46	Cost/KLB
Cooling Water		
Rate	1.11	MMGAL/H
Unit Cost	55	Cost/ MMGAL
Subtotal Cost	**1.09E+07**	**Cost/period**
Total Utilities Cost	**3.51E+07**	**Cost/period**

References

Aden, A., M. Ruth, K. Isben, J. Jechura, K. Neeves, J. Sheehan, B. Wallace, L. Montague, A. Slayton and J. Lukas, 2002, *Lignocellulose Biomass to Ethanol Process Design Utilizing Co-Current Dilute Acid Prehydrolysis and Enzymatic Hydrolysis for Corn Stover*, NREL/TP-510-32438, National Renewable Energy Laboratory, Golden, CO (June, 2002)

Basmadjian, D., 1997, *The Little Adsorption Book, A Practical Guide for Engineers and Scientists*, CRC Press, Boca Raton FL

Ciferno, J. P., T. E. Fout, A. P. Jones and J. A. Murphy, 2009, "Capturing Carbon from Existing Coal-Fired Power Plants," *Chemical Engineering Progress*, p. 33-47,April, 2009

Copeland, R. J., 2008, TDA Research Inc., private communication, April 1, 2008.

Copeland, R. J., 2009a, TDA Research Inc., private communication, August 31, 2009.

Copeland, R. J., 2009b, TDA Research Inc., private communication, September 28, 2009.

Davis, M. M. and M. D. Le Van, 1989, "Experiments on Optimization of Thermal Swing Adsorption," *Industrial & Engineering Chemistry Research*, Vol. 28, p. 778-785

Delgado, J. A., M. A. Uguina, J M. Gomez and L. Ortega, 2006, "Adsorption Equilibrium of Carbon Dioxide, Methane and Nitrogen onto Na- and H-Mordenite at High Pressures" *Separation and Purification Technology*, Vol. 48, p. 223-228

Elliott, J., 2009, TDA Research Inc., private communication, August 31, 2009.

Erbes, M.R. and R.H. Eustis, 1986 "A Computer Methodology for Predicting the Design and Off-Design Performance of Utility Steam Turbine-Generators", Proceedings of the American Power Conference, 48, pages 318-324, Chicago

Eustis, R.H., M.R. Erbes, and J.N. Phillips, 1987, *Analysis of the Off-Design Performance and Phased Construction of Integrated-Gasification-Combined-Cycle Power Plants Volume 2: Models and Procedures*, EPRI Report AP-5027, Volume 2

Fukunaga, P., K.C. Hwang, S. H. Davis and J. Winnick, 1968, Mixed-Gas Adsorption and Vacuum Desorption of Carbon Dioxide on Molecular Sieve," *I&EC Process Design and Development*, Vol. 7, No. 2, p.269f.

Garrett, D. E., 1989, *Chemical Engineering Economics*, Van Nostrand Reinhold, New York

Green, D. W., and R. H. Perry, 2008, *Chemical Engineers Handbook*, McGraw-Hill, New York

Hutchinson, D. O. 1997, private communication, September 19, 1997

Hyun, S. H., and R. P. Danner, 1982, "Equilibrium Adsorption of Ethane, Ethylene, Isobutane, Carbon Dioxide and Their Binary Mixtures on 13X Molecular Sieves," *Journal of Chemical Engineering Data*, Vol. 27, p. 196-200.

Keller, I. U., and R. Staudt, 2005*, Gas Adsorption Equilibria*, Chapter 7 Adsorption Isotherms, Springer US, New York

Keller, G. E., R. A. Anderson and C. M. Yon, 1987, *Handbook of Separation Process Technology*, Chapter 12 Adsorption, Editor R. W. Rousseau, Wiley, New York

Knaebel, K. S., 2002, "A 'How To' Guide to Adsorber Design," Adsorption Research, Inc., Dublin, OH 43016

Knopf, F. C., 2010, *Energy Systems Design and Optimization*, in press, Wiley, New York.

Kohl, A. A and R Nielson, 1997, *Gas Purification*, Chapter 12 Gas Dehydration and Purification by Adsorption, Gulf Publishing Company, Houston, TX

Lee, J. B., C. K. Ryu, J-I Back, T.H. Eom, and S.H. Kim, 2008, "Sodium-Based Dry Regenerable Sorbent for Carbon Dioxide Capture from Power Plant Flu Gas," *Industrial & Engineering Chemistry*, Vol. 47, p. 4465-4472

Lee, S. C., H. J. Chae, S. J. Lee, Y. H. Park and C. K. Ryu, 2009, "Novel Regenerable Potassium-Based Sorbents for CO_2 Capture at Low Temperatures," *Journal of Molecular Catalysis B: Enzymatic*, Vol. 56, p. 179-184

Liang Y., and D. P. Harrison, 2004, "Carbon Dioxide Capture Using Dry Sodium-Based Sorbents, *Energy & Fuels*, Vol. 18, p. 569-575

Le Van, M. D. and G. Carta, 2008, *Perry's Chemical Engineers' Handbook*, Section 16, Adsorption and Ion Exchange, Editors, D. W. Green and R. H. Perry, McGraw-Hill, New York

Lyderson, A. L., *Mass Transfer in Engineering Practice*, John Wiley and Sons, New York.

McCabe, W. L., J. C. Smith and P. Harriott, 2001, *Unit Operations of Chemical Engineering*, 6th Edition, p.821 f, McGraw-Hill, 2001

Park, Y. C., S-H Jo, K-W Park, Y. S. Park, C-K Yi, 2009, "Effect of Bed Height on the Carbon Dioxide Capture by Carbonation/Regeneration Cycle Operations Using Dry Potassium Based Sorbents," *Korean Journal of Chemical Engineering*, Vol. 26, No. 3 p. 874-878

Ramezan, M., et al., 2007a, Carbon Dioxide Capture from Existing Coal-Fired Power Plants, DOE/NETL-401/110907, Revised November 2007, National Energy Technology Laboratory, Department of Energy

Ramezan, M., et al., 2007b, Carbon Dioxide Capture from Existing Coal-Fired Power Plants, DOE/NETL-401/110907, Revised November 2007, National Energy Technology Laboratory, Department of Energy, AEP's Conesville #5 Power Plant, Stream 7, Flow from FGD to Stack (Table 2-1, p. 14, DOE Final Report Revised November 2007 DOE/NETL-401/110907)

Reynolds, S. P., A. D. Ebner and J. A. Ritter, 2006, "Stripping PSA Cycles for CO_2 Recovery from Flue Gas at High Temperature Using a Hydrotalcite-Like Adsorbent, *Industrial & Engineering Chemistry*, Vol. 45 p. 4278-4294

Rudistill, E. N., J. J. Hacskaylo and D. Le Van, 1992, "Co-adsorption of Hydrocarbons and Water on BPL Activated Carbon," Industrial & Engineering Chemistry, Fundamentals, Vol. 31, p. 1122-1130.

Ruthven, D. M., 1984, Principles of Adsorption and Adsorption Processes, Wiley, New York

Salisbury, J.K., *Steam Turbines and Their Cycles*, Robert E. Krieger Publishing Company, Huntington, N.Y., 1950.

Schork, J. M. and J. R. Fair, 1998, "Steaming of Activated Carbon Beds," *Industrial & Engineering Chemistry, Fundamentals*, Vol. 27, p. 1545-1547.

Schweiger, T. A. J., 1996, "A Design Method for Adsorption Bed Capacity: Steam-Regenerated Adsorbers," *Industrial & Engineering Chemistry*, Vol. 35, p. 1929-1934

Schweiger, T. A. J., and M. D. Le Van, 1993, "Steam Regeneration of Solvent Adsorbers," *Industrial & Engineering Chemistry*, Vol. 32, p. 2418-2429.

Slejko, F. J. 1985, *Adsorption Technology: A Step by Step Approach to Process Evaluation and Application* Marcel Dekker, New York.

Siriwardane, R., M. Shen, E. Fisher, J. Poston and A. Shamsi, 2001, "Adsorption and Desorption of CO_2 on Solid Adsorbents," DOE, NETL, Morgantown, VA, *Energy and Fuels*, accepted for publication in March 2001 issue.

Spencer, R.C., K.C. Cotton, and C.N. Cannon, 1963, *A Method of Predicting the Performance of Steam Turbine Generators … 16,500 kW and Larger*, Journal of Engineering for Power, pages 249-298 October, 1963.

Srinivas, G., R. Copeland and J. Elliott, 2008a, Technology for CO2 Capture, TDA Research, Proprietary, PowerPoint, March 13, 2008

Srinivas, G., R. Copeland and J. Elliott, 2008b, Modeling TDA's CO2 Capture System, TDA Research, Proprietary, PowerPoint, August 31, 2009

Striolo, A., et al, 2005, "Effect of Temperature on the Adsorption of Water in Porous Carbons" *Langmuir*, Vol. 21, p. 9457-9467

U. S. Army Corps of Engineers, 2001, "Adsorption Design Guide," Design Guide No. 1110-1-2, Department of the Army, U. S. Army Corps of Engineers,1 Mar 2001

Valenzuela, D. P. and A. L. Myers, 1989, *The Adsorption Equilibrium Data Handbook*, Prentice-Hall Englewood Cliffs, NJ

Walas, S. M. 1990, *Chemical Process Equipment – Selection and Design*, Chapter 15, Adsorption and Ion Exchange, Elsevier, New York

Wang, W-C and James Hoffman, 2009, "Exploratory Design Study on Reactor Configurations for Carbon Dioxide Capture from Conventional Power Plants Employing Regenerable Solid Sorbents," *I&EC Research*, Vol. 48, No., p. 341-351, American Chemical Society.

Yang, R. T., 1987, *Gas Separation by Adsorption Processes*, Butterworths, London

Yaws, C. L., 1999, *Handbook of Thermodynamic and Physical Properties of Chemical Compounds*, McGraw-Hill, New York

Appendix A: Power Plant Performance - Design and Off-Design Calculations

All carbon dioxide sequestration processes require regeneration and regeneration processes utilize steam extracted from the power plant. This steam extraction adversely affects power plant performance. Ultimate costing of the sequestration process requires accurate accounting for all sequestration costs (capital, labor, etc.) as well as accounting for the power lost from the power plant.

Power plants are designed and optimized for full-load operation, which is termed the design case or base-case. All operations which are not full-load operation are termed off-design operation. Sequestration with steam extraction will cause the power plant to operate in an off-design operation.

The first step in all power plant calculations is to determine design case plant performance including all pressures, temperatures, efficiencies, steam flows, turbine net heat rate, plant net heat rate, etc. All off-design performance calculations start from the design case.

In the next sections we discuss design and off-design power plant calculations. These calculations are particularized to the Conesville #5 Power Plant. The off-design calculations include steam extraction as needed for regeneration of the solid sorbent.

Power Plant Performance Design Case (Full-Load Operation) Design case performance calculations for steam turbine systems are standard calculations. Referring to Figure A-1 we can outline the calculation procedure as follows:

1.) Use the known turbine inlet conditions and exhaust conditions at each extraction point to determine enthalpy, entropy and steam quality in and out of each turbine section, as well as turbine section efficiency.

2.) Use the known pressure drops in the reheater and boiler, feedwater heater terminal temperature difference and the feedwater drain cooler approach temperature to determine steam properties at appropriate locations.

3.) Determine the steam extraction flowrates starting with feedwater heater (7) FWH-7, and continuing, FWH-6, FWH-5, …, until FWH-1 is reached.

4.) Calculate the power used by the auxiliary turbine and low-pressure feedwater pump.

5.) Calculate the turbine exhaust end loss using Spencer et al. (1963).

6.) Sum the output from all the turbines, account for all losses and determine turbine heat rate.

Normal full-load operational data for the Conesville #5 Power Plant were taken from the DOE report, DoE/NETL-401/110907, November 2007, page 19. This DoE report indicated the Conesville #5 plant has a steam turbine heat rate of 7773 Btu/kW-hr, a generator output of

463,478 kW and a net plant heat rate of 9309 Btu/kW-hr. The initial design case simulation developed for the present study, with results shown in Figure A-1, indicated a steam turbine heat rate of 7794 Btu/kW-hr, a generator output of 473,411 kW and a net plant heat rate of 9312 Btu/kW-hr. These later values are in agreement with the DOE report.

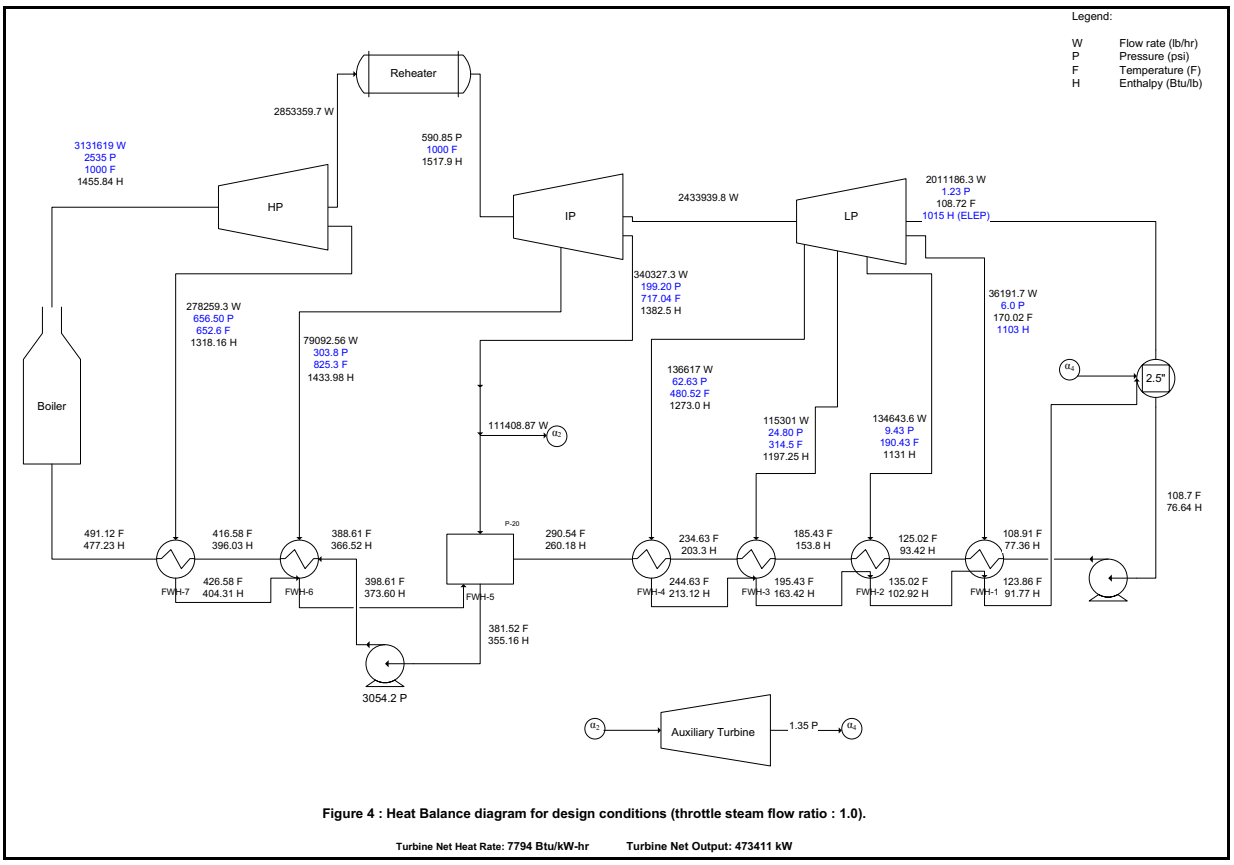

Figure A-1 Heat Balance Diagram for Design Conditions (Throttle Steam Flow Rate Ratio: 1.0)

Power Plant Performance Off-Design Operation: The solution to the off-design problems involves:

1.) Supplying initial estimates for all pressures and efficiencies in the turbine system.

2.) Modifying pressures in the turbine system based on the off-design turbine inlet conditions.

3.) Modifying the efficiencies based on the off-design velocity into each turbine section.

In the design case, we solved the full load operation material and energy balances for the turbine system using thermodynamic functions and known P and T or P and $\hat{h}$ (for 2-phase steam) at each turbine section inlet, outlet and extraction point. All standard commercial simulation packages – ASPEN, HYSYS, Pro/II, etc. – can determine power plant performance for the design case. However these packages can not directly solve for off-design performance. Here user written subroutines must be added to account for off-design pressure and efficiency

changes. Here we develop the needed subroutines to allow off-design calculation to be performed within the standard commercial packages. There are specialized commercial programs – GateCycle from General Electric – which can perform both design and off-design calculations for power systems.

We evaluated several methods for predicting off-design performance, for use with standard simulation packages, including the Spencer, Cotton, and Cannon Method as well as methods involving modifications to the Willians line. The most consistent off-design results were obtained using the method developed by Erbes and Eustis (1986) with addition of the Spencer, Cotton, and Cannon Method to determine turbine exhaust end loss.

To start the off-design calculations, the pressure at each stage i is modified from the design pressure by multiplication with the flow ratio,

$$P_{i,Off-Design} = P_{i,Design} * Flow\_Ratio \tag{A-1}$$

where the $Flow\_Ratio$ = Off Design Flow Rate / Design Flow Rate.

In CO_2 sequestration applications, steam extraction will change the flow rates determined in the design case for the LP turbine section. The off-design system performance can now be solved for the given off-design steam flow rates and using the design-case efficiencies, estimated pressures and assuming that all other conditions, including pump efficiencies and feedwater heater approach temperatures remain at design conditions.

Update Pressures for Off-Design Case: The process begins with the Stodola's ellipse law (1954) which provides a relation between steam flow and pressure drop in a turbine section as,

$$F_{Turbine\,Section} = K\sqrt{1-\frac{P_{Out}}{P_{In}}} \tag{A-2}$$

where, $F_{Turbine\,Section}$ = is the steam flow in the turbine section (lb/hr); K = a proportionality constant; and P_{Out} = pressure out of the section, and P_{In} = pressure in. But equation (A-2) cannot be used for off-design calculations since it does not take into account the effect of varying inlet temperature. Erbes and Eustis (1986) utilize a modification of the ellipse law suggested by Sylvestri, which accounts for varying inlet conditions as,

$$F_{Turbine\,Section} = K\sqrt{\frac{P_{In}^2 - P_{Out}^2}{\nu_{In}\,P_{In}}} \tag{A-3}$$

where ν_{In} = the stage inlet specific volume (ft^3/lb) and the remaining terms are the same as equation (A-2). In order to use equation (A-3) the constant K is first determined for each turbine section, which is done using design conditions.

With each $K_{Design}^{TurbineSection}$ determined, we can use equation (A-3) in a reverse-order iterative calculation, starting at the LP turbine outlet, to update the off-design pressure distribution in the turbine system. Equation (A-3) can be rearranged to solve for an updated value for P_{In} as,

$$P_{In}^{Stage\,i} = \frac{v_{In}^{Stage\,i}\left(\frac{F_{Turbine\,Section}^{Stage\,i}}{K_{Design}^{Stage\,i}}\right)^2 + \sqrt{\left(v_{In}^{Stage\,i}\left(\frac{F_{Turbine\,Section}^{Stage\,i}}{K_{Design}^{Stage\,i}}\right)^2\right)^2 + 4\left(P_{Out}^{Stage\,i}\right)^2}}{2} \qquad \text{(A-4)}$$

All the terms on the RHS of equation (A-4) are known from the initial estimate of the off-design conditions.

When updated values for all the P_{In}'s have been determined, these values can replace the initial estimated $P_{In}^{Stage\,i}$ values. These new P values, can be used to generate new flow rates, temperatures and steam specific volumes into each turbine section. The replacement (iteration process) continues until the pressure values remain unchanged.

With converged pressures for the IP and LP turbine sections, we next update the HP turbine stage. The HP section is not included in the iteration process as the pressure drop in the reheater, $\Delta P_{Reheater}^{Off-Design}$, fixes the outlet pressure of the HP turbine as,

$$P_{Out}^{HPT} = P_{In}^{IPT} + \Delta P_{Reheater}^{Off-Design} \qquad \text{(A-5)}$$

The pressure drop in the reheater can be determined by assuming a homogeneous flow model.

Update Efficiencies for the Off Design Case: In the off-design calculations we have utilized the $\eta^{Isentropic}$ values found in the design case. We next want to update these efficiency values using internal turbine considerations. Steam turbines are generally classified as impulse or reactive. In actual operation, most turbine sections show both impulse and reactive characteristics. Erbes and Eustis (1987) assume 50% reaction balding for each turbine section. From Salisbury (1950), stage efficiency can be found as,

$$\eta_{Design}^{Isentropic} = 2y\left[(a-y)+\sqrt{(a-y)^2+1-a^2}\right] \qquad \text{(A-6)}$$

where $a = \sqrt{1-x}$, x = fraction of stage energy released in the bucket system, $y = \frac{W_{Design}}{V_{Design}}$, W_{Design} = turbine rotational speed and, V_{Design} = inlet steam velocity to the turbine section. For a

50% reaction stage, x = 0.5 and a = 0.7071. Furthermore, for a 50% reaction stage, the maximum efficiency $y_{Optimal} = \left(\frac{W_{Design}}{V_{Design}}\right)_{Optimal} = 0.7071$.

In addition to the assumption of 50% reaction stages, Erbes and Eustis (1987) further suggest that the turbine rotational speed will remain constant in both the design and off design cases allowing us to write,

$$\frac{\left(\frac{W_{Off-Design}}{V_{Off-Design}}\right)}{\left(\frac{W_{Design}}{V_{Design}}\right)_{Optimal}} = \frac{\left(V_{Design}\right)_{Optimal}}{V_{Off-Design}} \qquad \text{(A-7)}$$

It is then possible to use equation (A-7) to ratio the off-design and design efficiencies. This efficiency correction is generally small.

Impact of CO_2 sequestration on power plant performance: We want to evaluate the impact of adding CO_2 sequestration to the Conesville #5 Power Plant base case power plant. Here we utilize a solid to adsorb CO_2. Regeneration of the sequestration system, when capturing 90% of the base-case generated CO_2, will require 1,240,233 lbs/hr of low pressure steam. This steam flow rate is ~ 40% of the total HP steam generated in the boiler.

We evaluate two possible extraction points for regeneration steam – Case A-1 with steam extraction from extraction point (5) and Case A-2 with steam extraction from extraction point (4). Steam extraction will lower the pressure in the turbine system both at the extraction point and downstream of the extraction. There will also be some lowering of pressure up-steam of the extraction point, but this will be to a much lesser extent. Care must be taken that the lower pressure and lower steam flow rate following extraction will not cause blade damage in the LP section of the turbine. Plant performance for Case A-1 is shown in Figure A-3, and Case A-2 results are shown in Figure A-4. Key results for power plant performance for the base case (full-load operation) and the two off-design steam extraction cases are summarized in Table A-1.

In both Case A-1 and Case A-2 extraction steam flow is set at 1,240,233 lbs/hr. For Case A-1 – with extraction immediately following the IP pressure turbine – the steam turbine heat rate is 10,060 Btu/kW-hr and generator output is 364,277 kW. For Case A-2 – with extraction after the first stage of the LP turbine – the steam turbine heat rate is 9,292 Btu/kW-hr and generator output is 390,097 kW. Some care must be exercised when using the Case A-2 results. There were stability issues in closing the feedwater heater energy balances when extracting the large amount of needed steam following the first stage in the LP turbine section. Additional plant data for design case operation, especially around the feedwater heaters, may be needed to address this difficulty. In addition, the off-design performance results should ultimately be confirmed using available packages such as GateCycle.

The results from Table A-1 show that in Case A-1 the power plant will deliver 94,890 kW less electricity due to steam extraction for the sequestration regeneration process. Case A-2

will deliver 70,878 kW less electricity due to steam extraction for sequestration. In order to properly determine the economics of the sequestration process we will need to purchase make-up electricity (either 94,890 or 70,878 kW). In addition the regeneration process itself will have associated capital costs, operations and maintenance costs, and utility costs. All these costs will need to be brought to a levelized energy cost basis to determine the impact of sequestration on utility pricing.

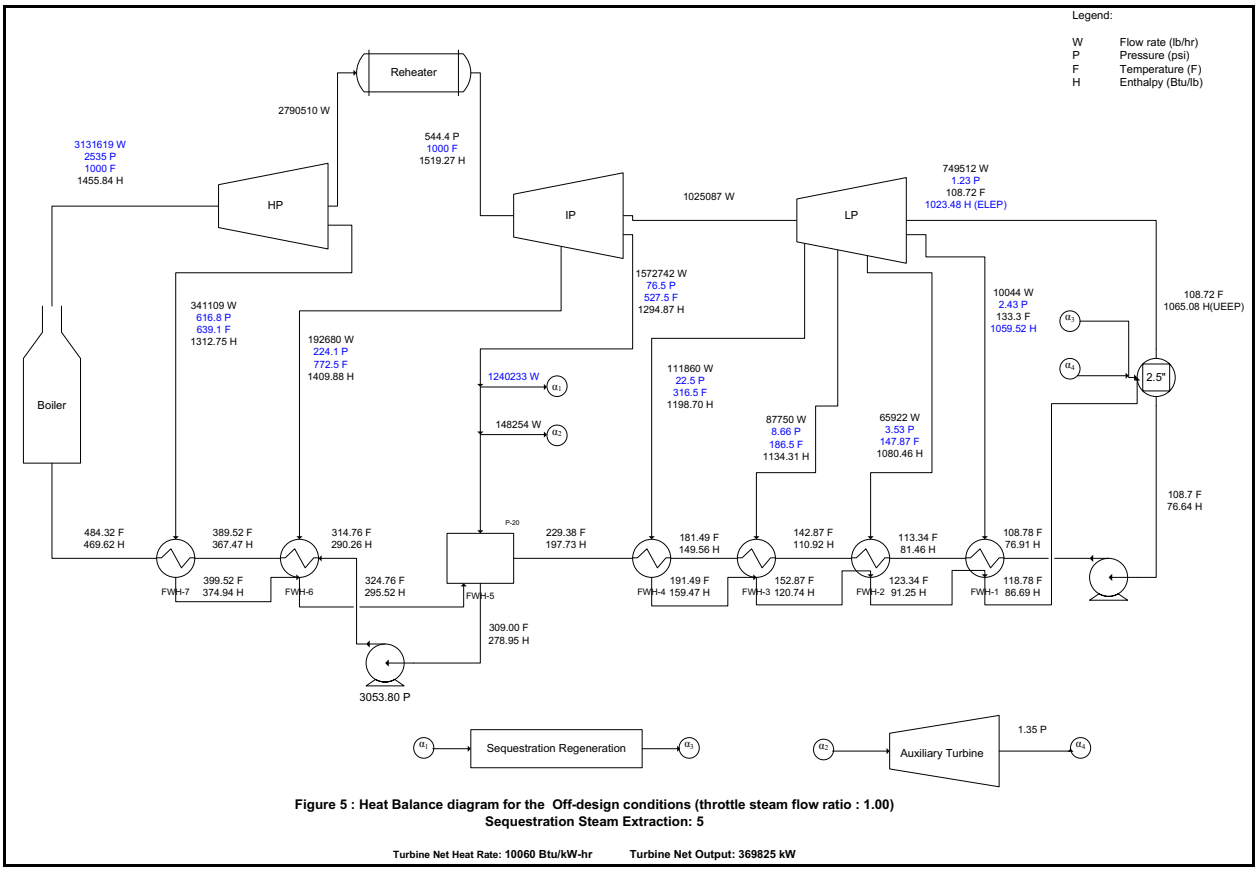

Figure 5 : Heat Balance diagram for the Off-design conditions (throttle steam flow ratio : 1.00)
Sequestration Steam Extraction: 5

Turbine Net Heat Rate: 10060 Btu/kW-hr **Turbine Net Output: 369825 kW**

Figure A-2 Heat Balance Diagram for the Off-Design Conditions (Throttle Steam Flow Ratio: 1.00)

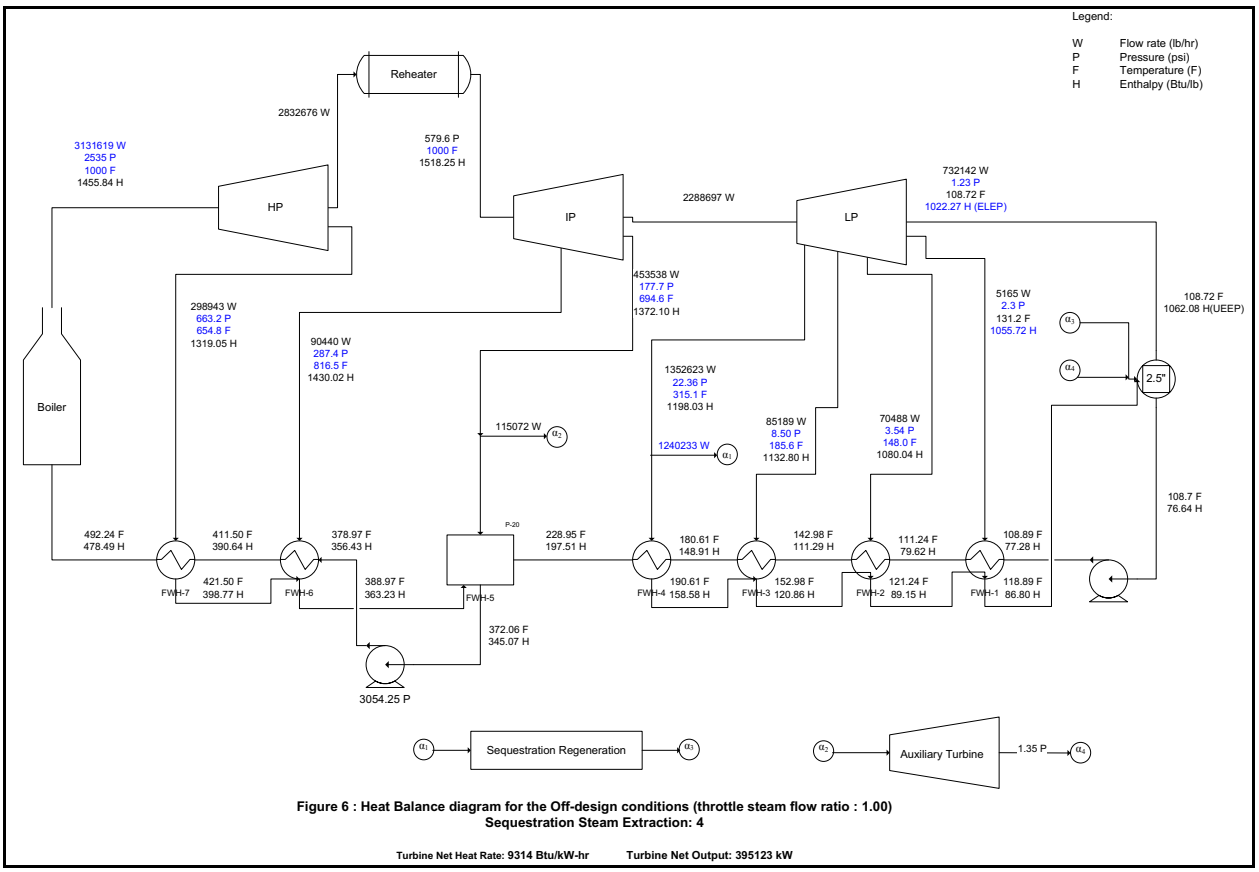

Figure 6 : Heat Balance diagram for the Off-design conditions (throttle steam flow ratio : 1.00)
Sequestration Steam Extraction: 4

Turbine Net Heat Rate: 9314 Btu/kW-hr **Turbine Net Output: 395123 kW**

Figure A-3 Heat Balance Diagram for the Off-Design Conditions (Throttle Steam Flow Ratio: 1.00, Sequestration Steam Extraction: 4)

Table A-1 Impact of CO_2 Sequestration on Power Plant Performance

	Base Case	Case A-1	Case A-2
Percent CO2 capture	0%	90%	90%
Extraction Point		(5)	(4)
Steam Turbine System (F, P, T, $\hat{h}$)			
Steam flow from Boiler (lb/hr)	3,131,619	3,131,619	3,131,619
Steam Pressure from Boiler (psia)	2,535	2,535	2,535
Steam Temperature from Boiler (F)	1,000	1,000	1,000
Steam Enthalpy from Boiler (Btu/lb)	1,455.835	1,455.835	1,455.835
Water Enthalpy into Boiler (Btu/lb)	477.23	469.62	478.49
Steam Pressure to IP Turbine Section (psia)	590.85	544.40	579.61
Steam Pressure to LP Turbine Section (psia)	199.20	76.52	177.68
Steam Extraction Rate for Regeneration (lb/hr)	NA	1,240,233	1,240,233
Steam Turbine System Heat Rate			
Turbine Net Output (kW)	473,411	369,825	396,038
Generator Efficiency (%)	98.5	98.5	98.5
Generator Net Output (kW)	466,310	364,277	390,097
Turbine Net Heat Rate (Btu/kW-hr)	7,794	10,060	9,292
Boiler Efficiency (%)	88.1	88.1	88.1
Steam Plant Auxiliary Power Consumption (%)	7.0	7.0	7.0
Plant Output (kW)	433,668	338,778	362,790
Plant Net Heat Rate (Btu/kW-hr)	9,513	12,279	11,341
Steam Turbine System CO_2 Emissions			
Coal Carbon wt %	63.2	63.2	63.2
Coal LHV (Btu/lb)	10,785	10,785	10,785
Coal Required, LHV (lb/hr)	382,526	385,699	381,508
CO_2 Produced (lb CO2 / lb Coal)	2.3159	2.3159	2.3159
Total CO_2 produced (lb/hr)	885,903	893,251	883,546

Appendix B: Aspen Technology's Engineering Suite

Aspen Technology's Engineering Suite includes over 50 engineering products that cover all aspects of design, analysis, control and optimization. Three of these programs could be used for the design and economic evaluation of the adsorber/regenerator and downstream processing: Aspen Adsorption, Aspen HYSYS and Aspen Icarus Project Manager (In-Plant Cost Estimator). Aspen Adsorption could be used to design the adsorber and regenerator. Aspen HYSYS could be used to design the flowsheet that goes from the power plant to the CO_2 pipeline and includes the adsorber and regenerator. Aspen Icarus Project Manager (In-Plant Cost Estimator) could be used for the economic analysis. These three programs are described briefly in the following paragraphs with information from the Aspen Technology's web site.

Aspen Adsorption is a comprehensive flowsheet simulator for the optimal design, simulation, optimization and analysis of industrial gas and liquid adsorption processes. It enables process simulation and optimization for a wide range of industrial gas and liquid adsorption processes including reactive adsorption, ion exchange and cyclic processes such as pressure-swing, temperature-swing, and vacuum-swing adsorption. It is used to select optimal adsorbents, design better adsorption cycles, and improve general plant operations. A rigorous rate-based adsorbent bed model includes: various geometries including axial column, horizontal bed and radial beds, options to include axial dispersion in the material balance, wide range of kinetic models including lumped resistance, micro/macro-pore and general rate model, and a range of standard equilibrium/isotherm models that allow for either pure component or multi-component/competitive behavior. A highly configurable energy balance to account for non - isothermal behavior, conduction, heat loss and wall effects, and a unique cyclic steady-state modeling paradigm allows use of steady-state estimation and optimization techniques for rapid design and optimization of cycles.

Aspen HYSYS is a process modeling tool for conceptual design, optimization, business planning, asset management and performance monitoring for the process industries. There is efficient workflow for process design, equipment sizing, and preliminary cost estimation within one environment through integration with other AspenONE Process Engineering tools including Aspen Process Economic Analyzer cost modeling software. Aspen HYSYS has a comprehensive thermodynamics foundation for accurate calculation of physical properties, transport properties, and phase behavior. A comprehensive library of unit operation models including distillation, reactions, heat transfer operations, rotating equipment, controller and logical operations in both the steady state and dynamics environments, but not adsorption. CAPE-OPEN compliant models are also fully supported.

Aspen In-Plant Cost Estimator (formerly Aspen Icarus Project Manager) is a powerful economic project management tool for in-plant capital and maintenance projects. By integrating the project economic capabilities of the Aspen Icarus technology with the industry-leading project management capabilities of Primavera Project Planner®, Aspen In-Plant Cost Estimator enables companies to optimize the constraints of quality, time and cost simultaneously. Aspen In-Plant Cost Estimator is a core element of AspenTech's aspenONE™ Process Engineering applications. Aspen In-Plant Cost Estimator focuses on small capital and maintenance projects where some or most of an existing process or facility infrastructure is existing or will be re-used

and should not need to be included in the project scope or schedule. The Aspen Icarus technology underlying Aspen In-Plant Cost Estimator is the industry standard for project and process evaluation. Unlike other approaches, the technology does not rely on capacity factored curves for equipment pricing, nor does it rely on factors to estimate installation quantities and installed cost from bare equipment. It follows a unique approach where equipment, with associated plant bulks, is represented by comprehensive design-based installation models. In this report, this program is referred to as Aspen Icarus.

Appendix C: Other Related Investigations

The following literature review covers research articles that are directly related to the design of an adsorber and regenerator for carbon dioxide capture from power plant flue gas. A summary of related information available in standard texts and handbooks on adsorption is included. Capabilities of process design programs for adsorption, regeneration, flowsheeting, cost estimation and economic evaluation are described.

An exploratory design study was conducted by Yang and Hoffman, 2009 for carbon dioxide removal from a flue gas with a flow rate of 3.4×10^4 m^3/min from a 500 MW power plant with an available pressure drop of 0.21 bar (3.0 psi) and carbon dioxide concentration of ~20%. They proposed two fluidized bed adsorber designs and two regenerator designs, one a fluidized bed and the other a moving bed. All used a dry, regenerable, amine-enhanced solid adsorbent with a carrying capacity of 0.264 kg CO_2/kg adsorbent. The adsorber operated at 54^0C (130^0F) with fast kinetics, and the regenerator operated at 99^0C (210^0F) with slow kinetics (tens of minutes in a laboratory scale packed bed). Fluidized bed operating velocities of 1.5 m/sec (5.0 ft/sec), 1.2 m/sec (4.0 ft/sec) and 0.9 m/sec (3.0 ft/sec) were used for a dense bubbling fluidized bed to determine fluid bed reactor size and number of modules as shown in Table C-1. For 90% carbon dioxide removal, an effective rate constant, K_f, of 2.04 sec^{-1} was determined from a first order reaction in a fine-particle bubbling bed, and a workable design had a minimum bed depth of 2.4 m operating with a velocity 1.34 m/sec. An optimum CO_2 adsorption bed temperature of 54^0C (130^0F) was determined using heat transfer constraints. Gas and solid properties used in the evaluations are given in Table C-1, and the fluidized bed adsorber design is summarized in Table C-3 with additional data on heat release and heat transfer given in Yang and Hoffman, 2009.

The fluidized bed adsorber was said to have a number of advantages over fixed and moving bed adsorbers according to Yang and Hoffman, 2009. The operating temperature can be controlled at the optimum adsorber temperature throughout the entire fluidized bed reactor. Moving bed adsorbers are said to be limited to the minimum fluidization velocity, and for all practical purposes a bed with particle that are less than 4,000 μm will operate as a fluidized bed. A correlation was obtained for the minimum fluidization velocity; and for 4,000 μm particles with a density of 1,500 kg/m^3 (93.6 lb/ft^3), the minimum fluidization velocity was about 1.2 m/sec (4.0 ft/sec). For higher velocities, the flow in packed and moving beds would have to be vertically downward, and this configuration is limited to the available pressure drop of about 0.21 bar (3.0 psi).

Similar limitations were encountered when moving beds are considered of regeneration. To prevent fluidization of the bed from the evolution of CO_2, gas is withdrawn from the bottom of the regenerator. Temperature control can use internal heat exchangers, and parallel plate heat exchangers were recommended by Yang and Hoffman, 2009. Their design of a moving bed regenerator had a bed height of 23 m (75 ft), to ensure the adsorbent reached the regeneration temperature of 95^0C. They concluded that direct injection of steam as not practical, since steam condensation would interfere with the movement of solids. They proposed conceptual designs for a fluidized bed adsorber and a moving bed regenerator that are shown below in Figure C-1

Table C-1 Number and Size of Fluidized Bed Reactor Modules as a Function of Operating Velocity for a Gas Flow of $3.4x10^4$ m^3/min ($1.2x10^6$ ft^3/min)* with Minimum Bed Height of 2.44 m (8.0 ft) for 90% CO_2 Capture from Yang and Hoffman, 2009

Operating Velocity m/sec (ft/sec)	Reactor Size Square Cross-Section one side m (ft)	Number of Modules	Adsorber Total Cross-Section m^2 (ft^2)
1.5 (5.0)	9.6 (30.8)	4	369 (3,795)
1.2 (4.0)	9.6 (30.8)	5	461 (4,743)
0.9 (3.0)	10.2 (33.5)	6	624 (6,734)

* $5.74x10^6$ lb/hr

Table C-2 Gas and Solid Properties from Yang and Hoffman, 2009

Flue Gas
Flow rate - $3.4x10^4$ m^3/min
$1.2x10^6$ ft^3/min

Pressure – 1.22 bar

Temperature – 54^0C (130^0F) adsorption,
99^0C (210^0F) regeneration

CO2 Capture
90% - CO2 removal
388,284 kg/hr
856,170 lb/hr

Solid Adsorbent
particle density 880 kg/m^3
0.880 gm/cm^3
bulk density 422 kg/m^3
0.422 gm/cm^3
fluid bed voidage 0.52
particle size 600μm
terminal velocity 0.12 m/sec
0.38 ft/sec

Minimum fluidization velocity 0.12 m/sec
0.38 ft/sec

Table C-3 Fluidized Bed Adsorber Design from Yang and Hoffman, 2009 with Flue Gas Flow Rate of $3.4x10^4$ m^3/min and 90% - CO_2 removal (388,284 kg/hr)

Adsorber

Number of Adsorbers	5
Fluidized Bed	
Width	9.15 m (30.0 ft)
Length	9.15 m (30.0 ft)
Minimum bed height	2.44 m (8.0 ft)
Total pressure drop	0.13 bar (1.9 psi)
Adsorbent	
CO_2 loading	0.264 kg CO_2/kg adsorbent
Total solids in bed	35,668 kg
Circulation rate	4,903 kg/min
Mean residence time	7.3 min

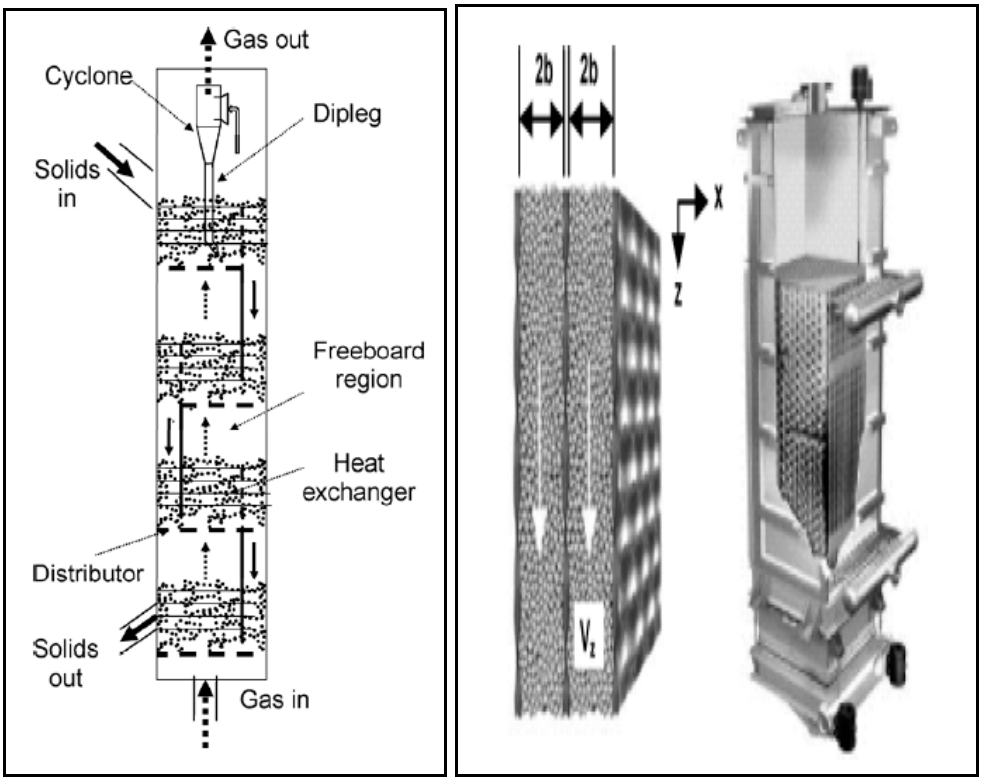

a Four stage, fluidized bed adsorber b Moving bed regenerator

Figure C-1 Conceptual Designs of a Fluidized Bed Adsorber and a Moving Bed Regenerator from Yang and Hoffman, 2009

from their paper. For the regenerator they would use recycled carbon dioxide as the fluidizing gas.

Modeling and experimental studies on steam regeneration of activated carbon beds with adsorbed n-hexane were made by Schweiger and Le Van, 1993. Steam was an effective regenerating agent because its high heat content increased the temperature to desorb the solvent, and water competes with the solvent for pore volume. They developed a one-dimensional, time dependent model using the species continuity and energy equations that used local equilibrium in a fixed bed. The Blake-Kozeny equation was used to compute the bed pressure drop. For adsorption equilibria of water and n-hexane, equations were given for pure components and for the interaction between water and n-hexane in the adsorbed phase where the interaction was significant, and adsorbed water displaced the n-hexane. These equations are shown below.

Adsorption Equilibria. Pure *n*-hexane (Hacskaylo, 1987):

$$\ln P_A\,(\text{MPa}) = A + \ln \theta_A - \frac{B + b_1(1-\theta_A)}{C+T} \quad \text{for} \quad \theta_A \le 1 \tag{29}$$

$$\ln P_A\,(\text{MPa}) = A - \frac{B}{C+T} \quad \text{for} \quad \theta_A \ge 1 \tag{30}$$

with $A = 6.98946, B = 2737.59, C = -46.87$, and $b_1 = 3356.89$. $\phi_A^s = 477.4 \times 10^{-6}\ \text{m}^3/\text{kg}$. $\rho_{A,l} = 654.71 - 0.9735(T - T_{ref})$.

Pure water:

$$\ln P_W\,(\text{MPa}) = A' - \frac{B + b_1(1-\theta_W)}{C+T} \quad \text{for} \quad \theta_W \le 1 \tag{31}$$

$$A' = A + \ln \theta_W + a_1(1-\theta_W) + a_2(1-\theta_W)^2 + a_3(1-\theta_W)^3 + a_4(1-\theta_W)^4 \tag{32}$$

$$\ln P_W\,(\text{MPa}) = A - \frac{B}{C+T} \quad \text{for} \quad \theta_W \ge 1 \tag{33}$$

with $A = 9.38086, B = 3816.41, C = -46.13, a_1 = 0.6856, a_2 = 4.8123, a_3 = -7.5767, a_4 = 5.9743$, and $b_1 = 438.165$. $\phi_W^s = 406.0 \times 10^{-6}\ \text{m}^3/\text{kg}$. $\rho_{W,l} = 997.01 - 0.5221(T - T_{ref})$.

Mixtures: The equations above are used to predict partial pressures empirically using values of θ_A and θ_W given by

$$\theta_A = \frac{\phi_A + (1 - \exp(-0.25 q_A^2))\phi_W}{\phi_A^s} \tag{34}$$

$$\theta_W = \frac{\phi_A + \phi_W}{\phi_W^s} \tag{35}$$

In these equations ϕ_A is the volume adsorbed based on liquid density, qM/ρ_l (m^3/kg), and q_A is the adsorbed/condensed phase concentration (moles/kg). These equations were used to predict the partial pressures empirically using the values of θ_A and θ_B.

Experiments measured breakthrough curves in a column (74 cm long, 7.2 cm dia., packed depth 58 cm) packed with BPL activated carbon. Steam flow rate and direction (up or down) and initial loading were varied and slightly above atmospheric pressure. There was general agreement between models and the five experiments. In the first experiment the flow rate was 0.021 gm/sec which is 0.85 superficial bed volumes per min. The breakthrough curves had three principle zones leaving the column. One was "a gentle purge of inerts" followed in about 60 minutes by a wave of desorbed n-hexane which lasted to about 110 minutes, and the third zone was breakthrough of steam.

Experimentally measured break-through curves were compared with model results. For five experiments, the model results agreed with experiments within the accuracy of the data, except for one case. Here, there were small differences between the curves because they stated that water competed with the solvent for pore volume. They said that more water must condense to provide the heat to desorb the larger quantity of solvent at the higher initial loading.

Concerns were expressed for the accuracy of the adsorbent equilibria correlation over the path of the steam regeneration experiments. This path began at room temperature with moderate solvent loadings, passes through moderate temperatures with high n-hexane solvent loadings and low water loadings, and finished with high temperatures with low solvent loadings and relatively high water loadings. The correlation used pore filling concepts with apparent pore volumes filled based on equilibrium partial pressures which were modified to account for n-hexane occupying the highest energy sites.

They described that most of the steam provided energy to heat the carbon adsorbent, the vessel, and any residual solvent and water. Only about one-fourth of the total energy from the steam went to desorb the n-hexane solvent. Additional details are provided by Schweiger and Le Van, 1993.

The co-adsorption of hydrocarbons and water on activated carbon was evaluated experimentally with a recirculating, constant volume apparatus by Rudisill, et al., 1992. Isotherm measurements were made for pure water, acetone, hexane and their mixtures from 25^0C to 125^0C. The measurements were presented as graphs of η_a (mol/kg) vs. reduced pressure ($P^r_w = P_w/P^s_w$) to show hysteresis loops, and the results for water are shown below in Figure 7 from their paper. A discussion was provided that related these results to previous work. The results given by Schweiger and Le Van, 1993 were based on isothermal equilibrium data from this paper.

For models of adsorption of hydrocarbon/water mixtures, Rudisill, et al., 1992 state that the approximation is made that an immiscible adsorbate, e.g., hexane, would act independent of the presence of water moderate at high loadings or at moderate water partial pressures. They argued that forces of adsorption are much stronger than water and that the water adsorption

would be a function of the pore volume occupied by the hexane. They said that data is available for the adsorption branch, but very little data are available for the desorption branch.

Regeneration of activated carbon bed with steam was evaluated by Schork and Fair, 1998 sing an instrumented packed column (7.44 cm i.d. by 30.5 cm long). They reported that during steaming, temperatures within the bed rose above the inlet value; and this was said to demonstrate the importance of the heat of adsorption. The rate of desorption was a strong function of temperature, and high temperatures were necessary to prevent long drying times. Having residual water on the bed reduces the maximum temperature. The heat of adsorption of water is an important source of energy for heating the bed. Analysis of 50-100 minute steam runs gave a better understanding of the physical phenomena. Steam generation cycles in industrial practice would be much shorter, and a rule of thumb is 4.0 lb steam per lb adsorbed organic. For the laboratory apparatus, about 10 minutes would regenerate the bed to 10% loading.

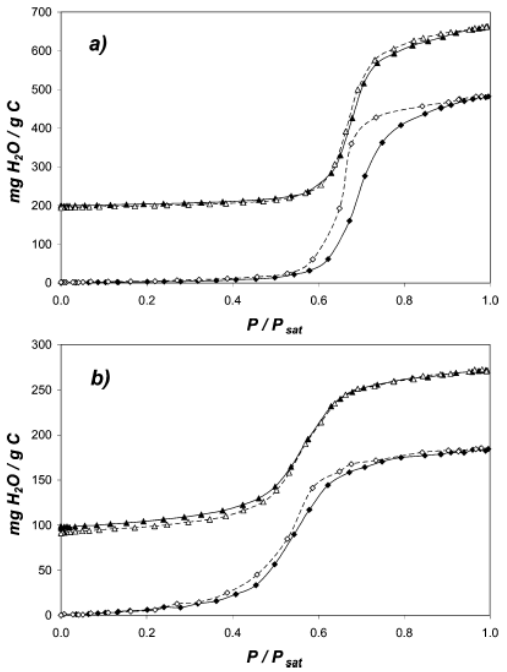

Figure 7. Experimental water adsorption isotherms in carbon-fiber monoliths. a is for SMS39; b is for SMM13. Diamonds are for $T = 378$ K; triangles are for $T = 423$ K (shifted for better visualization). Filled symbols are for adsorption; open symbols are for desorption. Lines are guide to the eye.

Experimental and simulation studies were used to investigate the effect of temperature on water in porous carbon (Striolo, A., et al, 2005). Results showed that there was negligible adsorption at low pressures, and this was followed by a sudden and complete pore filling once a threshold pressure was reached with wide adsorption-desorption hysteresis loops. The mechanism of how water affected the adsorption of other gases was not well understood. A mechanism was postulated that the coalescence of clusters of hydrogen-bonded molecules nucleate around high energy sites which causes a sharp rise in the water isotherm prior to reaching saturation. In the diagrams below, water adsorption and desorption isotherms were shown for diamonds and carbon-fiber monoliths. In these diagrams water adsorption is negligible at low pressure where pore filling occurs by capillary condensation, and adsorption-desorption isotherms have hysteresis loops. As the temperature increased, the size of the hysteresis loop decreased but the relative pressure which capillary condensation did not change significantly as shown in their two figures, Figures 4 and 7 given here. Additional discussion of the model development and comparison with experiments are given in the paper.

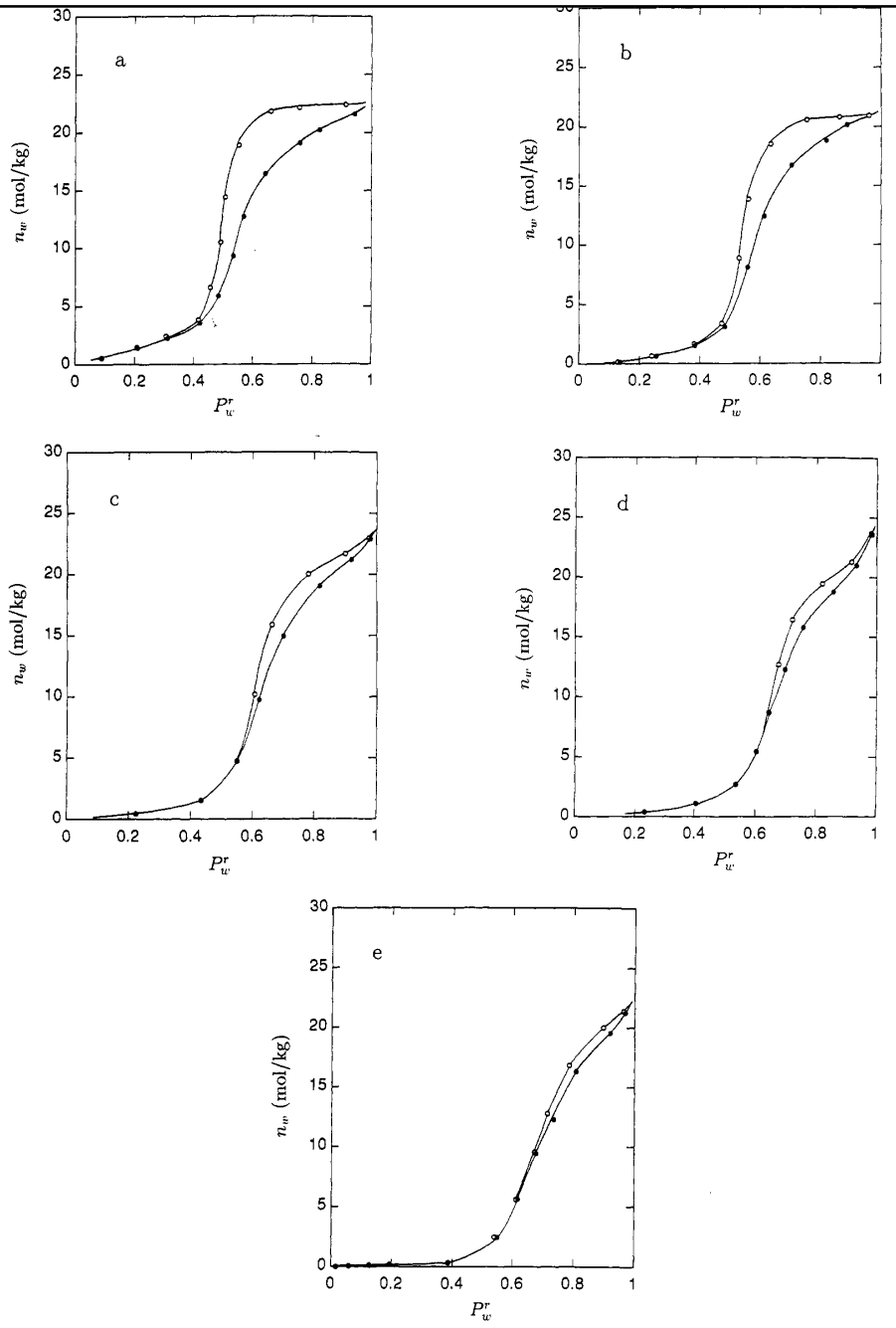

Figure 4. Isotherms for water adsorbed on BPL activated carbon. $P_w^r = P_w/P_w^s$. Filled circles denote adsorption, and open circles denote desorption. (a) 25 °C, P_w^s = 3.169 kPa. (b) 50 °C, P_w^s = 12.34 kPa. (c) 75 °C, P_w^s = 38.55 kPa. (d) 100 °C, P_w^s = 101.33 kPa. (e) 125 °C, P_w^s = 232.18 kPa.

In the Adsorption Equilibrium Data Handbook (Valenzuela and Myers, 1989), single-gas adsorption isotherms obtained from tabulated experimental data were given for about 130 gas-adsorbent combinations with constants for the Toth and UNILAN equations. Of these, there were eight for carbon dioxide mainly on activated carbon and a reference list for an additional 33 articles that present results graphically. There was no data for water, except for the 15 in the reference list. The equations from thermodynamics were given that apply to gas-solid adsorption, and procedures were described to calculate mixed-gas adsorption from single-gas isotherms using a general algorithm from IAS theory which requires a numerical solution. Experimental data was reported for about 20 binary mixtures (three with carbon dioxide and a hydrocarbon), along with the equilibrium concentrations using the algorithm.

A static, volumetric method was used by Hyun and Danner, 1982 to determine the adsorption equilibrium of ethane, ethylene, isobutene and carbon dioxide and their binary mixtures on 13X molecular sieves at a total pressure of 137.8 kPa and temperatures of 298, 323, and 373 K. There was an apparent adsorption azeotrope for two of the mixtures, one involving carbon dioxide. The Langmuir model, the simplest among others, was used to analyze the pure component data. This model had each site on the adsorbent surface accommodating only one adsorbed molecule with no surface heterogeneities and no interaction between adsorbed molecules. The pure gas isotherms were shown below (their Figure 1), along with the adsorption phase diagram (their Figure 2) and the isosteric heats of adsorption (their Table II).

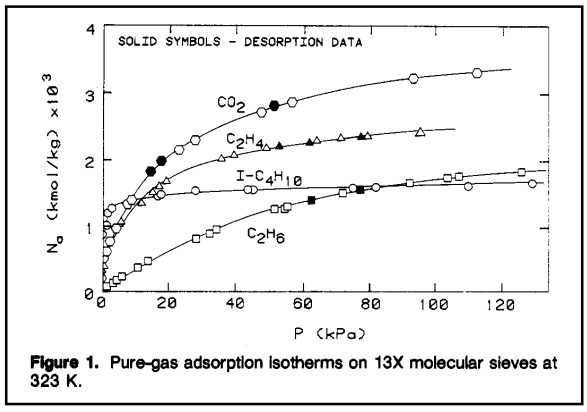

Figure 1. Pure-gas adsorption isotherms on 13X molecular sieves at 323 K.

Table II. Isosteric Heats of Adsorption for the Pure Gases on Molecular Sieve Type 13X

adsorbate gas	10^6(isosteric heat of adsorption), J/kmol			
	Langmuir model	SSTM[a]	VSM[b]	ref value
C_2H_4	27.91	35.75	40.12	38.10
C_2H_6	29.22	32.22	26.71	25.12
$i\text{-}C_4H_{10}$	39.31	43.13	58.93	
CO_2	34.44	33.57	70.67	76.62

[a] Simplified statistical thermodynamic model (*5*). [b] Vacancy solution model (*6*).

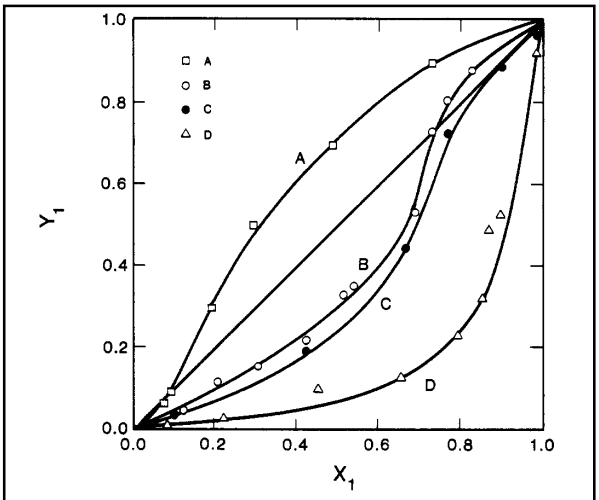

Figure 2. Adsorption phase diagrams for binary mixtures on 13X molecular sieves at 137.8 kPa: (A) C_2H_4 (1)–CO_2 (2) at 298 K; (B) $i\text{-}C_4H_{10}$ (1)–C_2H_4 (2) at 298 K; (C) $i\text{-}C_4H_{10}$ (1)–C_2H_4 (2) at 373 K; (D) $i\text{-}C_4H_{10}$ (1)–C_2H_6 (2) at 298 K.

Adsorption equilibrium isotherms were measured by Delgado, et al, 2006 for carbon dioxide, methane and nitrogen on Na- and H-mordenite at 279, 293 and 308 K for pressures up to 2.0 MPa using a volumetric apparatus. The results are shown in their Figure 2 below. The selectivity for one adsorbent at a given pressure was proportional to its adsorbed concentration, and the selectivity was carbon dioxide >> methane >> nitrogen for both adsorbents. The high selectivity for carbon dioxide was attributed to an electrostatic interaction of the quadrupole moment of carbon dioxide with the sodium cations in the adsorbent micropores. The Clausius-

Clapeyron equation was used to estimate the isosteric heat of adsorption, and the parameters in the Toth model were obtained from the equilibrium isotherm measurements. These results are shown in the following table (their Table 1).

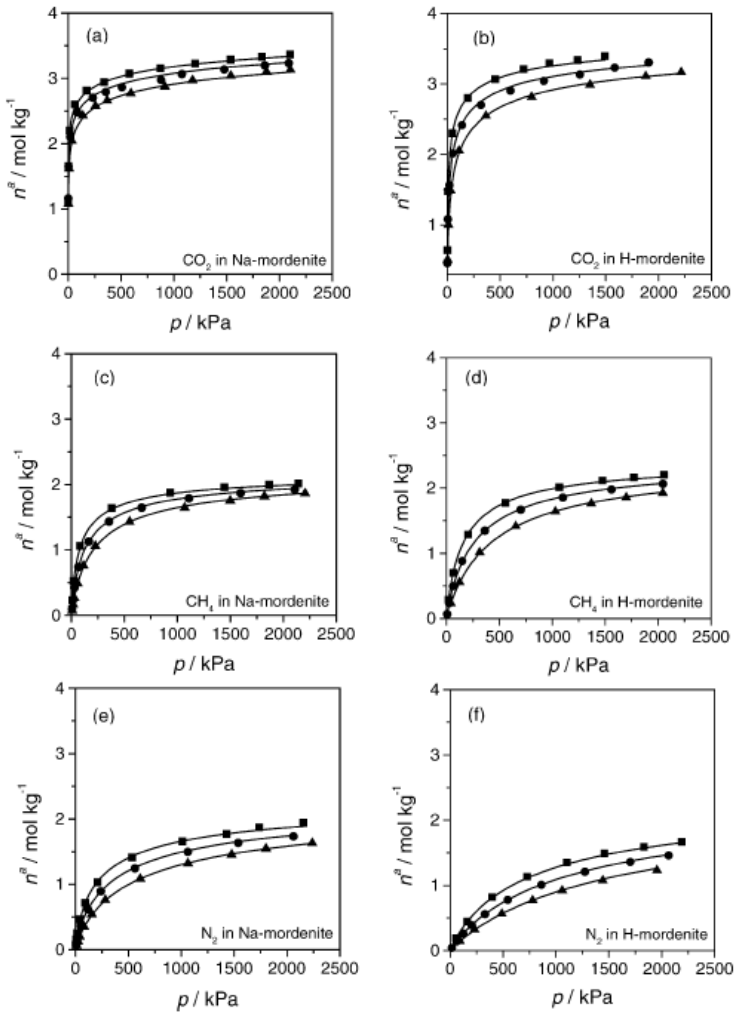

Fig. 2. Adsorption isotherms on mordenite at several temperatures: (a) carbon dioxide on Na-mordenite; (b) carbon dioxide on H-mordenite; (c) methane on Na-mordenite; (d) methane on H-mordenite; (e) nitrogen on Na-mordenite; (f) nitrogen on H-mordenite. (Squares) 279 K; (circles) 293 K; (triangles) 308 K. Lines are calculated with the Toth model.

Table 1
Fitting results for the Toth model

Adsorbent	Na-mordenite			H-mordenite		
Adsorbate	CO_2	CH_4	N_2	CO_2	CH_4	N_2
n^a_{max} (mol kg^{-1})	5.47	2.21	2.39	3.90	2.43	2.44
K_0 (Pa^{-1})	5.00×10^{-17}	5.52×10^{-11}	4.13×10^{-11}	3.65×10^{-12}	7.23×10^{-11}	1.81×10^{-10}
q_{st} (kJ mol^{-1})	103[a]	29.8	28.5	45.0	26.8	21.1
a	0.30	1.38	1.09	0.66	1.46	1.51
b (K)	46	193	131	76	174	200
r^2	0.9987	0.9995	0.9998	0.9984	0.9998	0.9997

[a] Extrapolated value, as equilibrium data are not available at low pressures for this system (in the linear part of the isotherms).

Mass transfer in adsorption was described by Fukunaga, et al, 1868 to be in the following steps: Adsorbate is carried by the bulk transfer in the gas stream, and mass is transferred from the bulk flow to the solid surface of the adsorbent. Mass is transferred from the surface of the adsorbent to the pores of the adsorbent. A model using these steps was developed and was shown to agree with experimental data from a gravimetric apparatus, and this model would apply to desorption, also. Equilibrium isotherms for carbon dioxide on a Linde Type 5A molecular sieve are shown in their Figure 2 below. Mass transfer coefficients were measured from breakthrough curves. The value of $k_a a$ and $k_d a$ were essentially the same, 0.315 lbmols/cu ft-hr-mmHg. There was surface resistance to mass transfer while there was equilibrium in the adsorbent. Vacuum desorption measurements were made, and this data is shown in their Figure 4 below.

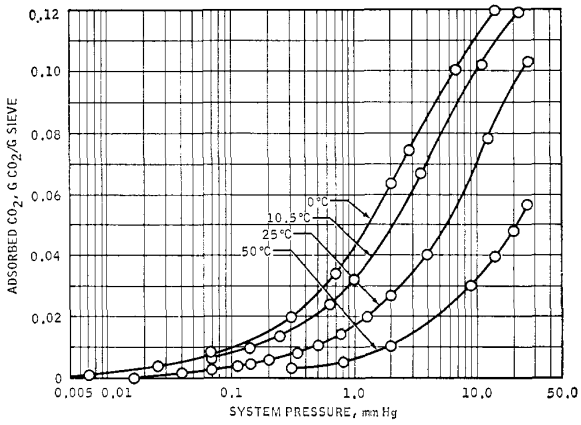

Figure 2. Equilibrium isotherms of CO_2 adsorption on Linde Type 5A molecular sieve

$^1/_{16}$-inch diameter pellets

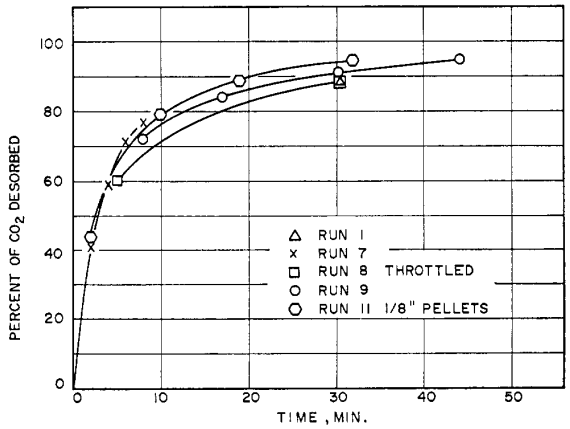

Figure 4. Vacuum desorption of CO_2 from Linde Type 5A molecular sieve at 25° C.

Full vacuum and $^1/_{16}$-inch pellets unless otherwise noted

A cyclic adsorption process simulator was developed and applied to six different high-temperature stripping pressure swing adsorption cycles (PSA) by Reynolds et al, 2006. The carbon dioxide adsorbent was a K-promoted hydrotalcite-like adsorbent, and a typical stack gas at 575 K was studied that had 15% (vol) CO_2. A number of cycle combinations were evaluated, and the best cycles depended on whether performance was measured by CO_2 purity, CO_2 recovered or feed throughput. It was said that this study substantiated the feasibility of a high temperature stripping PSA cycle for CO_2 capture and concentration. In their Table 2 below the parameters used in the model are given and in their Figure 2 below are the CO_2 adsorption isotherms for K-promoted HTlc.

Table 2. Bed Characteristics, Gas-Phase Species, and K-Promoted Hydrotalcite-like (HTlc) Adsorbent Transport and Thermodynamic Properties

parameter	value
Bed, K-Promoted HTlc Adsorbent, and Process Characteristics	
bed length, L (m)	0.2724
bed radius, r_b (m)	0.0387
bed porosity, ϵ	0.48
adsorbent particle density, ρ_p (kg/m^3)	1563
adsorbent particle heat capacity, $C_{p,p}$ (kJ kg^{-1} K^{-1})	0.850
CO_2−HTlc isosteric heat of adsorption, ΔH_i (kJ/mol)	9.29
heat-transfer coefficient, h (kW m^{-2} K^{-1})	0.00067
CO_2−HTlc mass-transfer coefficient (s^{-1})	
adsorption, k_a	0.0058
desorption, k_d	0.0006
feed mole fractions	
CO_2	0.15
N_2	0.75
H_2O	0.10
feed temperature, T_f (K)	575
wall temperature, T_o (K)	575
Adsorption Isotherm Parameters for CO_2 on K-Promoted HTlc	
$q^s_{i,1}$ (mol kg^{-1} K^{-1})	-1.5277×10^{-3}
$q^s_{i,2}$ (mol/kg)	1.7155
b_i^0 (kPa^{-1})	0.0203
B_i^0 (K)	1118.1
Gas (and Adsorbed) Phase Heat-Capacity Coefficients for CO_2, N_2, and H_2O	
A_i (kJ mol^{-1} K^{-1})	
CO_2	1.9795×10^{-2}
N_2	3.1123×10^{-2}
H_2O	3.2221×10^{-2}
B_i (kJ mol^{-1} K^{-2})	
CO_2	7.3437×10^{-5}
N_2	-1.3553×10^{-5}
H_2O	1.9217×10^{-6}
C_i (kJ mol^{-1} K^{-3})	
CO_2	-5.6019×10^{-8}
N_2	2.6772×10^{-8}
H_2O	1.0548×10^{-8}
D_i (kJ mol^{-1} K^{-4})	
CO_2	1.7153×10^{-11}
N_2	1.1671×10^{-11}
H_2O	-3.5930×10^{-12}

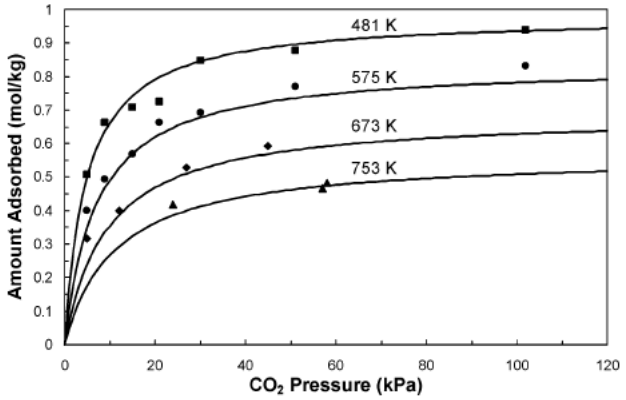

Figure 2. CO_2 adsorption isotherms for K-promoted HTlc. (From Ding and Alpay.[19,22]) Symbols represent experimental data points, and lines represent the fit of the experimental data points to the Langmuir adsorption isotherm model.

Evaluations were conducted on molecular sieves and activated carbon for the preferential adsorption of carbon dioxide from stack gases in a pressure swing adsorption (PSA) process by Siriwardane, et al, 2001. Adsorption and desorption isotherms were measured at 25^{0}C and up to equilibrium pressures of 300 psi (~2.0 MPa) in a volumetric adsorption apparatus. Adsorption-desorption isotherms for pure gases: carbon dioxide, nitrogen and hydrogen are shown in their Figure 1 below for a 13X molecular sieve. An atmospheric micro-reactor was used to evaluate competitive adsorption using a gas mixture of 15% CO_2, 82% N_2, 3%O_2, and water vapor on the molecular sieve at 25^{o}C. The CO_2 concentration decreased to almost zero until breakthrough as shown in their Figure 2 below. Using this data it was determined that the total amount of CO_2

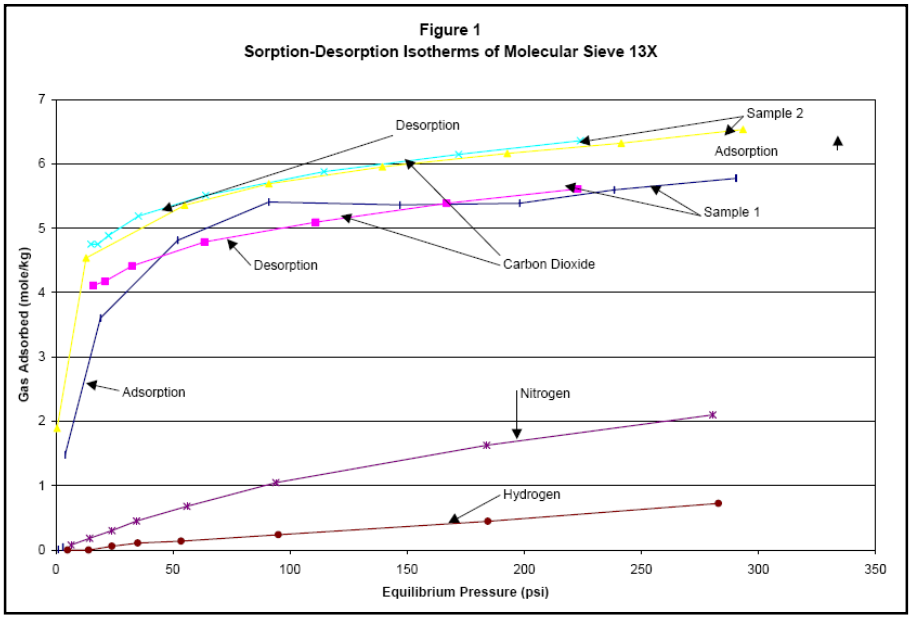

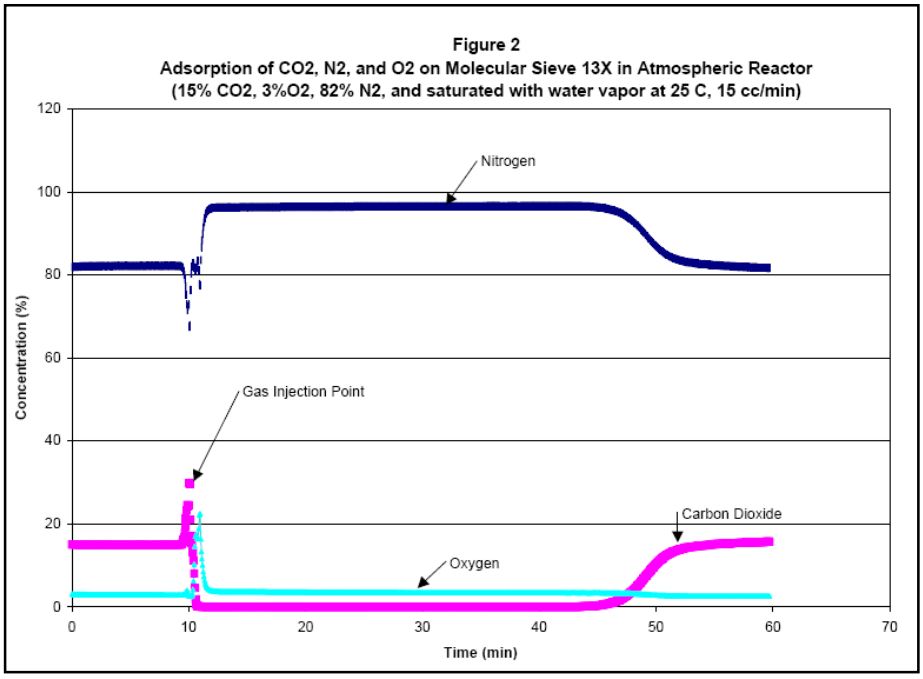

adsorbed was 3.0 moles/kg of adsorbent. Other adsorption studies were conducted at high pressure (250 psi) with 6-7moles/kg at breakthrough. Similar results were obtained with activated carbon.

A thermodynamic analysis was used by Lee, et al 2008 which identified alkali metal carbonates as potential materials to remove carbon dioxide from flue gas. Six adsorbents containing 20 to 50% Na_2CO_3 or $NaHCO_3$ were prepared by spray-drying, and their physical properties and TGA reactivity were determined. It was found that active components perform

more effectively with an appropriate inorganic matrix. The Sorb NX30 adsorbent had the best attrition resistance and reactivity with a spherical shape, 38-250 μm size distribution, bulk density of 0.87 gm/cc, CO_2 adsorption capacity of 10% (>80% sorbent utilization). Almost complete regeneration at less than 120^0C was obtained, and comparable performance was reported with a simulated flue gas to that of amine scrubbing.

An approximate solution to the material and energy balance equations for steam-regeneration of a fixed bed adsorber was developed by Schweiger, 1996. As shown in their Figure 1, first the effluent is a slow purge of inert gases at equilibrium with the adsorbent. Then a wave of desorbed solvent was said to roll-up ahead of the steam and saturate the adsorbent's pore structure and overflow. The solvent was said to behave as though it was being steam-distilled, and the water miscible solvent left at a high purity at a temperature approaching the boiling point. A second wave had a sudden drop in solvent concentration and a simultaneous rise in steam concentration and temperature. Following this wave, the steam acted as a purge gas. Regeneration was halted at this point since little additional solvent was desorbed. If the solvent's adsorption was not affected by water adsorption, the temperature throughout the adsorber was that of saturated steam. If the adsorption is "well characterized", the temperature, T, adsorbed phase concentration for water, q_w, and dimensionless velocity, $v^* = v/v_{in}$, can be determined from material and energy balance equations. The solvent desorption and water adsorption were related by an energy balance, and the difference between the heats of adsorption of the solvent and water meant that each mole of solvent that desorbs was not matched by the adsorption of one mole of water. Experimental and predicted recoveries were shown in their Table 1 for hexane and Freon-11, but the adsorbent was not specified in the paper. Steam use was about 0.2 kg steam/kg adsorbent, and solvent recovery was about 0.15 kg solvent/ kg adsorbent or about 0.2/0.15 = 1.3 kg steam/kg solvent.

Table 1. Predicted and Experimental Solvent Recoveries

			steam use	solvent recovery (kg/kg)		
exp	solvent	y_a	(kg/kg)	numerical	shortcut	expt
2	hexane	0.022	0.260	0.153	0.157	0.156
4	hexane	0.0024	0.169	0.090	0.096	0.081
5	hexane	0.175	0.201	0.195	0.201	0.171
plant	Freon-11	0.020	0.150		0.140	0.127

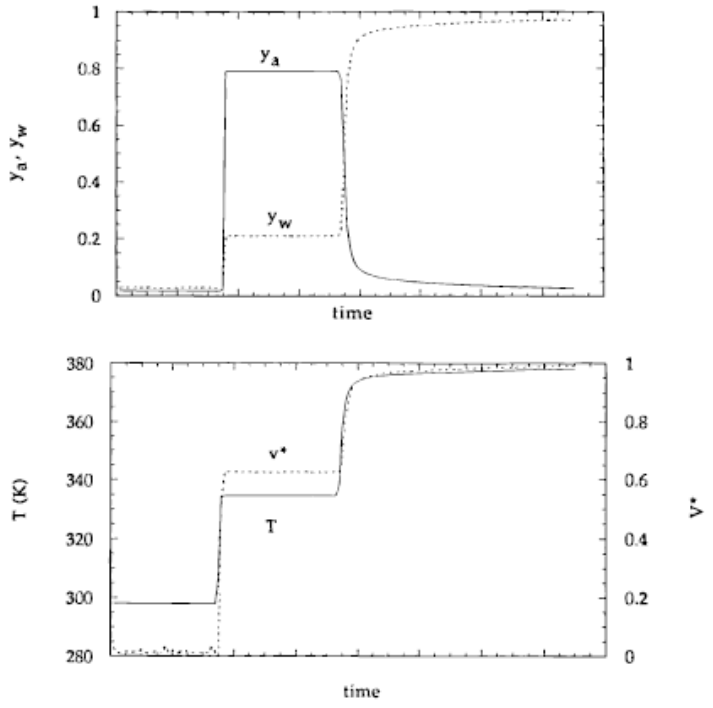

Figure 1. Typical conditions at the outlet of an adsorber during steam regeneration.

Electrobalance and fixed-bed reactors have been used by Liang and Harrison, 2004, to study the capture of CO2 from simulated flue gas using a regenerable Na_2CO_3 sorbent. The important reactions involved in the capture of CO_2 using Na_2CO_3 are:

$$Na_2CO_3(s) + CO_2(g) + H_2O(g) \leftrightarrow 2NaHCO_3(s) \quad (1)$$

$$\Delta H_r^\circ = -135 \text{ kJ/mol } Na_2CO_3$$

$$Na_2CO_3(s) + 0.6CO_2(g) + 0.6H_2O(g) \leftrightarrow 0.4[Na_2CO_3 \cdot 3NaHCO_3](s) \quad (2)$$

$$\Delta H_r^\circ = -82 \text{ kJ/mol } Na_2CO_3$$

CO_2 capture was effective in the temperature range of 60-70 °C, while regeneration occurred in the range of 120-200 °C, depending on the partial pressure of CO_2 in the regeneration gas. Equal molar quantities of CO_2 and H_2O are produced during sorbent regeneration, and pure CO_2 suitable for use or sequestration is available after condensation of the H_2O. Capture of as much as 90% of the CO_2 was possible at appropriate reaction conditions and little or no reduction in either carbonation rate or sorbent capacity was observed in limited multicycle tests. The concept is potentially applicable to the capture of CO_2 from existing fossil fuel-fired power plants, where amine scrubbing is the only CO_2 capture process currently available.

A novel potassium-based dry sorbent (KZrI) was developed for CO_2 capture at a low temperature range between 50^0C and 200^0C by Lee, et al, 2009. The CO_2 absorption and regeneration properties of this novel regenerable potassium-based dry sorbent were measured in a fixed-bed reactor during multiple absorption/regeneration cycles at low temperature conditions (CO_2 absorption at 50–100^0C and regeneration at 130–200^0C). The total CO_2 capture capacity of the KZrI sorbent was maintained during the multiple CO_2 absorption/regeneration cycles. The XRD patterns and FTIR analyses of the sorbents after CO_2 absorption showed the $KHCO_3$ phase only except for the ZrO_2 phase used as support. Even after 10 cycles, any other new structures resulting from the by-product during CO_2 absorption were not observed. This phase could be easily converted into the original phase during regeneration, even at a low temperature (130^0C). The KZrI sorbent developed in this study showed excellent characteristics in CO_2 absorption and regeneration in that it satisfies the requirements of a large amount of CO_2 absorption (91.6mg CO_2/g sorbent), and complete regeneration at a low temperature condition (1.0 atms., 150^0C) without deactivation.

The effect of bed height on CO_2 capture was investigated using carbonation/regeneration cyclic operations in a bubbling fluidized bed reactor by Park, et al, 2009. A potassium-based solid sorbent, SorbKX35T5 was used which was manufactured by the Korea Electric Power Research Institute. The sorbent consists of 35% K_2CO_3 for absorption and 65% supporters for mechanical strength. They used a fluidized bed reactor with an inner diameter of 0.05 m and a height of 0.8 m which was made of quartz and placed inside of a furnace. The operating temperatures were fixed at 70^0C and 150^0C for carbonation and regeneration, respectively. The carbonation/regeneration cyclic operations were performed three times at four different L/D (length vs. diameter) ratios such as one, two, three, and four. The amount of CO_2 captured was

the most when the L/D ratio was one, while the period of maintaining 100% CO_2 removal was the longest as 6.0 minutes when L/D ratio was three. At each cycle, CO_2 sorption capacity (g CO_2/g sorbent) was decreased as L/D ratio was increased. The results obtained in this study can be applied to design and operate a large scale CO_2 capture process composed of two fluidized bed reactors.

Thermal swing adsorption cycles in fixed beds were investigated by Davis and Le Van, 1989, using experiments and modeling to obtain the influence of process parameters on energy use and purge gas consumption. Cycle step times and regeneration conditions must be set to minimize costs. Objective functions involve heating and cooling demands, determining the extent of regeneration, and quantities of product produced. Experiments have been performed with a computer-controlled, pilot-scale, fixed-bed apparatus with n-hexane adsorbed from air onto BPL-activated carbon. The results agree well with model predictions. Short regeneration times were found to be efficient for energy and purge gas use. Proper timing of the cooling step can lead to significant energy savings.

A "How to" Guide was available from Knaebel, 2002 that gave an overview of adsorber design calculations. The U. S. Army Corps of Engineers, 2001, had developed an adsorption design guide that was said "to provide practical guidance for the design of liquid and vapor devices for the adsorption of organic chemicals." The Adsorption chapter in the Handbook of Separation Process Technology (Keller et al, 1987) describes adsorbents, cycles, flowsheets and process design considerations. The Adsorption and Ion Exchange chapter in the Chemical Process Equipment – Selection and Design (Walas, 1990) gave an overview of design procedures and process equipment. The Adsorption and Ion Exchange chapter in *Perry's Handbook* (Le Van and Carta, 2008) provided a detailed discussion of adsorption and ion exchange for process design. The *Yaws' Handbook of Thermodynamic and Physical Properties of Chemical Compounds* (Yaws, 2003) had data for the adsorption on activated carbon shown in the diagram but no data for water. Experimental measurements and analysis of data for adsorption isotherms were discussed in detail by Keller and Staudt, 2005. Purification of gas streams was described in *Gas Purification* by Kohl and Nielson, 1997 using molecular sieves for water and silica gel for hydrocarbons.

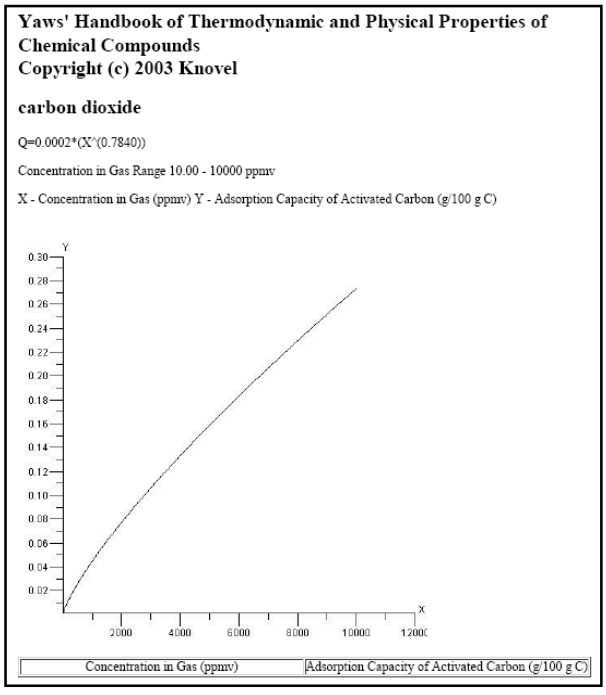

A comprehensive text by Yang, 1987, *Gas Separation by Adsorption Processes* covers equilibrium and rate processes, steady-state and dynamic adsorption and cyclic and pressure-swing adsorber operations. A practical guide to adsorption by Basmadjian, 1997, covers many aspects of adsorber design, and it states that with temperature rises of $>2^0$C an energy balance under equilibrium conditions provides an accurate estimate of the maximum temperature rise,

(see Equation 4.2, p.54). The text by Wankat, 1990, entitled *Rate-Controlled Separations* has chapters on sorption in packed columns described by linear and nonlinear theories, simulated moving beds, sequencing operations, among others. The notes that purge gas and desorbing systems were more complicated than pressure swing and thermal swing systems and were used only when necessary (p. 433). Moving bed adsorbers were mentioned on p. 500. An edited book by Slejko, 1985, on *Adsorption Technology: A Step by Step Approach to Process Evaluation and Application* included chapters by experts on adsorption theory and experiment, conceptual design and recovery of chemicals from liquids. The standard text by Ruthven, 1984, provided discussions of adsorbent characteristics, adsorption equilibria and kinetics, diffusion and flow through packed beds, the dynamics of single and multiple columns and cyclic systems. Most unit operations books have a chapter on adsorber design, and the chapter in McCabe, Smith and Harriott, 2001 was reasonably comprehensive.

Summary: An exploratory design study conducted by Yang and Hoffman, 2009 had results for carbon dioxide removal from a flue gas from a 500 MW power plant.

Flue gas flow rate of 3.4×10^4 m^3/min
Available pressure drop of 0.21 bar (3.0 psi)
Carbon dioxide concentration of ~20%
90% carbon dioxide removal
Dry, regenerable, amine-enhanced solid adsorbent
Carrying capacity of 0.264 kg CO_2/kg adsorbent
Adsorber operated at 54^0C (130^0F) with fast kinetics
Regenerator operated at 99^0C (210^0F) with slow kinetics
Dense bubbling fluidized bed
Fluidized bed operating velocities
1.5 m/sec (5.0 ft/sec), 1.2 m/sec (4.0 ft/sec) and 0.9 m/sec (3.0 ft/sec)
Effective rate constant, K_f, of 2.04 sec^{-1} for a first order reaction
Minimum bed depth of 2.4 m operating with a velocity 1.34 m/sec

Modeling and experimental studies on steam regeneration of activated carbon beds with adsorbed n-hexane were made by Schweiger and Le Van, 1993. They developed a one-dimensional, time dependent model using the species continuity and energy equations that used local equilibrium in a fixed bed. For adsorption equilibria of water and n-hexane, equations were given for pure components and for the interaction between water and n-hexane in the adsorbed phase where the interaction was significant, and adsorbed water displaced the n-hexane. Their model results agreed with experiments, and they stated that water competed with the solvent for pore volume. Water must condense to provide the heat to desorb the larger quantity of solvent at the higher initial loading.

Regeneration of activated carbon bed with steam was evaluated by Schork and Fair, 1998. The rate of desorption was a strong function of temperature, and high temperatures were necessary to prevent long drying times. Steam generation cycles in industrial practice would be much shorter, and a rule of thumb is 4.0 lb steam per lb adsorbed organic.

In the Adsorption Equilibrium Data Handbook (Valenzuela and Myers, 1989), there were eight single-gas adsorption isotherms for carbon dioxide mainly on activated carbon with constants for the Toth and UNILAN equations. There was no data for water. Procedures were described to calculate mixed-gas adsorption from single-gas isotherms using a general algorithm from IAS theory.

A static, volumetric method was used by Hyun and Danner, 1982 to determine the adsorption equilibrium of ethane, ethylene, isobutene and carbon dioxide and their binary mixtures on 13X molecular sieves at a total pressure of 137.8 kPa and temperatures of 298, 323, and 373 K. The Langmuir model, the simplest among others, was used to analyze the pure component data. This model had each site on the adsorbent surface accommodating only one adsorbed molecule with no surface heterogeneities and no interaction between adsorbed molecules.

Adsorption equilibrium isotherms were measured by Delgado, et al, 2006 for carbon dioxide, methane and nitrogen on Na- and H- mordenite at 279, 293 and 308 K for pressures up to 2.0 MPa using a volumetric apparatus. The selectivity for one adsorbent at a given pressure was proportional to its adsorbed concentration, and the selectivity was carbon dioxide >> methane >> nitrogen for both adsorbents. The parameters in the Toth model were obtained from the equilibrium isotherm measurements.

Mass transfer in adsorption was described by Fukunaga, et al, 1868. Equilibrium isotherms for carbon dioxide on a Linde Type 5A molecular sieve were obtained, and mass transfer coefficients were measured from breakthrough curves. The value of $k_a a$ and $k_d a$ were essentially the same, 0.315 lbmols/cu ft-hr-mmHg. There was surface resistance to mass transfer while there was equilibrium in the adsorbent.

Adsorption and desorption isotherms were measured for molecular sieves and activated carbon for the preferential adsorption of carbon dioxide from stack gases at 25^0C and up to equilibrium pressures of 300 psi (~2.0 MPa) by Siriwardane, et al, 2001. An atmospheric micro-reactor was used to evaluate competitive adsorption using a gas mixture of 15% CO_2, 82% N_2, 3% O_2, and water vapor on the molecular sieve at 25^oC. The CO_2 concentration decreases to almost zero until breakthrough, and the total amount of adsorbed was 3.0 moles/kg of adsorbent.

Lee, et al 2008 reported that Sorb NX30 adsorbent had the best attrition resistance and reactivity with a spherical shape, 38-250 μm size distribution, bulk density of 0.87 gm/cc, CO_2 adsorption capacity of 10% (>80% sorbent utilization). There was almost complete regeneration at less than 120^0C.

Appendix D: Fixed Bed Adsorber and Regenerator Designs

The following sections describe the fixed bed adsorber and regenerator designs and downstream processing to deliver CO2 to sequestration using flue gas from the AEP's Conesville #5 Power Plant. The designs are based on the procedure described in several books, including McCabe, Smith and Harriott, 2001 and Lyderson, 1983. The simulation of the Conesville #5 Power Plant has been validated against plant operational data. The adsorber and regenerator designs are being extended to include nonisothermal operations, and the power plant operations have been evaluated for the off-design case that produces steam and power for operation of the adsorber/regeneration process.

Adsorber Design

Referring to Figure D-1, the procedure for the design of the adsorber uses the following steps.

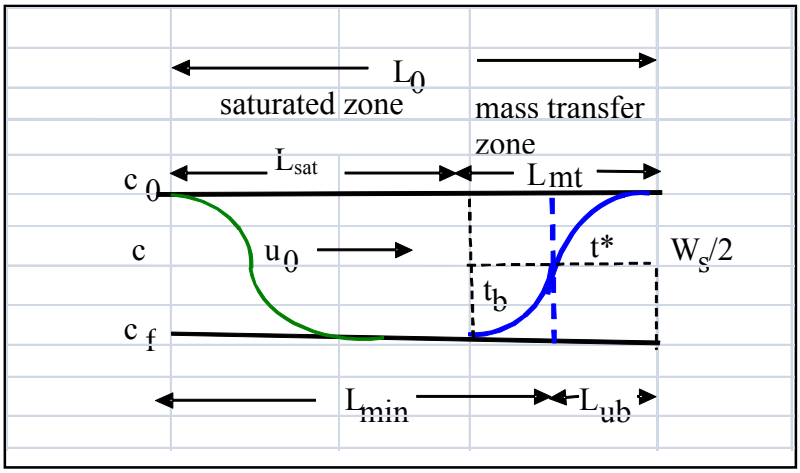

Figure D-1 Adsorber Diagram

1. For a known inlet carbon dioxide composition, c_0, to the adsorber and specified recovery of adsorbate (90% wt), the material balance around the adsorber is completed.

For a specified superficial velocity, u_0, in the adsorber, the cross-sectional area of the adsorber bed is evaluated, and the diameter of the bed, D, is determined for a circular cross-section.

2. The minimum bed length, L_{min}, is evaluated by a material balance knowing the equilibrium adsorption (saturated loading), W_s,, initial loading, W_0, initial adsorbate concentration in the gas, c_0, adsorbent bulk density, ρ_b, and ideal adsorption time for a vertical breakthrough curve, t*, that specifies cycle time for adsorber to give minimum length

3. The length of the mass transfer zone, L_{mt}, is evaluated using a material balance and rate equations for mass transfer from the bulk fluid to the gas solid interface and from this interface into the pores of the adsorbent.

4. The saturation zone length and the total bed length are evaluated based on the ideal adsorption time for a vertical breakthrough curve, t*, that specifies cycle time for adsorber to give the minimum length.

5. The breakthrough time is determined.

Specified Recovery of Adsorbate (90% CO_2): The inlet and outlet compositions to the adsorber are shown in Figure D-2 for a 90% wt recovery of CO_2 from flue gas by the adsorber. Inlet CO_2 mass flow rate is 866,156 lb/hr and the exit flow rate is 86,616 lb/hr with 779,540 lb/hr of CO2 captured.

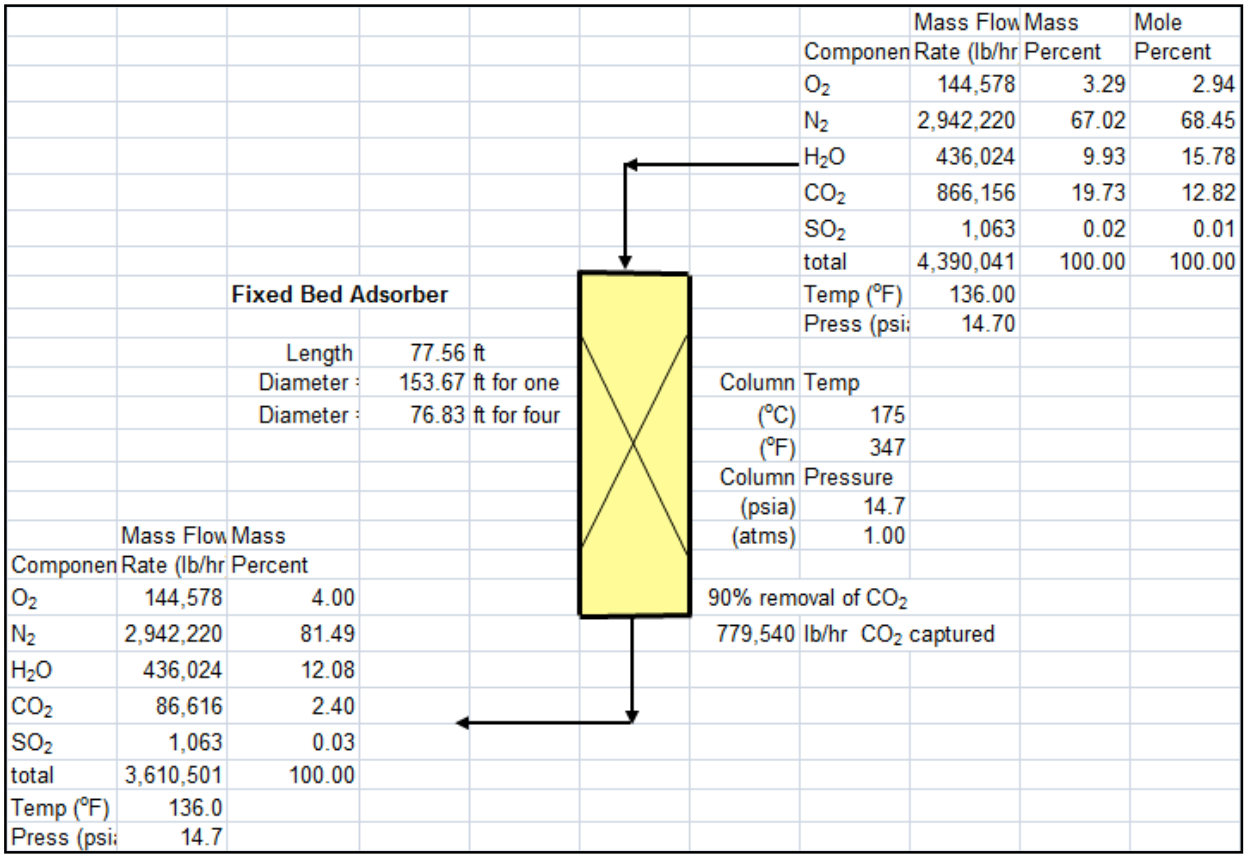

Componen	Mass Flow Rate (lb/hr	Mass Percent	Mole Percent
O_2	144,578	3.29	2.94
N_2	2,942,220	67.02	68.45
H_2O	436,024	9.93	15.78
CO_2	866,156	19.73	12.82
SO_2	1,063	0.02	0.01
total	4,390,041	100.00	100.00
Temp (°F)	136.00		
Press (psi	14.70		

Componen	Mass Flow Rate (lb/hr	Mass Percent
O_2	144,578	4.00
N_2	2,942,220	81.49
H_2O	436,024	12.08
CO_2	86,616	2.40
SO_2	1,063	0.03
total	3,610,501	100.00
Temp (°F)	136.0	
Press (psi	14.7	

Figure D-2 Flow Rates and Compositions to and from the Adsorber for 90% Recovery of CO_2 based on AEP's Conesville #5 Power Plant (Ramezan, 2007b) Stream 7, Flow from FGD to Stack (Table 2-1, p. 14, DOE Final Report Revised November 2007 DOE/NETL-401/110907)

Adsorber Bed Area: For a specified superficial velocity, u_0, in the adsorber, the cross-sectional area of the bed, A, is evaluated using the definition of the mass flow rate of the stack gas, m_g, that is equal to the density of the stack gas, ρ_g, times the cross-sectional area of the bed, A, times the gas superficial velocity, u_0.

$$m_g = \rho_g A\, u_0 \tag{D-1}$$

Using 359 s-ft^3/lb mol, and the volumetric flow rate, Q, the above equation can be written as:

$$A = m_g / u_0 \rho_g = Q / u_0 \quad and \quad Q = \frac{m_g}{Mw} \cdot \frac{359 sft^3}{lb-mol} \cdot \frac{T}{T_{ref}} \quad and \quad A = Q / u_0 \tag{D-2}$$

The temperature ratio adjusts the gas temperature from the reference temperature (32^0F) of the gas flowing in the adsorber.

The diameter of the bed (D) is determined for a circular cross-section by the following equation.

$$D = \left(4A / \pi\right)^{1/2} \tag{D-3}$$

Referring to Figure D-2, the following values were used to determine, A and D: m_g = 4,390,041 lb/hr, M_w = 28.60, T = 136^0F, volumetric flow rate, Q, = 18,546 ft^3/sec. Using u_0 = 1.0 ft/sec, the cross sectional area of the bed is, A, = 18,546 ft^2. For a circular cross-section the diameter, D = 153.7 ft for one adsorber, and for four adsorbers their diameter are D = 76.8 ft. For a superficial velocity of 2.0 ft/sec, the adsorber cross-section is 9,273 ft^2, and the diameter is 108.7 ft.

Equilibrium Adsorption: An adsorption isotherm gives the equilibrium relation between the concentration in the gas phase and the concentration in the gas phase that is equilibrium with the adsorbent at a given temperature. For gases the concentration is usually given in mole percent, and the concentration of adsorbate on the adsorbent is given as mass adsorbed per unit mass of original adsorbent. Linear isotherms go through the origin, and the amount adsorbed is proportional to the concentration in the fluid. Equilibrium isotherms that are concave upward are called favorable, because a relatively high solid loading can be obtained at low concentrations in the fluid. The limiting case of a very favorable isothermal is irreversible adsorption where the amount adsorbed is independent of concentration down to very low values. An isotherm that is concave upward is unfavorable because relatively low solid loadings are obtained, and there is a long mass transfer zone in the bed (McCabe, et al., 2001).

Equilibrium adsorption data has been reported for TDA Research's solid adsorbent in terms of loading as a function of CO_2 concentration and temperature. The theoretical maximum loading was reported to be ~9.0 %wt or 0.099 lb CO_2/lb adsorbent (Copeland, 2008) which was used in the adsorber design evaluations.

Equilibrium adsorption data for CO_2 on various adsorbents from the literature is summarized below in Table D-1. The standard reference is *The Adsorption Equilibrium Data Handbook* by Valenzuela and Myers, 1989; and this handbook contains data that was tabulated in journal articles, not including plots of data. It has nine adsorbents for CO_2 that are listed in Table D-1, and there are values of the parameters for the Toth model. (2.5 mmole/gm = 0.11

gm/gm). Perry's Chemical Engineers Handbook (Green and Perry, 2008) has tabulated data for the capacity of a number of adsorbents without reference to the adsorbate.

Table D-1 Equilibrium Adsorption Capacity for Carbon Dioxide on Various Adsorbents

		P and T		
Adsorbent	Capacity	kPa	K	Source
Carbon fiber	2.5 (mmole/gm)	100	273	Valenzuela & Myers, 1989
Activated carbon	1.5 (mmole/gm)	100	273	Valenzuela & Myers, 1989
Activated carbon	2.5 (mmole/gm)	100	273	Valenzuela & Myers, 1989
Activated carbon	5.0 (mmole/gm)	100	273	Valenzuela & Myers, 1989
Activated carbon	0.003 (gm/gm)	ns	ns	Yaws, 1999
Zeolite	4.0 (mmole/gm)	100	273	Valenzuela & Myers, 1989
Mordenite	2.5 (mmole/gm)	100	273	Valenzuela & Myers, 1989
Impregnated BPL	1.5 (mmole/gm)	100	273	Valenzuela & Myers, 1989
Columbia grade	1.6 (mmole/gm)	100	273	Valenzuela & Myers, 1989
BPL Pitt Chem. Co.	10.0 (mmole/gm)	100	273	Valenzuela & Myers, 1989
PPC Calgon	9.0 (mmole/gm)	100	273	Valenzuela & Myers,1989
ns	1.4 (mmole/gm)	100	223	Ruthven, 1984
4A Mol Sieve	0.14 (lb/lb)	100	323	Kohl & Nielson, 1997
5A Mol Sieve	0.65 (lb/lb)	50	323	Fukunaga, et al., 1968
13X Mol Sieve	6.5 (moles/kg)	1,700	295	Siriwardane, et al., 2001
13X Mol Sieve	0.1 (gm/gm)	20	596	Hyun and Danner, 1982
K-promoted HTlc	0.8 (kg/kg)	100	753	Reynolds, et al., 2006
Sorb NX30	0.10 (gm/gm)	101	323	Lee, et al., 2008
Mordenite	0.15 (gm/gm)	800	308	Delgado, et al., 2006
Various	0.10-0.50 (kg/kg)	ns	ns	Green and Perry, 2008

Minimum Bed Length: Referring to the adsorber diagram in Figure D-1, the minimum bed length, $L_{\min}$, for the adsorber is the case where the concentration profile is vertical and moves with a superficial velocity of u_0. The bed is saturated from the entrance to the vertical concentration profile. The time t* is the ideal adsorption time (hr) for a vertical breakthrough curve, and it is the cycle time for adsorber to have a minimum length.

A material balance can be written equating the amount of adsorbate in the fluid, Au_0ct^* equal to the amount of adsorbate that was transferred, $L_{\min}A\rho_b(W_s - W_0)$, over the time period, t*.

$$Au_0c_0t^* = L_{\min}A\rho_b(W_s - W_0) \tag{D-4}$$

This equation is used to determine the minimum bed length, $L_{\min}$, for a specified value of the cycle time for the adsorber, t*.

$$L_{\min} = u_0c_0t^* / \rho_b(W_s - W_0) \tag{D-5}$$

In this equation, ρ_b is the bulk density of the adsorbent, and W_s and W_0 are the saturated and initial value of the loading.

Applying Equation D-5 and using the theoretical maximum loading W_s of 9.0 % wt or 0.099 lb CO_2/lb adsorbent and no carbon dioxide on the adsorbent initially, W_0 = 0, the minimum bed length, $L_{\min}$, is 77.23 ft for t* = 8.0 hrs, the ideal adsorption time, and u_0 = 1.0 ft/sec. The time, t*, is called the cycle time for the minimum length of the adsorber. The minimum bed length increases to 154.5 ft for a superficial velocity of 2.0 ft/sec.

Mass Transfer and Saturated Zones: Referring to Figure D-1, the length of the saturation zone, L_{sat}, is the length where the adsorbent had been saturated with adsorbate. In the length of the mass transfer zone, L_{mt}, the rate of mass transfer, m_c of the adsorbate from the fluid to the adsorbent was described by an overall mass transfer coefficient, K_c, which incorporated a diffusion coefficient from the bulk flow to the surface of the adsorbent, $k_{c,ext}$ and a diffusion coefficient from the surface of the adsorbent into the pores of the adsorbent, $k_{c,int}$. These coefficients are related by the following equation.

$$\frac{1}{K_c} = \frac{1}{k_{c,ext}} + \frac{1}{k_{c,\text{int}}} \qquad \text{(D-6)}$$

Methods to evaluate $k_{c,ext}$ and $k_{c,\text{int}}$ are given by McCabe, et al., 2001 and Hutchinson, 1997. Following these procedures a value for K_c of 0.25 cm/sec was estimated.

The rate of mass transfer is given by the following equation.

$$m_c = K_c a(c - c^*) \qquad \text{(D-7)}$$

In this equation a is the mass transfer area that is given by the external surface area of the adsorbent, c is the concentration of the adsorbate in the bulk flow and c* is the concentration of the adsorbate in equilibrium with the concentration in the solid as measured by W_s. A typical value of a is 13.0 cm^2/cm^3 (Hutchinson, 1997).

As shown in Figure D-3, to relate the rate of mass transfer from the bulk fluid to the solid adsorbent, the species continuity equation is applied to a section of adsorber length, dL_{mt}, in the mass transfer zone. There is an accumulation (depletion) of c in the differential volume, AdL_{mt}, that is equal to the mass flow rate into and out of the control volume, AdL_{mt}. In this control volume the concentration of the adsorbate in the bulk flow decreases, and the concentration of the adsorbate in the adsorbent increase as measured by the change in adsorbate loading. The control volume with solids and voids can be described in terms of the porosity, ε, (volume of voids per total volume).

The change of mass of c, the concentration of the adsorbate, with time in the voids is:

$$\frac{\partial}{\partial t}\varepsilon A dL_{mt} c = \varepsilon A dL_{mt}\frac{\partial c}{\partial t} \tag{D-8}$$

The change of mass of W, the concentration (loading) of the adsorbate on the adsorbent, with time in the porous solid is:

$$\frac{\partial}{\partial t}\left((1-\varepsilon)A dL_{mt}\rho_p W\right) = (1-\varepsilon)A dL_{mt}\rho_p\frac{\partial W}{\partial t} \tag{D-9}$$

In this equation, ρ_p is the particle density, and W is the adsorbent loading.

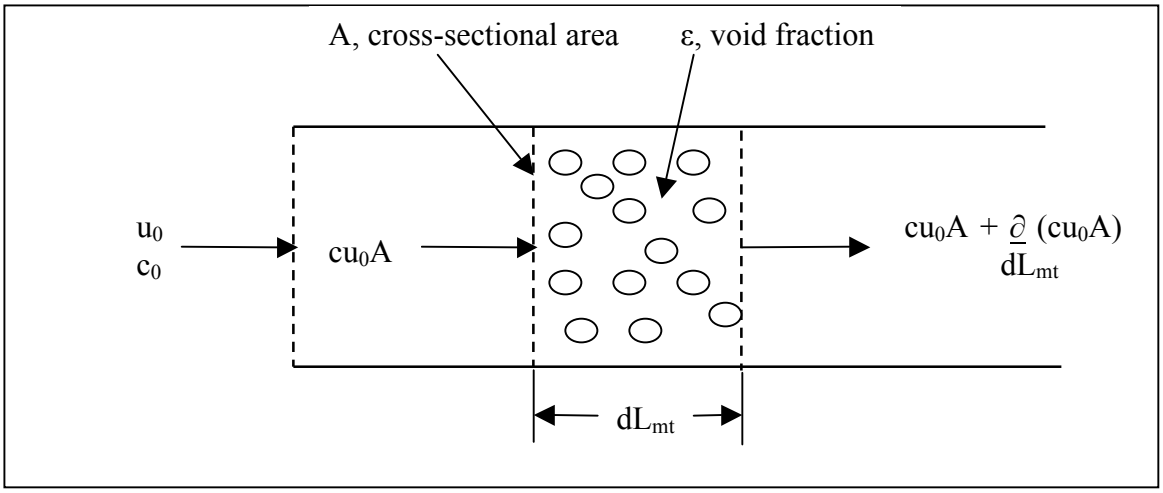

Figure D-3 Species Material Balance on a Differential Section of the Adsorber in the Mass Transfer Zone

In the adsorber control volume of AdL_{mt}, the species continuity equation has the mass accumulation of c equal to the mass flow rate of c into the control volume minus the mass flow rate of c from the control volume (acc = input – output), as shown in Figure D-3.

Mass flow rate into the control volume = $cu_0 A$ (D-10)

Mass flow rate from the control volume = $cu_0 A + \frac{\partial cu_0 A}{\partial L}dL = cu_0 A + u_0 A\frac{\partial c}{\partial L}dL$ (D-11)

Combining Equations D-9, D-10 and D-11 gives:

$$\varepsilon A dL_{mt}\frac{\partial c}{\partial t} + (1-\varepsilon)A dL_{mt}\rho_p\frac{\partial W}{\partial t} = cu_0 A - cu_0 A - u_0 A\frac{\partial c}{\partial L}dL_{mt} \tag{D-12}$$

Simplifying gives:

$$\varepsilon \frac{\partial c}{\partial t} + (1-\varepsilon)\rho_p \frac{\partial W}{\partial t} = -u_0 \frac{\partial c}{\partial L} \tag{D-13}$$

The second term on the left hand side is the rate of mass transfer of c from the bulk of the fluid to the pores that is described by Equation D-7.

$$m_c = K_c a(c - c^*) = (1-\varepsilon)\rho_p \frac{\partial W}{\partial t} \tag{D-14}$$

Equation 13 can be written as:

$$\varepsilon \frac{\partial c}{\partial t} + K_c a(c - c^*) = -u_0 \frac{\partial c}{\partial L} \tag{D-15}$$

The first term on the left is the accumulation (depletion) with time of the adsorbate in the bulk fluid. This term is usually very small compared to the second term which is the accumulation with time of adsorbate on the porous solid. Neglecting the first term on the left as small compared to the other terms gives:

$$K_c a(c - c^*) = -u_0 \frac{\partial c}{\partial L} \tag{D-16}$$

Strongly favorable adsorption has the equilibrium concentration c* essentially zero and Equation D-16 can be integrated over the mass transfer zone to give:

$$\ln \frac{c}{c_0} = -\frac{K_c a L_{mt}}{u_0} \tag{D-17}$$

This equation is used to determine the length of the mass transfer zone, L_{mt}.

$$L_{mt} = \frac{u_0}{K_c a} \ln \frac{c}{c_0} \tag{D-18}$$

Using $c/c_0 = 0.12$, $u_0 = 1.0$ ft/sec, and $K_c a = 3.275$ sec^{-1}, the value of $L_{mt} = 0.64$ ft. Repeating the evaluation with $u_0 = 2.0$ ft/sec gives $L_{mt} = 1.27$ ft.

Referring to Figure 1, the total length of the adsorber bed is the sum of the saturated bed and the mass transfer zone, $L_0 = L_{sat} + L_{mt}$. The amount of adsorbate in the mass transfer zone can be evaluated using a symmetric breakthrough curve with equilibrium adsorption having W = 0.5 W_s. The amount of CO_2 adsorbate in this zone is:

$$L_{mt} A \rho_b W_s / 2 \tag{D-19}$$

Referring to Equation D-4, the total amount of CO_2 adsorbate transferred to the adsorbent for time t* is given by:

$$t^* u_0 c_0 A \tag{D-20}$$

The saturated zone holds the total amount of adsorbent transferred for t* minus the amount in the mass transfer zone.

$$L_{sat} A \rho_b W_s = t^* u_0 c_0 A - L_{mt} A \rho_b W_s / 2 \tag{D-21}$$

This equation can be written as:

$$L_{sat} = (t^* u_0 c_0 - L_{mt} \rho_b W_s / 2) / W_s \rho_b A \tag{D-22}$$

Referring to Figure 1, the total length of the adsorber bed is the sum of the saturated bed length, L_{sat} = 76.91 ft, and the mass transfer zone length, L_{mt} = 0.64 gives:

$$L_0 = L_{sat} + L_{mt} = \quad 76.91 + 0.64 = 77.56 \text{ ft}$$

Breakthrough Time: The breakthrough time is determined by writing two differential mass balances on the transfer of the mass of the adsorbate, m_c, from the bulk fluid to the surface adsorbent and from the surface to the pores of the adsorbent.

For the rate of accumulation (depletion) differential amount of mass of c transferred from the bulk of the gas to the surface of the adsorbent in the length dL is (acc = input – output):

$$\frac{dm_c}{dt} = cu_0 A - \left(cu0A + \frac{\partial cu_0 A}{\partial L} dL \right) \tag{D-23}$$

For the differential amount of mass of c transferred from the surface of the adsorbent to the pores of the adsorbent in the length dL is:

$$dm_c = (W_s - W_0) \rho_b A dL \tag{D-24}$$

Simplifying Equation D-23 gives:

$$\frac{dm_c}{dt} = -u_0 A dc = -u_0 (c_f - c_0) \tag{D-(25)}$$

where dc is equal to ($c_f - c_0$), the change in concentration across the stoichiometric front.

Writing Equation D-24 as:

$$\frac{dm_c}{dL} = (W_s - W_0)\rho_b A \tag{D-26}$$

Eliminating dm_c by combining Equations D-25 and D-26 and rearranging, the result is:

$$dL = \frac{u_0(c_0 - c_f)}{(W_s - W_0)\rho_b} dt \tag{D-27}$$

Referring to Figure D-1, Equation D-27 can be integrated between limits of L = 0 at t = 0 and to $L = L_{min}$ at t* to give:

$$L_{\min} = \frac{u_0(c_0 - c_f)}{(W_s - W_0)\rho_b} t^* \tag{D-28}$$

Referring to Figure 1, Equation D-27 can be integrated between limits of L = 0 at t = 0 and $L = L_{sat}$ at $t = t_b$ to give:

$$L_{sat} = \frac{u_0(c_0 - c_f)}{(W_s - W_0)\rho_b} t_b \tag{D-29}$$

Combining Equations D-28 and D-29, using $L_{sat} = L_0 - L_{mt}$, $L_{min} = L_0 - L_{ub}$ and $2L_{ub} = L_{mt}$, rearranging gives:

$$\frac{t_b}{t^*} = \frac{L_0 - L_{ub}}{L_0} = 1 - \frac{L_{ub}}{L_0 - L_{ub}} \tag{D-30}$$

Equation D-30 is a basic equation used to analyze breakthrough data (Lyderson, 1983) and is essentially the same equation that is given by McCabe et al., 2001.

With $L_{ub} = ½ L_{mt} = 0.64/2 = 0.32$ ft, $L_0 = 77.56$ ft, and t* = 8.0 hrs, using EquationD-30 gives a breakout time of $t_b = 7.97$ hrs. This time agrees with the specified theoretical adorption time (or cycle time) of 8.0 hrs.

Plant-Scale, Fixed Bed Adsorbers: In an exploratory design study by Yang and Hoffman, 2009, they designed a fluidized bed adsorber for carbon dioxide removal from a flue gas which had a total adsorber cross-sectional area of 4,743 ft^2. According to Slejko, 1985, plant-scale, fixed bed adsorbers were two to ten feet in diameter and four to ten feet high. In Perry's Handbook (Green and Perry, 2008), there is a discussion of the design of adsorption equipment, and pressure drops of 1 to 4 kPa are used in compressed gas adsorption. Also, there is a section on moving-bed adsorption which uses cross-flow systems configured with panel beds, adsorbent wheels or rotating annular beds. A diagram of a 1969 patented moving bed was described by Walas, 1990. Design of a molecular sieve, ethylene purification plant is described

by Kohl and Nielson, 1997 which had an adsorber diameter of 5.0 ft and a height of 32 ft. The design of a vapor-phase, activated carbon adsorber for removal of volatile organic chemicals, e.g., benzene, had an adsorber diameter of 7.1 ft and a height of 23 ft (U. S. Army Corps of Engineers, 2001). Yang, 1987 describes a commercial process for air separation that used three adsorbers with 6-10 ft bed lengths.

Summary: A preliminary design of a fixed bed adsorber for carbon capture from the flue gas from the AEP's Conesville #5 Power Plant has been completed. The results from the adsorber design and parameters used in the evaluation are shown in Table D-2. To have a 90% removal of carbon dioxide, the adsorber height was 78 ft. and the diameters of four adsorbers in parallel are 79 ft each. A summary of the design procedure developed is given in Table D-3. This procedure was incorporated in an Excel spreadsheet. The adsorber and regenerator designs could be extended to include nonisothermal operations using Aspen Adsim program and Excel spreadsheet

Table D-2 Adsorber Design Results and Parameters Used in Excel Calculations

W_s	equilibrium or saturated value (lb CO2/lb adsorbent)	0.0989	lb CO_2/lb-adsorbent		
	loading (theoretical maximum TDA-R data (wt%))	9.00	%wt		
W_0	initial adsorbent loading (lb CO_2/lb adsorbent)	0.00	lb CO_2/lb-adsorbent		
u_0	superficial velocity (ft/sec)	1.00	ft/sec		
c_0	concentration of CO_2 in gas entering adsorber (lb/ft^3)	0.0157	lb/ft^3		
c_f	concentration of CO_2 in gas leaving adsorber (lb/ft^3)	0.0019	lb/ft^3		
Mw_{avg}	average molecular weight	28.60	lb/mole		
Q	gas flow rate into adsorber	18,546	ft^3/sec		
ρ_b	adsorbent bulk density (gm/cc)	0.95	gm-adsorb/cm^3	59.25	lb-adsorb/ft^3
t*	ideal adsorption time for a vertical breakthrough curve (hr)	8.00	hr	28,800.00	sec
	specifies cycle time for adsorber to give minimum length				
t_b	time at breakthrough	7.967	hr		
t_1	time to saturate the first portion of the bed	TBD			
K_c	overall mass transfer coefficient	0.25	cm/sec	estimated	
a	surface area of adsorbant	13.1	cm^2/cm^3	estimated	
L_{mt}	length of the mass transfer zone	0.6434	ft		
c_f/c_0	concentration ratio	0.12	dimensionless		
K_ca	mass transfer coefficient times surface area of adsorbant	3.275	sec^{-1}		
L_{min}	Minimum bed length with equilibrium adsorption	77.23	ft		
L_{sat}	Length of the saturated zone	76.91	ft		
L_{UB}	Length of unused bed, L_0 - L_{min}	0.32	ft		
L_0	Total length of the adsorber = L_{sat} + L_{min}	77.56	ft		
A	adsorber cross-sectional area	18,546	ft^2		
D	Diameter of one adsorber	153.67	ft		
L_{mt}	Length of mass transfer zone	0.6434	ft		

Table D-3 Summary of Adsorber Design Procedure

Procedure: Calculate	
1. Determine bed area	
'A = w/ρv = wV/u_0	
2. Equilibrium adsorption - minimum bed length	
Minimum bed length for an 8.0 hr adsorption cycle with an ideal adsorption curve	
' Lmin = t*u0c0/ρb(Wsat - W0)	
3. Length of the mass transfer zone	
Determine kc_{ext} from a mass transfer correlation	
Determine kc_{int} from a mass transfer correlation with $D_e = D_v/10$	
Determine overall mass transfer coefficient K_c	
Determine area of bed knowing void fraction ε and surface area a	
Determine $K_c a$	
Determine length of mass transfer zone with $c/c_0 = 0.05$	
4. Total length of bed	
Determine the amount of adsorbate in the mass transfer zone using $W = W_s/2$	
Compute length of the saturated bed to account for CO_2 in the mass transfer zone	
Determine the total length of the bed $L_0 = L_{sat} + L_{mt}$	
5. Calculate the breakout time $\frac{t_b}{t^*} = 1 - \frac{L_{ub}}{L_0 - L_{ub}}$	

Regenerator Design

Referring to Figure D-1, the procedure for the design of the regenerator follows the same steps as the design of the adsorber.

1. For a known inlet steam conditions, c_0, to the regenerator and a specified ratio of steam to carbon dioxide required to displace carbon dioxide from the adsorbent, the material balance around the regenerator is completed.

For a specified superficial velocity, u_0, in the regenerator, the cross-sectional area of the regenerator bed is evaluated, and the diameter of the bed, D, is determined for a circular cross-section.

2. The minimum bed length, L_{min}, is evaluated by a material balance knowing the equilibrium adsorption (saturated loading), W_s; initial loading, W_0; initial adsorbate concentration in the gas,

c_0, adsorbent bulk density, ρ_b, and ideal adsorption time for a vertical breakthrough curve, t*, that specifies cycle time for adsorber to give the minimum length.

3. The length of the mass transfer zone, L_{mt}, is evaluated using a material balance and rate equations for mass transfer from the bulk fluid to the gas solid interface and from this interface into the pores of the adsorbent.

4. The saturation zone length and the total bed length are evaluated based on the ideal adsorption time for a vertical breakthrough curve, t*, that specifies cycle time for adsorber to give the minimum length.

5. The breakthrough time is determined.

Specified Regeneration of Adsorbent: The inlet and outlet flow rates to and from the regenerator are shown in Figure 4. For a known inlet steam conditions to the regenerator and a specified ratio of steam to carbon dioxide required displace carbon dioxide from the adsorbent, the material balance around the regenerator is completed.

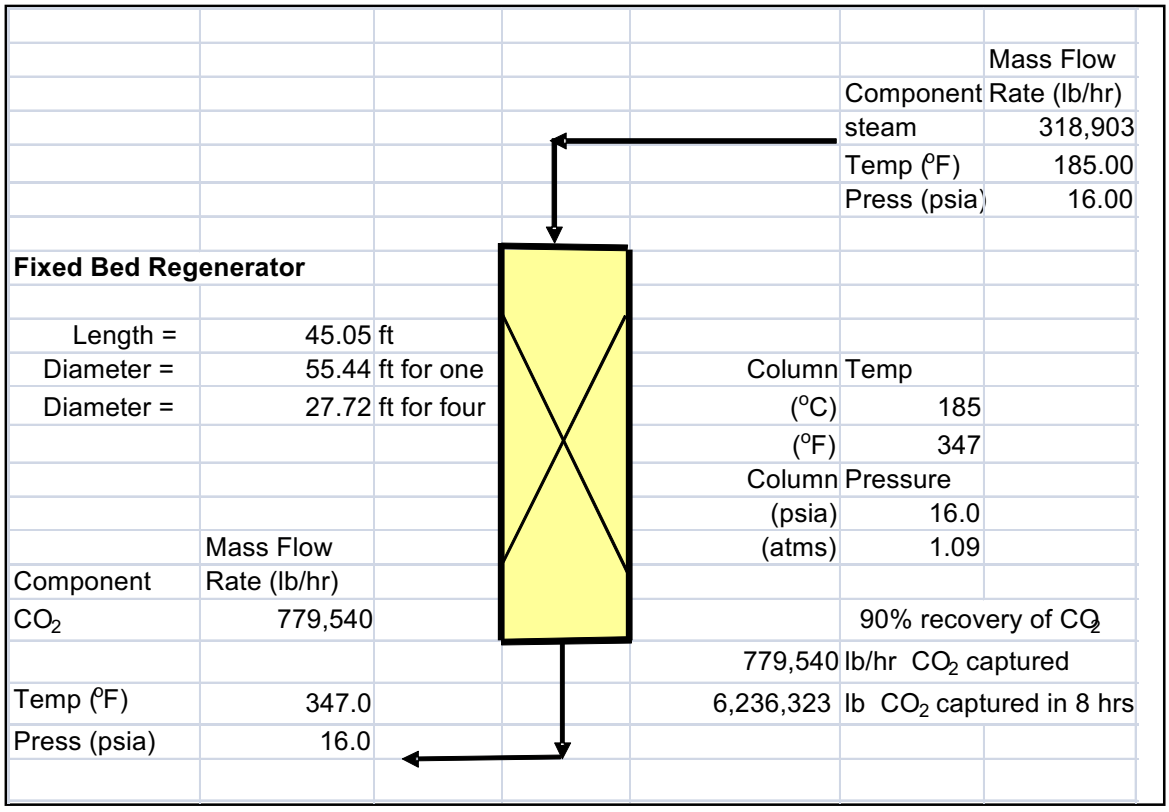

Figure D-4 Flow Rates and Compositions to and from the regenerator for removal of CO_2 based on AEP's Conesville #5 Power Plant (Ramezan, 2007b) DOE Final Report Revised November 2007 DOE/NETL-401/110907)

Regenerator Bed Area: For a specified superficial velocity, u_0, in the regenerator, the cross-sectional area of the bed, A, is evaluated using the definition of the mass flow rate of

steam, m_s, which is equal to the density of the steam, ρ_s, times the cross-sectional area of the bed, A, times the gas superficial velocity, u_0, in Equation (D-31).

$$m_s = \rho_s A\, u_0 =_s \; A u_0 / V_s \tag{D-31}$$

This equation can be solved for the area of the regenerator, A, as:

$$A = m_s / u_0 \rho_s = m_s V_s / u_0 \quad = Q / u_0 \tag{D-32}$$

Using the mass flow rate of steam, m_s = 318,903 lb_m/hr, the specific volume of steam at 280^0F and 16.0 psia (60^0F of superheat), V_s = 27.25 ft^3/lb, and the superficial velocity, u_0 = 1.0 ft/sec, the cross-sectional area, A, is 2,414 ft^2 using Equation 32.

The diameter of the bed, D, is determined for a circular cross-section by the following equation.

$$D = \left(4A / \pi\right)^{1/2} \tag{D-33}$$

Using the circular cross-sectional area of the bed, A, as 2,414 ft^2, the diameter, D = 55.44 ft for one regenerator, and for four regenerators their diameter are D = 27.72 ft. Increasing the superficial velocity to 2.0 ft/sec, the regenerator cross-section is 1,207 ft^2, and the diameter is 39.20 ft.

Equilibrium Adsorption: There is very limited data on water as an adsorbate, and equilibrium adsorption data for water on four adsorbents from the literature is summarized below in Table D-4. The standard reference, *The Adsorption Equilibrium Data Handbook* by Valenzuela and Myers, 1989, did not have any date for water adsorption.

Table D-4 Equilibrium Adsorption Capacity for Water Vapor on Various Adsorbents

		P and T		
Adsorbent	Capacity	kPa	K	Source
4A Mol Sieve	0.2 (gm/gm)	ns	293	Ruthven, 1984
Zeolites	1.0 – 28 %wt	ns	ns	Wankat, 1990
Activated alumina	0.07 – 0.25 (kg/kg)	ns	373	Wankat, 1990
Activated carbon	1.0 (gm/gm)	101	398	Rudistill, et al., 1992
Activated carbon	4 lb steam/lb organic	101	302	Schork and Fair, 1998
Activated carbon	0.5 (gm/gm)	101	334	Schweiger and Le Van, 1993
Activated carbon	0.26 (kg/kg)	101	303	Schweiger, 1996
Carbon fibers	0.65 gm/gm	468	423	Striolo, 2005

Minimum Bed Length: Referring to the regenerator diagram in Figure D-4, the minimum bed length, $L_{\min}$, for the regenerator is the case where the concentration profile is vertical and moves with a superficial velocity of u_0. The bed is saturated from the entrance to the

vertical concentration profile. The time t* is the ideal adsorption time for a vertical breakthrough curve (hr), and it is the cycle time for regenerator to have a minimum length.

A material balance can be written equating the amount of adsorbate in the fluid, Au_0ct^* equal to the amount of adsorbate that was transferred, $L_{\min}A\rho_b(W_s - W_0)$, over the time period, t*, Equation D-4. This equation is used to determine the minimum bed length, $L_{\min}$, for a specified value of the cycle time for the regenerator, t*.

$$L_{\min} = u_0 c_0 t^* / \rho_b (W_s - W_0) \tag{D-34}$$

In this equation, ρ_b is the bulk density of the adsorbent, and W_s and W_0 are the saturated and initial value of the steam loading.

An approximate average of the equilibrium adsorption capacities given in Table D-4 is W_s = 0.4 lb steam/lb adsorbent. This value is used for the saturation loading. There is no steam on the adsorbent initially, W_0 = 0. The initial concentration of steam entering the regenerator c_0 = 0.0367 lb/ft^3, is the density of steam with 20 degree of superheated at 16.0 psia and 280^{0}F. The minimum bed length, $L_{\min}$ = 44.59 ft was determined using Equation 34 for t* = 8.0 hrs, the ideal adsorption time. This time is the cycle time for the minimum length of the adsorber.

Mass Transfer and Saturated Zones: Referring to Figure D-1, the length of the saturation zone L_{sat} is the length where the adsorbent is saturated with adsorbate. In the length of the mass transfer zone, L_{mt}, the rate of mass transfer, m_c of the adsorbate from the fluid to the adsorbent is described by an overall mass transfer coefficient, K_c, which incorporates a diffusion coefficient from the bulk flow to the surface of the adsorbent, $k_{c,ext}$ and a diffusion coefficient from the surface of the adsorbent into the pores of the adsorbent, $k_{c,int}$. These coefficients are related by Equation D-6. Methods to evaluate $k_{c,ext}$ and $k_{c,int}$ are given by McCabe, et al., 2001 and Hutchinson, 1997. Following these procedures a value for K_c of 0.25 cm/sec was estimated.

The rate of mass transfer is given by Equation D-7. In this equation a is the mass transfer area that is given by the external surface area of the adsorbent, c is the concentration of the adsorbate in the bulk flow and c* is the concentration of the adsorbate in equilibrium with the concentration in the solid as measured by W_s. A typical value of a is 13.0 cm^2/cm^3 (Hutchinson, 1997).

As shown in Figure D-3, to relate the rate of mass transfer from the bulk fluid to the solid adsorbent, the species continuity equation is applied to a section of adsorber length, dL_{mt}. The change of mass of c, the concentration of the adsorbate, with time in the voids is given by Equation D-8. The change of mass of W, the concentration (loading) of the adsorbate on the adsorbent, with time in the porous solid is by Equation D-9. The species continuity equation has the mass accumulation of c in the adsorber control volume of AdL_{mt} equal to the mass flow rate of c into the control volume minus the mass flow rate of c from the control volume (acc = input – output), as shown in Figure D-3. Combining, simplifying and integrating these equations as described in the adsorber design section, the following equation is obtained.

$$L_{mt} = \frac{u_0}{K_c a} \ln \frac{c}{c_0} \tag{D-35}$$

Using $c/c_0 = 0.05$, $u_0 = 1.0$ ft/sec, and $K_c a = 3.275$ sec^{-1}, the value of $L_{mt} = 0.9147$ ft was obtained.

Referring to Figure D-1, the total length of the adsorber bed is the sum of the saturated bed and the mass transfer zone, $L_0 = L_{sat} + L_{mt}$. The amount of adsorbate in the mass transfer zone can be evaluated using a symmetric breakthrough curve with equilibrium adsorption having $W = 0.5\ W_s$. The amount of adsorbate in this zone in lb of steam is given by Equation D-35. The saturated zone holds the total amount of adsorbent transferred for t* minus the amount in the mass transfer zone. The resulting equation can be written as: (See adsorber section for details.)

$$L_{sat} = (t^* u_0 c_0 - L_{mt} \rho_b W_s / 2) / W_s \rho_b A \tag{D-36}$$

Using the previously specified values of the parameters, the saturated bed length, $L_{sat} = 44.13$ ft.

Referring to Figure D-1, the total length of the regenerator bed is the sum of the saturated bed length, L_{sat} and the mass transfer zone length, L_{mt}:

$$L_0 = L_{sat} + L_{mt} = \ 44.13 + 0.91 = 45.05 \text{ ft} \tag{D-37}$$

Breakthrough Time: The description and equations to obtain the breakthrough time are given in the adsorber section. The final result is Equation D-30. Using this equation with $L_{ub} = ½\ L_{mt} = 0.9147/2 = 0.4574$ft, $L_0 = 45.74$ft, and t* = 8.0 hrs, a breakout time of $t_b = 7.92$ hrs.

Summary: In Table D-5 the results are given for the preliminary design of a fixed bed regenerator for steam regeneration of the adsorbent. To regenerate the adsorbent, a column height of 45 ft is required, and the diameters of four adsorbers in parallel are 27 ft each. A summary of the design procedure developed above is given in Table D-6. This procedure is incorporated in an Excel spreadsheet. The regenerator design is being extended to include nonisothermal operations using Aspen Adsim program and Excel spreadsheet.

Table D-5 Regenerator Design Results and Parameters Used in Excel Calculations

W_s	equilibrium or saturated value (lb CO2/lb adsorbent)	0.4000	lb steam/lb-adsorbent			
W_0	initial adsorbent loading (lb steam/lb adsorbent)	0.00	lb steam/lb-adsorbent			
u_0	superficial velocity (ft/sec)	1.00	ft/sec			
$c_0 = \rho$	concentration of steam in gas entering adsorber (lb/ft^3)	0.0367	lb/ft^3	density of steam at 16.0 psia and 280^0F		
c_f	concentration of steam in gas leaving adsorber (lb/ft^3)		lb/ft^3			
V	specific volume of steam	27.25	ft^3/lb specific volume at 16.0 psia and 280^0F			
Q	gas flow rate into adsorber w*V	2,414	ft^3/sec			
ρ_b	adsorbent bulk density (gm/cc)	0.95	gm-adsorb	59.25	lb-adsorb/ft^3	
t*	ideal adsorption time for a vertical breakthrough curve (hr)	8.00	hr	28,800.00	sec	
	specifies cycle time for adsorber to give minimum length					
t_b	time at breakthrough	7.919	hr			
t_1	time to saturate the first portion of the bed	TBD				
K_c	overall mass transfer coefficient	0.25	cm/sec	estimated		
a	surface area of adsorbant	13.1	cm^2/cm^3	estimated		
L_{mt}	length of the mass transfer zone	0.9147	ft			
c_f/c_0	concentration ratio	0.05	dimensionless			
K_ca	mass transfer coefficient times surface area of adsorbant	3.275	sec^{-1}			
L_{min}	Minimum bed length with equilibrium adsorption	44.59	ft			
L_{sat}	Length of the saturated zone	44.13	ft			
L_{UB}	Length of unused bed, L - L_{min}	0.46	ft			
L_0	Total length of the adsorber = L_{sat} + L_{min}	45.05	ft			
A	adsorber cross-sectional area	2,414	ft			
D	Diameter of one adsorber	55.44	ft			
L_{mt}	Length of mass transfer zone	0.9147	ft			

Table D-6 Summary of Regenerator Design Procedure

Procedure:	
1. Determine bed area	
'A = w/ρv = wV/u_0	
2. Equilibrium adsorption - minimum bed length	
Minimum bed length for an 8.0 hr regeneration cycle with an ideal adsorption curve	
' Lmin = t*$u_0c_0/\rho_b(W_{sat} - W_0)$	
3. Length of the mass transfer zone	
	Determine kc_{ext} from a mass transfer correlation
	Determine kc_{int} from a mass transfer correlation with $D_e = D_v/10$
	Determine overall mass transfer coefficient K_c
	Determine area of bed knowing void fraction ε and surface area a
	Determine K_ca
	Determine length of mass transfer zone with $c/c_0 = 0.05$
4. Total length of bed	
	Determine the amount of adsorbate in the mass transfer zone using $W = W_s/2$
	Compute length of the saturated bed to account for steam in the mass transfer zone
	Determine the total length of the bed $L_0 = L_{sat} + L_{mt}$
5. Calculate the breakout time	$\frac{t_b}{t^*} = 1 - \frac{L_{ub}}{L_0 - L_{UB}}$

Comparison of Effects of Steam to Carbon Dioxide Ratio and Superficial Velocity on the Regenerator Design

In Table D-7, a comparison is given for the effect of changing the ratio of steam to CO_2 in the regenerator and changing the superficial velocity. These results were obtained using the Excel spreadsheets for the design of the adsorber and regenerator. Increasing the moles steam/mole CO_2 for a constant superficial velocity of 1.0 ft/sec had the effect of increasing the regenerator diameter but not affecting the regenerator length. Increasing the steam/CO_2 ratio increased the flow rate to the regenerator, and according to Equation 32 the area and diameter increased. According to Equations D-18, D-22, D-23 and D-34, the regenerator length was not affected by the increase in increasing the steam/CO_2 ratio. Increasing the superficial velocity for a constant 2.0 moles steam/mole CO_2 had the effect of increasing the length from 45 ft to 135 ft, and decreasing the diameter from 39 ft to 23 ft as shown in Table D-7. According to Equation 32 increasing the superficial velocity for a constant flow rate decreased the required area and diameter. Increasing the superficial velocity increased the length as can be seen in Equations D-18, D-22, D-23 and D-34. Comparable results can be obtained for the adsorber, since the equations used for the adsorber design are the same as those used for the regenerator.

Table D-7 Comparison of Changing the Steam to Carbon Dioxide Ratio and Superficial Velocity on the Design of the Regenerator

		Regenerator					
		1.0 ft/sec superficial velocity			2.0 moles steam/ mole CO_2		
	Adsorber	Moles steam/mole CO_2			Superficial velocity (ft/sec)		
		1.00	2.00	3.00	1.00	2.00	3.00
Length (ft)	78	45	45	45	45	90	135
Diameter (ft)	154	55	78	96	78	55	45
Diameter (ft)*	77	28	39	48	39	28	23

*Four adsorbers or regenerators

Aspen HYSYS Adsorber/Regenerator Process Design

A preliminary Aspen HYSYS process flow diagram is shown in Figure D-5 for the Adsorber/Regenerator process. Using HYSYS, the process was designed to have the carbon dioxide from the Adsorber/Regenerator be delivered to the sequestration pipeline at 2,200 psia. The units required were two compressors, a high pressure pump and intercooling heat exchangers. The design was within the limitations of industrial equipment in compressing CO_2 from 16.1 psia to 2,200 psia, and it ensured that the carbon dioxide was in the single phase region since compressing or pumping two-phase mixtures is not practical. The path from the Adsorber/Regenerator to the high pressure outlet is shown in Figure D-6 on a T vs. P diagram for carbon dioxide to demonstrate the process units operated in the single phase region, either as a supercritical fluid or liquid.

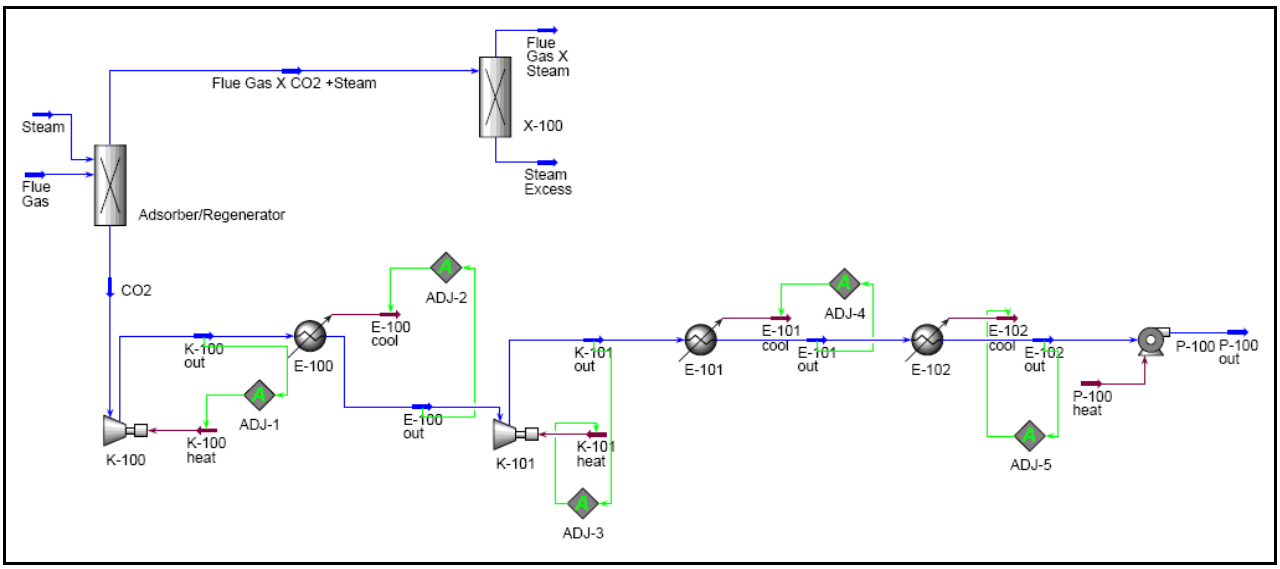

Figure D-5 Preliminary Aspen HYSYS Process Flow Diagram for Adsorber/Regenerator Process

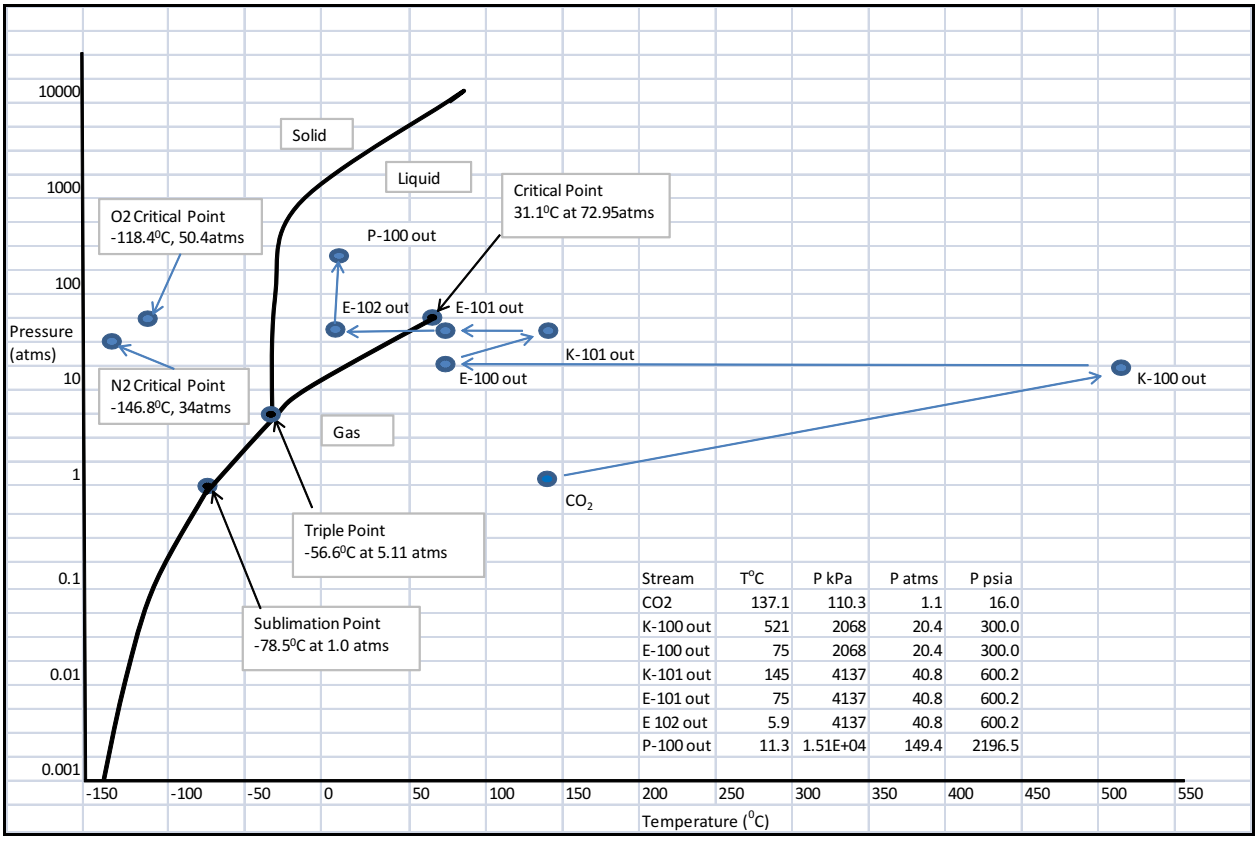

Figure D-6 Temperature–Pressure Phase Diagram for Carbon Dioxide Showing Streams in the Process Flow Diagram

The data associated with Figures D-5 and D-6 was obtained from standard HYSYS Workbook. The first of the 22 Workbook pages is shown in Figure D-7. The Workbook

provides data on the material streams including flow rate, temperature, pressure and composition. Heat flows for the energy streams are included in the Workbook, along with a unit operations summary. In Table D-8 the energy required is given for the compressors, pump and heat exchangers that was taken from the Aspen HYSYS Workbook.

Table D-8 Preliminary Energy Requirements for the Adsorber/Regenerator Process

				Compressors and Pump		
Heat Exchangers	Heat Flow				Heat Flow	
	kJ/hr	BTU/hr			kJ/hr	BTU/hr
E-100 cool	1.634E+08	1.632E+08		P-100 heat	5.796E+06	5.788E+06
E-101 cool	2.310E+07	2.307E+07		K-100 heat	1.431E+08	1.429E+08
E-102 cool	1.195E+08	1.193E+08		K-101 heat	2.311E+07	2.308E+07
	Total	3.056E+08			Total	1.718E+08

Based on the above design, Aspen In-Plant Cost Estimator program could be used to develop equipment and operating costs and related economic evaluations. Aspen Adsorption could be used to extend the adsorber/regenerator design for nonisothermal operations.

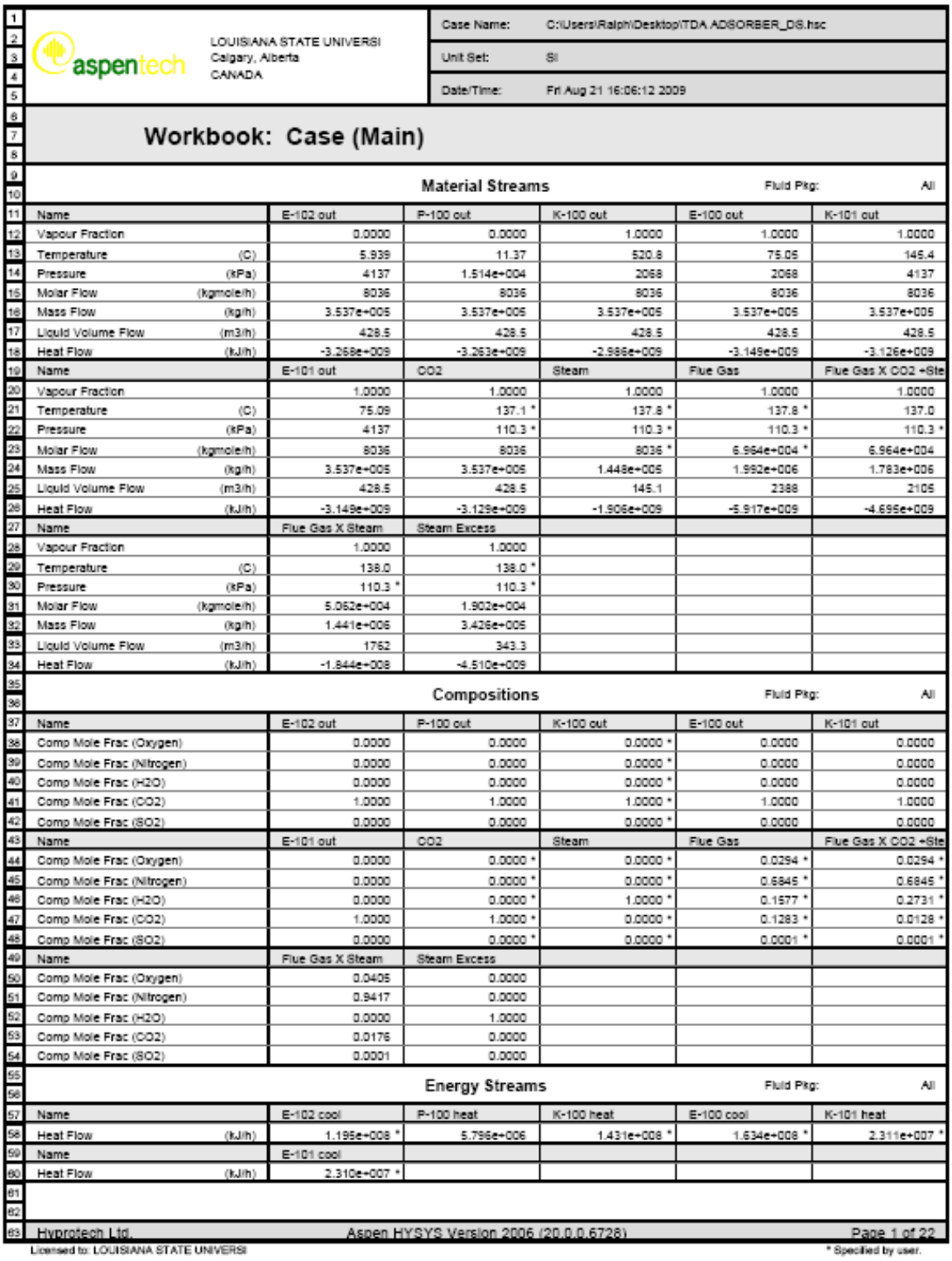

aspentech

LOUISIANA STATE UNIVERSI
Calgary, Alberta
CANADA

Case Name: C:\Users\Ralph\Desktop\TDA ADSORBER_DS.hsc
Unit Set: SI
Date/Time: Fri Aug 21 16:06:12 2009

Workbook: Case (Main)

Material Streams

Fluid Pkg: All

Name		E-102 out	P-100 out	K-100 out	E-100 out	K-101 out
Vapour Fraction		0.0000	0.0000	1.0000	1.0000	1.0000
Temperature	(C)	5.939	11.37	520.8	75.05	145.4
Pressure	(kPa)	4137	1.514e+004	2068	2068	4137
Molar Flow	(kgmole/h)	8036	8036	8036	8036	8036
Mass Flow	(kg/h)	3.537e+005	3.537e+005	3.537e+005	3.537e+005	3.537e+005
Liquid Volume Flow	(m3/h)	428.5	428.5	428.5	428.5	428.5
Heat Flow	(kJ/h)	-3.268e+009	-3.263e+009	-2.986e+009	-3.149e+009	-3.126e+009

Name		E-101 out	CO2	Steam	Flue Gas	Flue Gas X CO2 +Ste
Vapour Fraction		1.0000	1.0000	1.0000	1.0000	1.0000
Temperature	(C)	75.09	137.1 *	137.8 *	137.8 *	137.0
Pressure	(kPa)	4137	110.3 *	110.3 *	110.3 *	110.3 *
Molar Flow	(kgmole/h)	8036	8036	8036 *	6.964e+004 *	6.964e+004
Mass Flow	(kg/h)	3.537e+005	3.537e+005	1.448e+005	1.992e+006	1.783e+006
Liquid Volume Flow	(m3/h)	428.5	428.5	145.1	2388	2105
Heat Flow	(kJ/h)	-3.149e+009	-3.129e+009	-1.906e+009	-5.917e+009	-4.695e+009

Name		Flue Gas X Steam	Steam Excess			
Vapour Fraction		1.0000	1.0000			
Temperature	(C)	138.0	138.0 *			
Pressure	(kPa)	110.3 *	110.3 *			
Molar Flow	(kgmole/h)	5.062e+004	1.902e+004			
Mass Flow	(kg/h)	1.441e+006	3.426e+005			
Liquid Volume Flow	(m3/h)	1762	343.3			
Heat Flow	(kJ/h)	-1.844e+008	-4.510e+009			

Compositions

Fluid Pkg: All

Name	E-102 out	P-100 out	K-100 out	E-100 out	K-101 out
Comp Mole Frac (Oxygen)	0.0000	0.0000	0.0000 *	0.0000	0.0000
Comp Mole Frac (Nitrogen)	0.0000	0.0000	0.0000 *	0.0000	0.0000
Comp Mole Frac (H2O)	0.0000	0.0000	0.0000 *	0.0000	0.0000
Comp Mole Frac (CO2)	1.0000	1.0000	1.0000 *	1.0000	1.0000
Comp Mole Frac (SO2)	0.0000	0.0000	0.0000 *	0.0000	0.0000

Name	E-101 out	CO2	Steam	Flue Gas	Flue Gas X CO2 +Ste
Comp Mole Frac (Oxygen)	0.0000	0.0000 *	0.0000 *	0.0294 *	0.0294 *
Comp Mole Frac (Nitrogen)	0.0000	0.0000 *	0.0000 *	0.6845 *	0.6845 *
Comp Mole Frac (H2O)	0.0000	0.0000 *	1.0000 *	0.1577 *	0.2731 *
Comp Mole Frac (CO2)	1.0000	1.0000 *	0.0000 *	0.1283 *	0.0128 *
Comp Mole Frac (SO2)	0.0000	0.0000 *	0.0000 *	0.0001 *	0.0001 *

Name	Flue Gas X Steam	Steam Excess			
Comp Mole Frac (Oxygen)	0.0405	0.0000			
Comp Mole Frac (Nitrogen)	0.9417	0.0000			
Comp Mole Frac (H2O)	0.0000	1.0000			
Comp Mole Frac (CO2)	0.0176	0.0000			
Comp Mole Frac (SO2)	0.0001	0.0000			

Energy Streams

Fluid Pkg: All

Name		E-102 cool	P-100 heat	K-100 heat	E-100 cool	K-101 heat
Heat Flow	(kJ/h)	1.195e+008 *	5.796e+006	1.431e+008 *	1.634e+008 *	2.311e+007 *

Name		E-101 cool
Heat Flow	(kJ/h)	2.310e+007 *

* Specified by user.

Figure D-7 Aspen HYSYS Workbook for the Preliminary Design of Adsorber/Regenerator Process